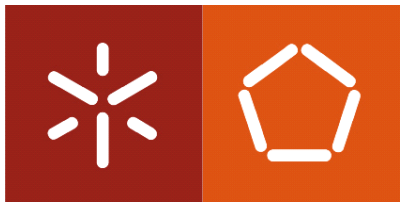

Universidade do Minho
Escola de Engenharia

Nuno Miguel Dias Cerca

Virulence aspects of *Staphylococcus epidermidis*: biofilm formation and Poly-N-Acetyl-Glucosamine production

Dissertation for PhD degree

Supervisor: Joana Azeredo

2006

Universidade do Minho,
Braga, 2006

Acknowledgments

The work presented in this thesis was only possible due to a fantastic team of researchers that I want to acknowledge: **Casie Kelly-Quintos** (chapter 10), **Danielle Pier** (chapter 10), **Donald Goldmann** (chapters 10 and 12), **Filipe Cerca** (chapters 4 and 9), **Kimberly Jefferson** (chapters 4, 6, 8, 10, 11 and 12), **Luzia Teixeira** (chapter 9), **Manuel Vilanova** (chapters 2, 3 and 9), **Martha Grout** (chapters 10 and 12), **Pedro Madureira** (chapter 9), **Sanna Sillankorva** (chapter 6 and 7), **Silvia Martins** (chapters 4, 5 and 6) and **Tomas Maira-Litran** (chapters 10 and 12).

I specially acknowledge **Joana Azeredo**, **Rosário Oliveira** and **Gerald Pier** for guidance through my PhD research work.

I extend my thanks to everyone of the Biofilm Group Laboratory in the Minho University, Channing Laboratory Pier's Lab, and Mario Aralla-Chaves Laboratory in the ICBAS for a good working environment and for their understanding for all the times I was using somebody else's bench space. I also want to thank Aidan Coffey and Tyrone Pitt for helpful hints regarding the use of staphylococcal phages and Christine Anderson for providing training to work in BL2+ laboratory.

The work presented here was done in: Centro de Engenharia Biológica of Universidade do Minho, Braga, Portugal; The Channing Laboratory, Brigham and Women's Hospital, Harvard Medical School, Boston, USA and Instituto de Ciências Biomédicas Abel Salazar from Universidade do Porto, Porto, Portugal.

I acknowledge the financial support by FCT through grant SFRH/BD/8676/2002. I also acknowledge the Portuguese Fulbright Commission, Brigham and Women's Hospital, FLAD, and Fundação Calouste Gulbenkian.

My mother sometimes tells me the story of how I was infected by staphylococcus, when I was 4 years old. I had several skin irritations, generalized pain, and I lost some of my teeth, presumably as a side effect of the potent antibiotics that I was taking to fight the infection. For many, many years, this early encounter with this common human pathogen was forgotten deep inside my mother's memories. When I started my PhD research work on staphylococcal biofilms, my mother told me about this episode of my childhood. Interesting how life is! Twenty years later I found myself dealing once again with these "bugs", but this time, on a completely different perspective…

Virulence aspects of *Staphylococcus epidermidis*: biofilm formation and Poly-N-Acetyl-Glucosamine production

Summary

Staphylococcus epidermidis and other *Staphylococci* are now well established as major nosocomial pathogens associated with infections of indwelling medical devices. The major virulence factor of these organisms is their ability to adhere to devices and form biofilms. Biofilms are complex microbial communities wherein bacteria acquire different characteristics from their planktonic counterparts, like enhanced resistance to antibiotics and host defenses. The work described in this thesis was aimed at evaluating the adhesion and biofilm formation abilities of several clinical isolates of *Staphylococci* as well as the phenotypic alterations triggered by the sessile mode of growth. The determination of the role of Poly-N-Acetyl-Glucosamine (PNAG), a major constituent of the biofilm matrix, in *S. epidermidis* pathogenesis was also a goal of the described work. Some experimental approaches were developed or optimized in order to assess initial adhesion, biofilm formation and PNAG production with accurate and expeditious methods. According to the results, initial adhesion and biofilm maturation are two distinct phenomena, and may influence virulence differently. Initial adhesion was found to be dependent on the surface composition, hydrophobic surfaces being more prone to bacterial adhesion. Biofilm formation was not so strongly affected by the substrata surface properties. It was also demonstrated that sub-inhibitory concentrations of antibiotics differentially influence initial adhesion and biofilm formation abilities. Additionally, biofilms formed in the presence of sub-inhibitory concentrations of antibiotics exhibit alterations in their structures and matrix compositions and the biofilm cells acquire enhanced resistance to antibiotics. The results also revealed that *S. epidermidis* biofilm cells are more resistant to antibiotics that target cell wall synthesis but fairly susceptible to antibiotics that target RNA and protein synthesis, when compared to their equivalent planktonic populations. Biofilm cells proved to be more resistant to the lytic action of phage K than their exponentially grown planktonic counterparts, possibly due to the lower growth rate of biofilm bacteria. Furthermore, it was also demonstrated that biofilm cells are more resistant to phagocytosis (evaluated in vitro and in vivo), probably due to the high levels of PNAG expression, since PNAG is a known inhibitor of phagocytosis. The role of PNAG in Staphylococcal virulence was also established by the direct correlation between biofilm formation and level of PNAG expression. The molecular studies of PNAG production demonstrated that the *icaB* gene, present in the intercellular adhesion locus (*ica*), plays an important role in the virulence of *Staphylococcus spp*, mediating PNAG anchorage to the cell surface or release into the

extracellular media, acting as a possible decoy to the immune system. This newly described mechanism highlighted the role of PNAG in biofilm resistance to the immune system. Finally, and focusing on the role of PNAG as a target for vaccine development, several pathogenic genera were screened for PNAG production. The fact that a polysaccharide immunologically similar to the Staphylococcal PNAG was detected on the cell surface of several strains of *E. coli*, *Yersinia spp*. and *Bordatela spp*, opens the possibility for the development of a broad vaccine against some major human pathogens.

Factores de virulência de *Estafilococos epidermidis*: formação de biofilme e produção de Poli-N-Acetil-Glucosamina

Sumário

A espécie *Estafilococos epidermidis* assim como outras espécies de *Estafilococos* é actualmente reconhecida com uma importante espécie nosocomial patogénica associada a um grande número de infecções relacionadas com a utilização de implantes médicos invasivos. A capacidade que esta espécie apresenta para aderir a superfícies e para formar biofilmes é considerada um dos factores de virulência preponderantes. Os biofilmes são estruturas complexas que conferem às células bacterianas resistência aos antibióticos e às defesas naturais do organismo. O trabalho descrito nesta dissertação teve como objectivo principal o estudo da capacidade de adesão e formação de biofilmes de várias estirpes clínicas de *Estafilococos* bem como a determinação das alterações fisiológicas induzidas pelo fenótipo de biofilme e a importância da segregação do polissacárido poli-N-acetilglucosamina (PNAG), um constituinte importante do biofilme. Os estudos conduzidos e aqui descritos pretendem explicar as implicações das características fenótipicas dos biofilmes de *Estafilococos* na virulência desta espécie. Foi necessário desenvolver um conjunto de metodologias que permitem de forma expedita e fidedigna estudar a capacidade de adesão, de formação de biofilme, bem como de quantificação de PNAG. Os resultados obtidos permitiram concluir que a capacidade de adesão é dissociada da capacidade de formação de biofilme pelo que adesão e formação de biofilme devem se considerados dois fenómenos distintos. Consequentemente demonstrou-se que a composição da superfície de adesão implica o fenómeno de adesão, sendo ele mais favorável a superfícies hidrofóbicas, afectando de forma não linear a formação de biofilme. Do mesmo modo demonstrou-se que concentrações sub-inibitórias de antibióticos afectam de forma diferente a adesão a superfícies e a formação de biofilme, e verificou-se também que os biofilmes formados na presença de concentrações sub-inibitórias de antibióticos apresentam alterações na composição e estrutura da matriz e aumento de resistência a certos antibióticos. Os estudos realizados permitiram ainda concluir que os biofilmes de *Estafilococos* são mais resistentes à acção de antibióticos do que as células suspensas, especialmente os que actuam ao nível da síntese da parede, tendo no entanto sido susceptíveis a antibióticos que afectam a replicação de RNA e a produção de proteínas. Os biofilmes de *Estafilococos* mostraram-se também mais resistentes à acção lítica do bacteriófago K, possivelmente devido à baixa taxa de crescimento das células no biofilme. Também se verificou que populações de bactérias crescidas em biofilmes apresentavam maior resistência à fagocitose (avaliada *in vitro* e *in*

vivo), possivelmente devido à elevada quantidade de PNAG detectada na sua superfície celular e na matriz do biofilme, visto que PNAG é um conhecido inibidor da fagocitose. Esta molécula parece ser determinante na formação dos biofilmes uma vez que biofilmes mais espessos apresentam maior quantidade de PNAG. Os estudos moleculares realizados permitiram concluir que o gene *icaB*, presente no operão *ica*, desempenha um papel crucial na virulência de *Estafilococos*, mediando a fixação da PNAG na superfície celular ou a libertação para o meio externo, funcionado então como uma possível defesa contra o sistema imune do hospedeiro, sendo este um novo mecanismo descrito elucidando melhor a capacidade de resistência dos biofilmes de *Estafilococos* ao sistema imune. A PNAG parece ser ubíqua em espécies de importância clínica, uma vez que se detectou a presença de uma molécula imunologicamente semelhante à PNAG em estirpes clínicas de *Escherichia coli, Yersinia spp*. e *Bordatela spp*. Esta descoberta poderá abrir novas perspectivas no desenvolvimento de vacinas capazes de combater diferentes agentes patogénicos.

I dedicate this thesis to my parents, brother and sister

Abbreviations

α-. Anti-

Ab. Antibody

Agr. Accessory gene regulator

β-gal. β-galactosidase

BHI. Brain heart infusion

BSA. Bovine serum albumin

BSS. Balanced salt solution

CFU. Colony forming unit

CFZ. Cefazolin

CoNS. Coagulase-negative staphylococci

CSLM. Confocal scanning laser microscopy

DCX. Dicloxacillin

DNA. Deoxyribonucleic acid

dPNAG. Deacetylated Poly-N-Acetyl-Glucosamine

EDTA. Ethylenediaminetetraacetic acid

ELISA. Enzyme-linked immunosorbent assay

EPS. Extracellular polysaccharide

FBS. Fetal bovine serum

FITC. Fluoroscein isothiocyanate

HRP. Horseradish peroxidase

IP. Inter-peritoneal

IV. Intra-venous

IgG. Immunoglobulin class G

IgM. Immunoglobulin class M

LB. Luria Broth

Mab. Monoclonal antibody

MBEC. Minimum biofilm eradication concentration

MIC. Minimum inhibitory concentration

MOI. Multiplicity of infection

NCCLS. National Committee for Clinical Laboratory Standards

NGS. Normal goat sera

NRS. Normal rabbit sera

NICU. Neonatal intensive care unit

OD. Optical density

PBS. Phosphate buffer saline

PCR. Polymerase chain reaction

PE. Phycoerythrin

PFU. Plaque forming unit

PIA. Polysaccharide intercellular adhesion

PMN's. Polymorphonuclear cells

PMS. Phenazine methosulfate

PNAG. Poly-N-Acetyl-Glucosamine

dPNAG. deacetylated Poly-N-Acetyl-Glucosamine

PS. Peak serum concentration

RIF. Rifampicin

RNA. Ribonucleic acid

RPMI. Roswell Park Memorial Institute

RT-PCR. Reverse transcription polymerase chain reaction

SD. Standard deviation

SEM. Scanning electron microscopy

Sub-MIC. Sub-minimal inhibitory concentrations

TET. Tetracycline

TBS. Tris Buffer Saline

TBST. Tris Buffer Saline with 0.4% Tween

TSA. Trypic soy agar

TSB. Trypic soy broth

TSBG. Trypic soy broth with 1% extra glucose

UTI. Urinary tract infections

VAN. Vancomycin

Vs. Versus

WGA. Wheat germ agglutinin

XPS. X-Ray photoelectron spectroscopy

XTT. 2,3-bis (2-methoxy-4-nitro-5-sulfophenyl) – 5 - [(phenyalamino)carbonyl] - 2H-tetrazolium hydroxide

Page index

General Introduction

General introduction cover image is a Scanning Electron Microscope (SEM) observation with 5000x magnification of a S. epidermidis 9142 biofilm formed on acrylic. Centre of Materials, University of Minho, Braga, Portugal.

Microbial biofilms

For a long time, the laboratory study of microorganisms was based upon the pure-culture paradigm. It was considered that in order to study a certain microorganism, it should be diluted to a single cell and studied in liquid culture. Bacteria were therefore described as unicellular life forms [56]. The first descriptions of bacterial communities came from environmental microbiologists. However, due to the lack of appropriate microscopy and molecular technologies, the ability to study these communities *in situ* was until recently limited [56]. Direct observation of a wide variety of natural habitats has established that the majority of microorganisms persist attached to surfaces within a structured biofilm ecosystem and not as free-floating organisms [48,63].

A biofilm can therefore be defined as a community of bacteria that is attached to a surface and is encased in a matrix of extrapolymeric substance. This matrix is composed of a mixture of components, such as extracellular polysaccharide (EPS), protein, nucleic acids and other substances [56] and accounts for the majority (~85%) of the biofilm volume [60].

Bacteria has several advantages when residing within a biofilm: (a) they experience a certain degree of protection due to the existence of the surrounding matrix [78,165,166,168] against biocides, antibiotics, antibodies, surfactants, bacteriophages and predator organisms (like free-living amoebae) [63], (b) this micro-environment allows the establishment of symbiotic relationship providing crucial nutrients to some strains [26,199] and (c) the close contact between different species enhances the transmission of genetic elements [126,192].

Bacterial biofilms play an important role in nature by: (a) production and degradation of organic matter, (b) degradation of environmental pollutants and (c) cycling of nitrogen, sulphur and many metals [56].

Many species have shown distinct developmental steps in biofilm formation, which include: (a) initial attachment to a surface, (b) formation of microcolonies and finally (c) maturation of the microcolonies into an EPS-encases mature biofilm [56]. It is believed that biofilm formation begins when bacteria sense certain environmental parameters that trigger the transition from planktonic growth to biofilm growth by a mechanism known as quorum sensing [169,173,174,186,187,209,241].

Biofilms can be composed of a population derived from a single species or a community of multiple species. In both situations, the development of biofilms requires a multicellular behavior [56]. Biofilm formation and structure is affected by several conditions like: surface properties [42], nutrient availability [41], hydrodynamics [214] and composition of the microbial community [213].

Biofilms are dynamic and heterogeneous communities in constant evolution. Cells in a biofilm have different metabolic activities, depending on the special position inside the biofilm, and this can change over time [186].

Biofilms and infectious diseases

Although multi-species biofilms are more common in nature, single species biofilms play an important role in infectious diseases [56]. Single species biofilms develop on medical implants [34,84] as well as dead and living tissue [47,184], contributing to a variety of persistent infections. Biofilms can release antigens and/or bacteria and stimulate the production on antibodies, but the bacteria resident within the biofilm are normally resistant to these defense mechanisms, providing the basis for persistent infections [49].

Biofilm-based infections pose a serious threat to patients, mainly due to the high resistance to antibiotics [140,211] and also resistance to the host immune system [60,105]. These types of infections are associated with medical devices [60,234] like: prosthetic heart valves [112], contact lenses [54], intrauterine devices [147,246], artificial bone replacements [53], voice prostheses [30], intracardiac devices [234] and catheters [65,76,144,197] (see figure i.1).

Figure i.1. Scanning electron microscopy analysis of a cut section of a catheter collected from a patient with a urinary tract infection, showing the massive presence of *Cocci* and *Bacilli*. Adapted from Clinic Microb Rev (2002), 15: 167-193.

Millions of catheters are inserted into patients every year, and these implants serve as potential surfaces for biofilm formation. Up to 60% of all nosocomial infections are due to biofilms on medical surfaces [56,60] Often, the removal and reinsertion of colonized devices becomes necessary [234], which carries an additional economic and health cost [96,234].

Although less so than with medical devices, biofilm infections have also been associated with native valve endocarditis [225], otitis media [60], chronic bacterial prostatitis [167], cystic fibrosis [148], and peridontitis [188].

Staphylococcal, biofilms and infection

Pathogenic staphylococci are ubiquitous: they are carried on skin and mucous membranes of healthy individuals, with a higher incidence in hospital patients and personnel. *Staphylococcus aureus* is considered the classical staphylococcal pathogen, causing serious diseases in healthy individuals. Non-S. *aureus* staphylococci, also known as coagulase-negative staphylococci (CoNS), are opportunistic pathogens, normally only causing infections in immunocompromised individuals [172]. CoNS are widely distributed over the surface of the human body, where they constitute the majority of the commensal bacterial microflora, *Staphylococcus epidermidis* being the most frequent isolated CoNS species [172,239]. Furthermore, *S. epidermidis* is the most important bacterial pathogen involved in nosocomial infections [239]. Contrary to *S. aureus*, *S. epidermidis* is limited in the number of virulence factors elaborated: while *S. aureus* virulence can be attributed to protein A, clumping factor, biofilm formation, some proteolytic enzymes, and several toxins, *S. epidermidis* virulence is mainly attributed to its ability to form thick biofilms [239]. Probably due to this shortage of virulence factors, as compared to *S. aureus*, *S. epidermidis* is associated with persistent and relapsing infections while *S. aureus* is typically associated with severe acute tissue-related infections [172].

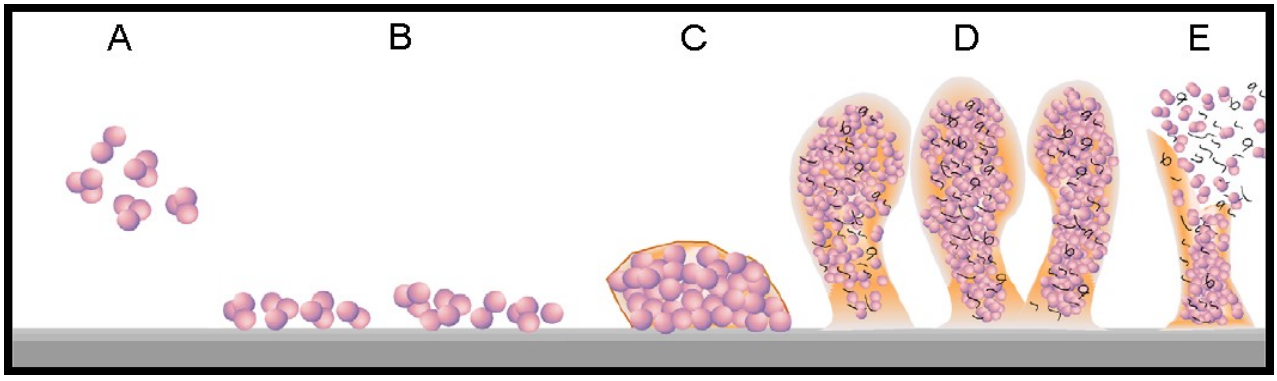

Figure i.2. The *S. epidermidis* biofilm cycle: planktonic cells can adhere to a solid surface (A). Adhered cells can then grow in clusters (B) due to the production of PNAG that acts as a polysaccharide intercellular adhesin (PIA) (C). A mature biofilm is a mixture of bacteria embedded in an extracellular matrix composed of proteins, nucleic acids and polysaccharides (D). Mature biofilms can then undergo a detachment process that will release planktonic bacteria that can then colonize another region of the host (E). Adapted from Microb Infect (2002), 4, 481-489.

Biofilm formation in *S. epidermidis* (see figure i.2) and also *S. aureus* is strongly associate with the production of Poly-N-Acetyl-Glucosamine (PNAG) [50,151], which is synthesized by the genes encoded in the *icaADBC* locus [51,88,137]. Biofilm formation (and other virulence factors) is controlled by a quorum-sensing system, that enables cell-to-cell communication, called staphylococcal accessory gene regulator (*agr*) [249]. The *agr* system has been found initially in *S. aureus,* but now it as also been described in *S. epidermidis* [177].

Objectives and outline of this thesis

The main objective of this thesis is to provide an insight into the properties that CoNS biofilm-grown cells present compared to their planktonic counterparts, evaluating the most important virulence factors of CoNS: biofilm formation and PNAG production. The first section addresses the topic of biofilm formation on clinical relevantly surfaces by clinical isolates of CoNS strains. In the second section, the topic of biofilm resistance to antimicrobial agents was addressed. Some aspects of the immune response to biofilm infections were also studied and are described in the third section. Molecular studies were also performed on the production and detection of the major *S. epidermidis* virulence factor, PNAG, and possible roles of the *icaB* gene in PNAG function, as described in the fourth section. The fifth and last section explores the presence and role of PNAG in several other important pathogens and the eventual relationship with staphylococcal PNAG.

The present thesis is divided in 5 sections that are then subdivided in chapters. Each section has an introduction, followed by some chapters, most of them being versions of scientific publications available for public reviewing.

Section I

Biofilms and Staphylococcus spp

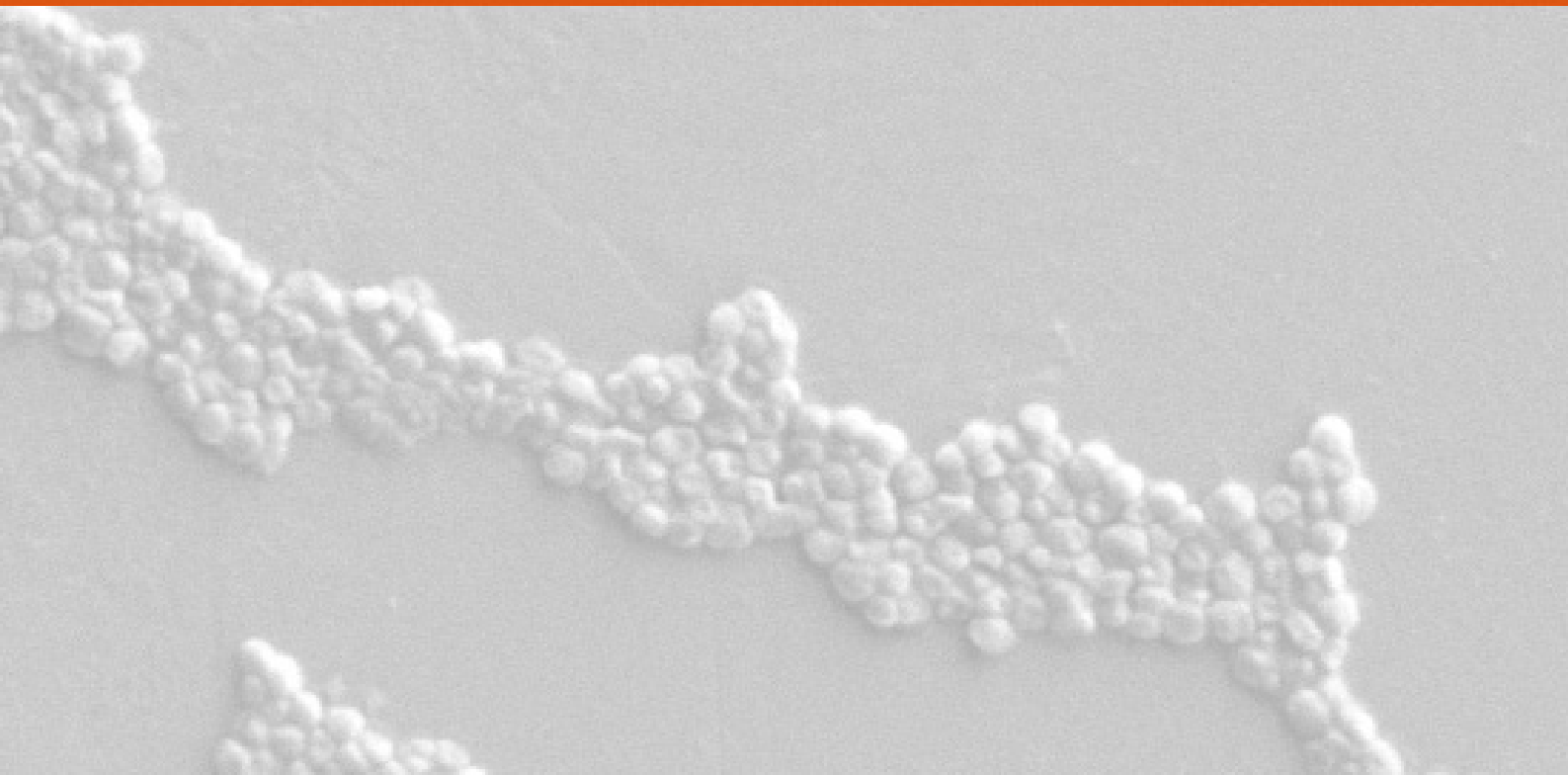

Section I cover image is a SEM observation with 1000x magnification of S. epidermidis 9142 adhered to acrylic. Centre of Materials, University of Minho, Braga, Portugal.

Introduction

The healthy human skin and mucous membranes represent the natural habitat of coagulase-negative staphylococci (CoNS) such as *Staphylococcus epidermidis* and *Staphylococcus haemolyticus* [236]. In predisposed hosts, usually with an indwelling medical device, CoNS have become significant nosocomial pathogens [124]. The major virulence factor associated with this organism's ability to cause infections is dependent on adhesion to medical devices and formation of a biofilm [236].

Acrylic is a polymer often used in the manufacture of medical implants like bone-cement, intraocular artificial lenses and cranioplastic implants [53] and adhesion to acrylic surfaces may contribute to serious clinical consequences like persistent and chronic infections [172].

Microbial adhesion to surfaces has been shown to be a complex process, involving physico-chemical [22,52,109,120], protein [30,85,156] and polysaccharide factors [32,63]. From an overall physico-chemical point of view, microbial adhesion can be mediated by non-specific interactions, with long-range characteristics, including Lifshitz-van der Waals forces, electrostatic forces, acid-base interactions, and Brownian motion forces [229]. As soon as microorganisms reach a surface, they will be attracted or repelled to it, depending on the sum of the different non-specific interactions [71] (see figure I). In biological systems, hydrophobic interactions are usually the strongest of all long-range non-covalent forces [20], and adhesion to surfaces is often mediated by these types of interactions [221]. It has been demonstrated that hydrophobicity plays an important role in a wide range of microbial infections [61]. Microbial hydrophobicity is defined by the energy of attraction between apolar or slightly polar cells immersed in an aqueous phase [230], and can be assessed by several methods, although, according to Doyle [61], the best method to determine bacterial hydrophobicity is by contact angle measurements.

A wide variety of experimental systems have been developed to study microbial adhesion to inert surfaces but there is no consensus as to which is most representative of the infectious process in a human. One of the simplest methods to study bacterial adhesion is the static adherence method [18]. In this method, a slide or similar piece of substratum such as a catheter is immersed in a microbial suspension and a batch adhesion process is allowed to occur. After exposure, the substratum is washed for removal of non-adherent bacteria and then adhering bacteria can be enumerated *in situ*. More elaborate methods are available for studying microbial adhesion, one of which, the parallel-plate flow chamber, is considered by many investigators to have important advantages [18]. With the parallel-plate flow chamber, adhesion to surfaces can be studied in a more controlled hydrodynamic environment, and more experimental parameters can be measured, such as the initial adhesion rate or the removal rate after passage of an air-liquid interface [22]. According to some authors, this type

of system provides a more accurate evaluation of bacterial adhesion than the static adhesion system, on account of the washing step required with the later method [18]. This washing procedure, required to remove non- or loosely adhered cells, strongly influences the adhesion results. Although this is a crucial step in static adhesion assays, most of the reported data result from adhesion assays performed under uncontrolled washing procedures.

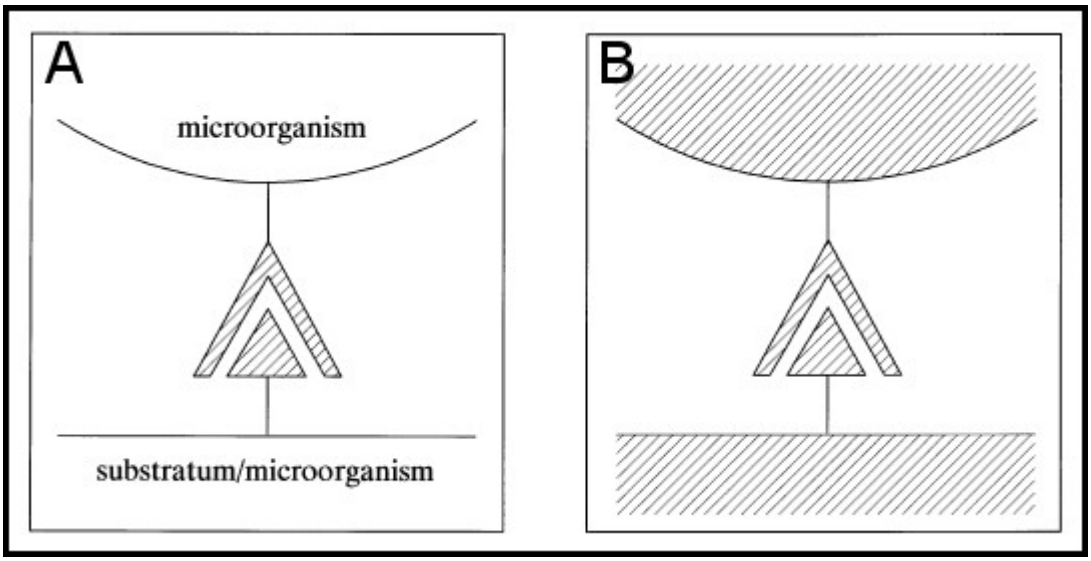

Figure I. Both specific (A) and non-specific (B) interactions originate from the same fundamental, physico-chemical forces. In the case of so called specific interactions, only those forces between highly localized, stereochemical molecular groups are considered, whereas the forces between the entire body of the interacting surfaces, whether microbial or not, constitute the so-called non-specific interaction. The shaded areas indicate the regions from where the interaction forces are assumed to originate. Adapted from FEMS Microbiol Rev (1999), 23:179-230.

After initial adhesion, mature biofilm formation is often associated with the production of specific molecules by the microorganisms that mediate cell-to-cell adhesion. In *S. epidermidis* a polymer of N-acetyl glucosamine, initially defined biologically as the polysaccharide intercellular adhesin (PIA) and chemically as Poly-N-acetyl-glucosamine (PNAG) has been identified as the molecule responsible for biofilm formation [41,88,151]. The PNAG molecule is synthesized by proteins encoded by genes contained in the *ica* locus [151]. PNAG is also involved in the agglutination of erythrocytes, which is a common property of *S. epidermidis* strains [136,195]. This characteristic can therefore be used to identify the presence of PNAG in a *S. epidermidis* strain by a hemagglutination assay.

Several different methods have been developed for testing biofilm formation [60] although most of them are based on a 1-day batch culture [88,90,134,135,154,158]. However, in clinical situations biofilms develop over a long period of time, in conditions hardly similar to batch systems [67]. While a 1-day batch culture is an easy and fast way to evaluate biofilm formation, this might not be the most accurate method to quantitatively compare biofilm

formation by a range of bacteria. Expression of PNAG, adhesion to synthetic surfaces and biofilm formation are virulence factors of *S. epidermidis* clinical strains and therefore these parameters should be evaluated using clinical isolates, and adequate experimental methods.

Comparative evaluation of coagulase-negative staphylococci (CoNS) adherence to acrylic by a static method and a parallel-plate flow dynamic method

Summary

In this first chapter, the study of the adhesion of several clinical strains of S. epidermidis and S. haemolyticus to inert surfaces, the first stage of biofilm formation, using both static and dynamic adhesion methods, is described. While static methods are easier to perform, recent discussions in the scientific community pointed out some disadvantages of static adhesion assays. The advantages and disadvantages of these 2 methods were first compared. S. epidermidis adhesion, assessed by both methods, was greater than that of S. haemolyticus. It was found that the simple static method, when performed using an accurate washing procedure, could be as useful as the dynamic flow method for assessing differences in the adherence of strains. Although the dynamic flow method yielded more overall information, its greater complexity and cost may not always justify its use for certain experimental comparisons.

Part of the work described in this chapter was published in 2004, in Research in Microbiology, 155:755-760

1.1. Experimental procedure

1.1.1. Bacterial strains

In this work, 5 *S. epidermidis* strains and 2 *S. haemolyticus* strains were used: *S. epidermidis* 9142, 9142-M10, IE75, IE186, M187, *S. haemolyticus* M176 and IE246. Detailed information about these strains is present in the supplements section, page 179.

1.1.2. Media and growth conditions

Tryptic soy broth (TSB) and tryptic soy agar (TSA) were prepared according to the manufacturer's instructions. All strains were incubated in 15 ml of TSB inoculated with bacteria grown on TSA plates not older than 2 days, and grown for 24 (± 2) H at 37ºC in a shaking rotator at 130 rpm. Then, 200 µl of each cell suspension was transferred to 150 ml of fresh TSB, which was incubated for 18 (± 2) H at 37ºC, at 130 rpm. After being harvested by centrifugation (for 5 min at 10,500 g and 4ºC), cells were washed twice and resuspended in a saline solution (0.9% NaCl prepared in distilled water).

1.1.3. Substrate preparation

Acrylic was cut into 2 cm x 2 cm squares (for static method) or into 7.6 cm x 5 cm plates (for dynamic method). These substrata were immersed in a 0.2% solution of a commercial detergent overnight, after which they were transferred to a new solution of 0.2% of a commercial detergent and washed in warm water with strong agitation for 5 min. The squares and plates were then well rinsed with distilled water and finally each individual substratum was well rinsed with ultra-pure water and dried at 60ºC, overnight.

1.1.4. Static adhesion methods

1.1.4.1. Optimization of the adhesion assays

In order to ascertain the influence of the initial inoculum to the amount of adhered cells, adhesion was allowed to occur during 30 min using different cell concentrations. In order to determine the influence of the adhesion time on the amount of adherent bacterial cells, adhesion was allowed to occur for different times, using a standard cell concentration.

To evaluate the effect of the washing step, 3 approaches were considered: no washing, washing by multiple immersions in water and finally washing by rinsing with a spurt of water. When using the immersion method, the acrylic surfaces were gently transferred to 100 ml glass beakers containing distilled water, and were allowed to rest there for approximately 10 s. Next, the surfaces were transfered to a different 100 ml glass beaker with distilled water, followed by a third transfer 10 s later. In the other method, the substrate surfaces were

carefully removed from the adhesion medium and were rinsed with a spurt of distilled water for approximately 20 s. After the washing steps, all surfaces were allowed to dry at 60ºC.

S. epidermidis 9142 was selected as the strain to be used in all the optimization assays, since it is a strain already used in other works [136,137].

1.1.4.2. Static adhesion

Squares of acrylic were placed in 6 well polystyrene tissue-culture plates containing 5 ml of a cell suspension at an optimal concentration in saline solution (see table 1.1). Initial adhesion to each substratum was allowed to occur during the optimal adhesion time (see table 1.1) at 37ºC, in a shaker at 120 rpm. Negative controls were obtained by placing acrylic in a saline solution without bacterial cells. The squares were then carefully washed by immersion. The substratum squares with adhered cells were dried at 60ºC. All experiments were done in triplicate, with 4 repeats.

1.1.4.3. Image analysis

For image observation and enumeration of adherent bacterial cells, the substratum squares were stained with a 0.2% safranin solution. Direct bacterial counts were done using a phase contrast microscope coupled to a 3CCD video camera that acquires images with 820×560 pixels resolution at a magnification of 400×. With this magnification 1cm^2 is equivalent to 1.823×10^4 captured images (as determined by a Neubauer chamber). For each surface analyzed, 20 images were taken. Images were processed using the software Sigma Scan Pro, as illustrated on figure 1.1. For each surface analyzed a background image was acquired (1.1.A). This image was used to subtract the noise from the images containing the adhered bacteria (1.1.B) resulting in clean image with a uniform background (1.1.C). The software analyzes the intensity of the pixels and sets the optimal greyscale threshold to quantify the amount of black pixels (1.1.D) representing adhered bacteria. With the use of a Neubauer chamber the average pixel size of 1 bacteria was determined using more than 100 measurements from several independent surfaces.

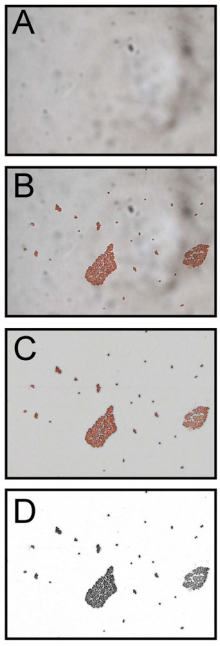

Figure 1.1. Image analysis procedure using the software Sigma Scan Pro.

1.1.5. Dynamic adhesion methods

1.1.5.1. The parallel-plate flow chamber and image analysis

The parallel-plate flow chamber and image analysis system has been previously described [18]. Briefly, images were taken from the center of the bottom of the plate, with a CCD video camera mounted on a phase-contrast inverted microscope equipped with a 40× ultra-long working distance objective. Images containing 768×576 pixels were acquired by the image analysis software. Each 10 s 1 image was obtained by adding 5 consecutive images captured with a time interval of 500 ms in order to eliminate moving bacteria and to enhance the signal-to-noise ratio. At the magnification used, $1cm^2$ is equivalent to 3.148×10^4 captured images (as determined with a Neubauer chamber).

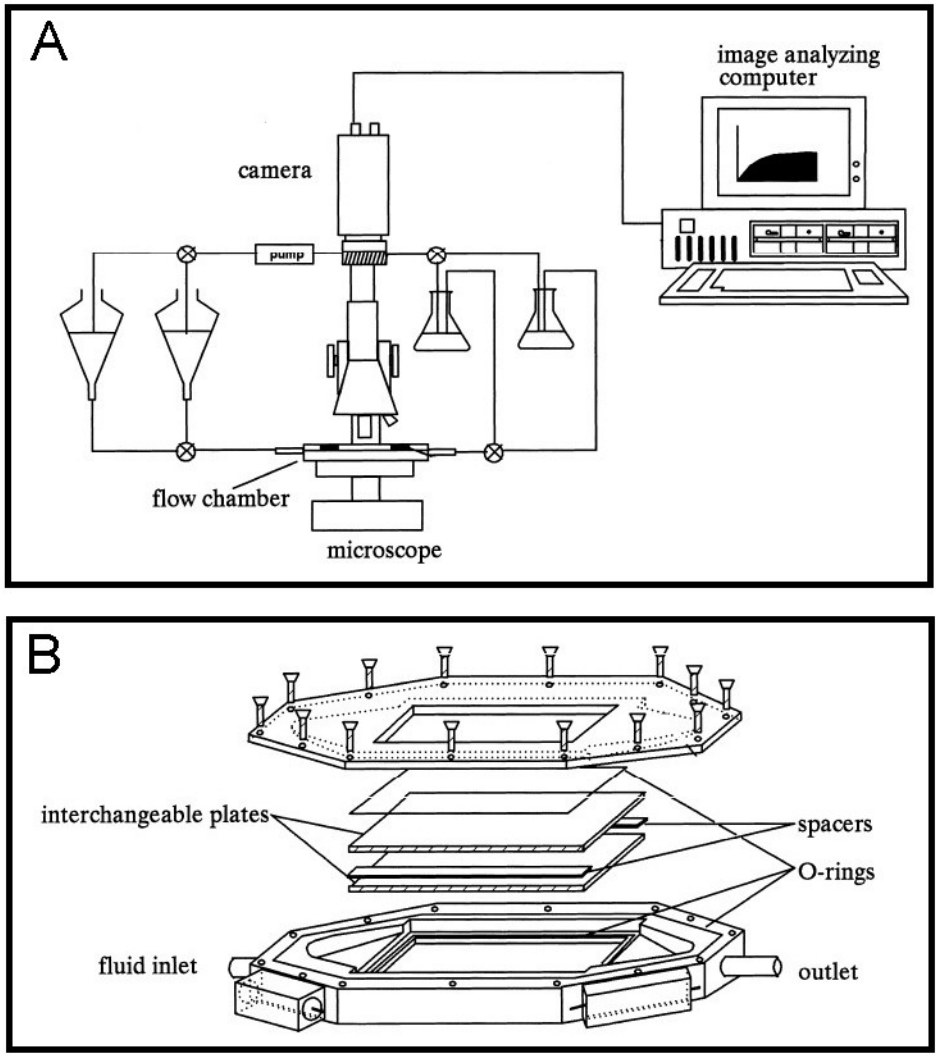

Figure 1.2. Schematic overview of the parallel plate flow chamber system used in the study described in this chapter (A) and detailed view of the chamber it self (B). Adapted from FEMS Microbiol Rev (1999), 23:179-230.

1.1.5.2. Dynamic adhesion

Prior to each experiment, all tubes and the flow chamber were filled with a saline solution with special attention to removing all air bubbles from the system. A saline solution was circulated through the system until the stationary operation conditions were obtained (0.18 ± 0.02 ml/s), which yields a laminar flow (Reynolds number of 4.8 ± 0.6). A pulse-free flow was established by hydrostatic pressure, and the suspension was recirculated using a peristaltic roller pump. Afterwards, the flow was switched to the bacterial suspension (at the same concentration used in the static assays) that was circulated trough the system at room temperature for 60 min while images were captured with a time interval of 10 s. After the enumeration of adhering bacteria, an air-liquid interface was passed through the system and the amount of cells removed was determined. Besides the determination of adherent bacteria at a stationary end-point, the initial deposition rate was also calculated during the first minutes of the adhesion assays. All experiments were done at least 4 times, with independent cultures.

1.2. Results

1.2.1. Optimization of the adhesion assays

A summary of the optimization of the static adhesion parameters is presented in table 1.1. When no washing step was performed, the number of adherent cells was found to be constant at different adhesion times. On the other hand, when using immersion or rinsing washing procedures, the number of adherent cells increased with increasing adhesion times (as illustrated on figure 1.3). However, only using washing by immersion was this increase found to be significantly different at the $p<0.05$ level (ANOVA and Tukey's multiple comparison test).

As expected, a lower initial cellular concentration yielded a lower number of adherent organisms but interestingly, the differences in adherent organisms over a broad range of initial inocula were not large. Clearly there is a maximum number of bacterial cells that can adhere to the substrate, as shown by the similar level of adhesion achieved by a cell suspension with an initial OD_{640nm} of 1.5 compared with another suspension with an initial OD_{640nm} of 2.4.

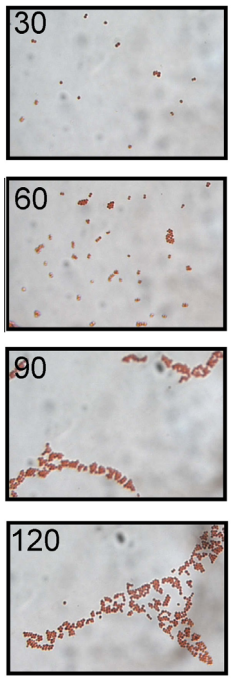

Figure 1.3. *S. epidermidis* 9142 adhesion to glass at 30, 60, 90 and 120 min.

When comparing the number of adherent cells after different exposure times, it was verified that lower exposure times yielded a lower level of adherent cells (2.3×10^6 cells/cm^2 after 30 min of exposure and 4.2×10^6 cells/cm^2 after 90 min of exposure). The plateau was attained at 120 min of exposure, as there was no significant increase in adherence at the $p<0.05$ level (ANOVA and Tukey's multiple comparison test) after 150 min of exposure (4.6×10^6 cells/cm^2 and 4.5×10^6 cells/cm^2, respectively).

Table 1.1. Optimization of the static adhesion parameters.

Adhesion Time (min) [(a)]	10^6 cell/cm^2	Initial inoculum (b)	10^6 cell/cm^2
15	1.2 (±0.3)	0.1	0.3 (±0.2)
30	2.3 (±0.2)	0.4	0.7 (±0.2)
60	3.6 (±0.4)*	1.0 #	1.3 (±0.2)*
120	4.6 (±0.5)	1.8 #	2.1 (±0.2)
180	4.6 (±0.4)	2.4 #	2.2 (±0.3)

Washing step (c)	Adhesion time (min)	10^6 cell cm^{-2}
None	20	35.2 (±5.7)
	40	36.4 (±9.9)
Immersion	20	1.2 (±0.3)*
	40	2.3 (±0.4)*
Rinsing	20	0.6 (±0.5)
	40	0.9 (±0.5)

(a) Influence of the adhesion time on the amount of adhered cells. A standard inoculum was used with an OD_{640nm} of 2.0 (diluted 4 fold, measured 0.5 at 640 nm); (b) Influence of the initial cell density in the amount of adhered cells (cell densities described above 0.8 (#) were diluted 4 fold as measured at 640 nm); (c) Influence of the washing steps at different times of adhesion in the amount of adhered cells. The SD is between brackets. * represents a mean difference significant at the $p<0.05$ level (ANOVA and Tukey's multiple comparison test).

1.2.2. Comparison of static with dynamic adhesion

A summary of the adhesion parameters using both methods is presented in table 1.2. A linear relation was obtained between the adhesion levels (in 10^6 cell/cm^2) in the dynamic method (D) and the static method (S): $D = 3.4011 \times S + 5.6288$, $r = 0.9555$. When using the static method the only information that can be obtained is the amount of cells adherent at the end of the assay. When using the dynamic method, more information is available.

As it can be seen in figure 1.4, the 3 strains were representative of the distinct behaviors observed, reached a maximal adhesion phase very quickly (less than 30 min) compared with 120 min using the static method. Furthermore, the number of adherent bacterial cells with the dynamic method was almost 10 fold higher than the adhesion achieved in the static method ($p<0.05$, paired samples t-test). The results obtained by the static adhesion method revealed

that *S. epidermidis* strains adhered at higher extents to acrylic than *S. haemolyticus* strains (table 1.2).

Table 1.2. CoNS adhesion to acrylic in both dynamic and static methods.

Strain	Dynamic method			Static method
	j_0 (a)	n_{30min} (b)	d % (c)	n_{120min} (d)
S. epidermidis 9142	7.2 (±1.2)	36.8 (±7.4) *	91 (± 5)	4.5 (±0.5)
S. epidermidis 9142-M10	9.3 (±1.3)	40.2 (±4.7) *	82 (± 11)	4.8 (±3.8)
S. epidermidis IE75	5.9 (±0.9)	23.4 (±5.1)	87 (± 12)	2.2 (±0.7)
S. epidermidis IE186	12.2 (±0.9)	44.3 (±4.0) *	80 (± 12)	5.2 (±1.9)
S. epidermidis M187	10.7 (±0.2)	40.4 (±5.9) *	79 (± 3)	4.6 (±1.4)
S. haemolyticus IE246	3.5 (±0.5) *	14.4 (±1.4)	89 (± 7)	2.6 (±0.5)
S. haemolyticus M176	3.3 (±0.6) *	17.1 (±1.9)	91 (± 7)	3.1 (±1.1)

(a) Initial adhesion rate (j_0, 10^4 cell/cm^2 s^1); (b) number of adhered bacteria at stationary deposition phase (n_{30mi}n, 10^6 cell/cm^2); (c) percentage of detached bacteria by passing an air-bubble through the chamber; (d) number of adhered bacteria at stationary deposition phase (n_{120min} ,10^6/cm^2). The SD is between brackets. * represent a mean difference significant at the $p<0.05$ level (ANOVA and Tukey's multiple comparison test)

The only exception was *S. epidermidis* IE75 that adhered at the same level of *S. haemolyticus* IE246 and *S. haemolyticus* M176 (2.2×10^6 cells/cm^2, 2.6×10^6 cells/cm^2 and 3.1×10^6 cells/cm^2 respectively). With the dynamic adhesion assay, the extent of adherence of most of the *S. epidermidis* strains were again significantly different ($p<0.05$, ANOVA and Tukey's multiple comparison test) from the *S. haemolyticus* strains, when comparing the adhesion achieved at the stationary phase.

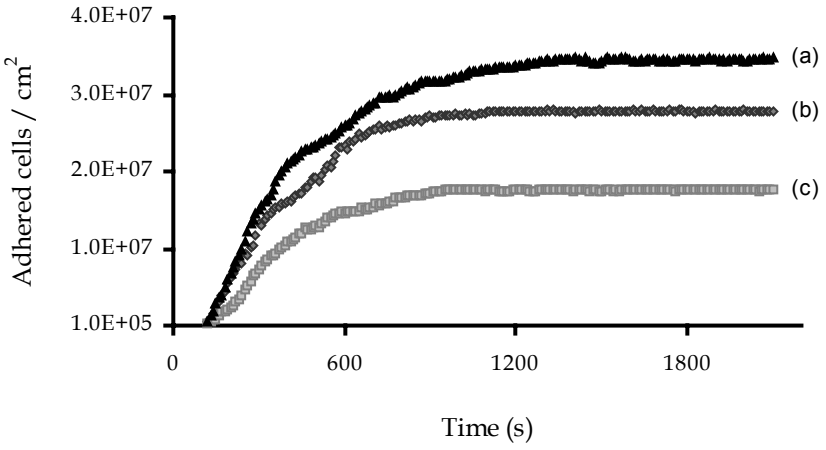

Figure 1.4. Adherence kinetics of *S. epidermidis* 9142 (a), *S. epidermidis* IE75 (b) and *S. haemolyticus* M176 (c) using the dynamic parallel flow chamber assay.

Regarding the comparison of the initial adhesion rates, *S. haemolyticus* strains had the slowest rates, significantly different from the rates of the *S. epidermidis* strains ($p<0.05$, ANOVA and Tukey's multiple comparison test). The effect of passing an air-bubble through adherent cells in the parallel plate flow chamber resulted in removal of a large proportion of the adherent organisms. This can be explained by the formation of an air-liquid interface, that induces a shear force of about 10^{-7} N, which is in the range of the adhesion strength evaluated by atomic force microscopy [68].

1.3. Discussion

Many investigators have evaluated the adherence of bacteria such as CoNS to polymers and medical devices to understand the processes of colonization and biofilm formation [2,85,176]. However, comparisons of the parameters used that would be important in evaluating the results achieved, such as the amount of the inoculum, incubation period and washing procedure are not fully discussed in the literature. Additionally, there is a lack of detailed studies comparing both the static and the dynamic methods of assessing initial adhesion. In the study described in this chapter several critical parameters that could affect the outcome of adherence assays were evaluated in order to provide insights into which steps of this process are affected by variations in experimental conditions.

In the present case, when no washing step was used, a great number of adherent bacterial cells were obtained. Furthermore, without washing, there was no difference between levels of adherent cells regardless of the exposure times to the substratum. Probably the cells enumerated include those that adhered, plus the loosely attached cells and the cells deposited by sedimentation. While it might seem obvious that some washing must occur to discriminate effectively adherent from merely deposited cells, the findings without washing point out the need for defining a proper set of washing conditions to accurately gauge and compare among different experimental conditions the number of adherent cells on a substratum.

When further comparing the 2 distinct washing procedures, both of which are described in the literature [4,10,151], it was found that adhesion levels determined by both methods were different for each time of exposure evaluated, demonstrating the importance of choosing an adequate method to remove non-adherent cells when using static adhesion assays. Moreover, both methods revealed an increase on the number of adherent cells with increasing time of exposure. Washing by immersion was considered to be more reliable since it is more reproducible. Moreover, the spurt method is subjected to variations dependent on the operator since the amount and flow of water used will most probably vary between repeated experiments. Based on the methodological investigations, a static adherence assays along

with the immersion method of washing the surfaces, were used to compare bacterial adherence after 2 H, a time found to yield maximal adherence. The initial cell suspension had a concentration equivalent to 1×10^9 cells/ml, which was found to be the "breakthrough concentration", in the sense that it corresponds to the highest level of adherence with the lowest input inoculum.

A clear difference was found when comparing the extent of adhesion of *S. epidermidis* with *S. haemolyticus*, with most *S. epidermidis* adhering in a greater extent than *S. haemolyticus* strains. This was also seen in the 3 parameters measured with the dynamic method: generally, *S. epidermidis* has a higher initial rate of adherence, reached higher cell densities in the stationary phase of adhesion which was also attained sooner; and they were more resistant to removal after passing an air-bubble through the parallel plate flow chamber. Although the static method allows only 1 parameter to be measured (the number of adhering cells at the stationary point), it was also found that *S. epidermidis* generally adheres to a larger extent to acrylic than *S. haemolyticus*.

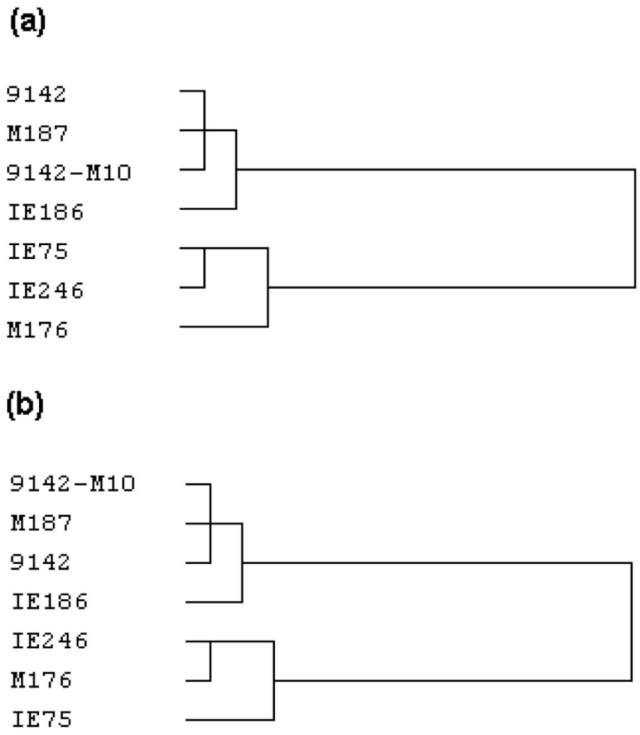

Figure 1.5. Hierarchal Cluster analysis based on squared Euclidean distances of (a) static adhesion assays and (b) dynamic adhesion assays.

On account of that, 2 hierarchal cluster analyses, based on squared Euclidean distances, were performed as described by Bosch *et al.* [19] using the data from static and dynamic adhesion assays. From both cluster analysis (figure 1.5), 2 distinct groups could be identified: both *S. haemolyticus* strains and *S. epidermidis* IE75 belong to the same group,

showing the lowest extent of adhesion; the remaining *S. epidermidis* strains belong to another distinct group, displaying the greatest number of adhered cells.

With the dynamic method, adherence was almost 10 fold higher than that achieved with the static method. This can be explained by the differences in the transport phenomena in the 2 methods. With the static method, transport of bacteria is by diffusion only, while with the dynamic method, in addition to diffusion, there are also convection phenomena [156] that could contribute to bacterial accumulation. It has been demonstrated previously that the transport phenomena involved in adhesion processes greatly influence the adhesion extent [13].

It has been suggested that, since the slide method would always be affected by the air-liquid interface in the washing and drying processes, this method evaluates the retention of cells rather than adhesion [18], i.e. the ability to adhere to a surface and to resist shear forces that exist in many natural environments [22,29,30]. However, the effect of the air-liquid interface varies and is dependent on the substratum properties, cell surface properties and the velocity of the passing air-bubble [33,81]. It has been demonstrated that the passage of an air-liquid interface through a lawn of adherent bacteria can detach some of the cells [81], although this effect is attenuated in the presence of a more hydrophilic substrate or with more rapid washing of adherent cells [82]. In a previous study [52], several different washing procedures were assayed and the effect of each was evaluated as reported by Suárez *et al*. [81]. The results obtained suggested that when using hydrophilic glass no effect is observed from the different washing procedures. Conversely, for the hydrophobic acrylic substrate, an effect was sometimes observed, but attenuated by rapid washing to minimize the time of exposure of the adherent cells to an the air-liquid interface. In the study described in this chapter, the washing procedure was performed carefully in order to avoid the formation of an air-liquid interface.

Overall, the results obtained in the present work suggest that both static and dynamic methods are equally valid to compare adhesion behaviors among CoNS clinical strains. The linear relation obtained between adhesion levels in both the dynamic method and the static method had a very high correlation ($p<0.05$). Additionally, the cluster analysis performed using either static or dynamic adhesion results yielded the same 2 distinct groups, differentiating the strains by their adhesion capabilities. For instance, the high capacity of adhesion of *S. epidermidis* IE186 compared to any of the *S. haemolyticus* can be detected by both static and dynamic methods. Although dynamic methods do provide more information, the ease and practicality of a well-defined static method can also be useful for discerning differences among CoNS strains in regard to their adherence ability.

Summarizing, a static adhesion method can be used for evaluating differences in adhesion capabilities, even if it can only provide information about the final level of adherence achieved. Since it is a low cost method that is very easy to perform and less-time consuming, the slide static adherence method has some advantages over the dynamic parallel-plate flow chamber method, such as evaluating adherence capability of a high number of strains. The dynamic adhesion assay using the parallel-plate flow chamber is more time consuming and needs more expensive equipment, and is thus more appropriate to study fundamental aspects of adhesion with a limited number of strains, as has been demonstrated by many authors [81,155,191].

Influence of batch or fed-batch growth on S. epidermidis biofilm formation

Summary

After addressing initial adhesion to surfaces in the previous chapter, the work described in this second chapter aims at studying biofilm formation and maturation using batch or fed-batch systems. Dry-weight measurements of biofilms formed in batch and fed-batch conditions were compared with hemagglutination titers, which is an indirect measure of the amount of PNAG produced. The results revealed that strains grown in batch systems developed less biofilm than when grown in fed-batch systems and a good correlation between the amount of biofilm formed and the hemagglutination titters was only found with the fed-batch system. Differences in biofilm formation and PNAG production by S. epidermidis were proved to be dependent on the availability of nutrients, with higher availability correlating with more biofilm and PNAG production. These results may explain some disparity of conclusions among different investigations where different systems of biofilm formation were used and stress the importance of choosing an appropriate system to study biofilm formation.

Part of the work described in this chapter was published in 2004, in Letters in Applied Microbiology, 39:420-424.

2.1. Experimental procedures

2.1.1. Bacteria strains

S. epidermidis strains used in this work were: *S. epidermidis* 9142, 9142-M10, FJ6, JI6, LE7 and PE9. Detailed information about these strains is presented in the supplements section, page 179.

2.1.2. Media and Growth conditions

TSB and TSA were prepared according to the manufacturer instruction. Physiological saline was prepared adding 0.9% of NaCl to distilled water.

All strains were incubated in 15 ml of TSB inoculated from TSA plates not older than 2 days, for 24 (± 2) H at 37ºC with agitation of 130 rpm, in an orbital shaker. Then, 50 µl were transferred to 30 ml of fresh TSB, and allowed to grow for 18 (± 2) H, at 37ºC with agitation of 130 rpm, before cells were harvested by centrifugation for 5 minutes at 10,500 g and 4ºC. Cells were then resuspended in physiological saline at a density of approximately 1×10^9 cells/ml.

2.1.3. Surface preparation

Acrylic was cut into 2 cm x 2 cm surfaces and then immersed in a 0.2% commercial detergent solution overnight, after which the surfaces were transferred to a new 0.2% commercial detergent solution and washed in warm water with strong agitation for 5 min. The detergent was removed by thoroughly rinsing with distilled water. Finally, each individual surface was rinsed thoroughly with ultra-pure water and sterilized by immersion in a flask filled with distilled water and autoclaved for 15 min at 121 ºC.

2.1.4. Biofilms formed in batch mode

Sterilized acrylic surfaces were inserted in each well of 6 well polystyrene tissue culture plates containing 5 ml of TSB supplemented with 0.25% of glucose. Then 20 µl of a 0.9% NaCl solution containing 1×10^9 bacterial cells/ml was added and growth was allowed to occur during 24 or 72 H, at 37ºC, in a shaker at 120 rpm. Negative controls were obtained by incubating the surfaces in TSB supplemented with 0.25% glucose without adding any bacterial cells. All experiments were done in quadruplicate with 3 repeats.

2.1.5. Biofilms formed in fed-batch mode

Biofilms were formed on sterilized acrylic surfaces as described above, except that at every 12 H the TSB medium containing suspended bacterial cells was removed and an equal volume of fresh TSB with 0.25% of glucose was added. Negative controls were obtained by

incubating the surfaces in TSB with 0.25 % glucose without adding any bacterial cells. All experiments were done in quadruplicate with 3 repeats.

2.1.6. Biofilm dry-weight determination

Biofilm dry-weight determinations were performed as previously described [4] with some modifications. Briefly, the colonized surfaces were removed from the plates and placed at 80ºC, overnight. Then the weight of the surface was determined on a digital scale. Surfaces were placed again at 80ºC for 2 H, and weighed again, to check the stability of the dry weight. Then, the biofilm was mechanically removed from the surface, and the surfaces were thoroughly cleaned with 0.2% commercial detergent solution. Cleaned surfaces were kept overnight at 80ºC, prior to a third weight determination. The difference in the weight of the surface with and without the biomass attached is the biofilm dry-weight. Figure 2.1 shows an acrylic surface after dry-weight determination.

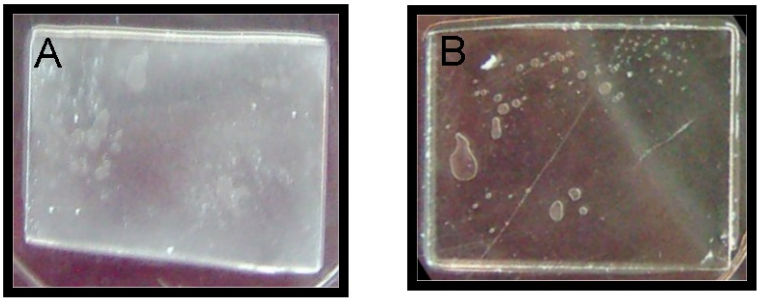

Figure 2.1. Image of an acrylic plate washed 3 times in distilled water, after 72 H of growth of a biofilm forming strain (A) or biofilm negative strain (B).

2.1.7. Hemagglutination assays

The hemagglutination assays were performed as previously described [195] with some modifications. Briefly, a *S. epidermidis* biofilm was formed in 96 well (U-shaped) polystyrene microtiter plate for 24 H, at 150 rpm and 37ºC, in TSB supplemented with 0.25% glucose. Planktonic cells were then removed and the biofilm was scraped from the surface and resuspended in saline, followed by sonication (20 W, 20 s) to disrupt the cell aggregates. The cell density was then adjusted to a concentration of approximately 3×10^9 cells/ml. Five 2-fold dilutions of each cell suspension were made (100 μl) in 96 well (U-shaped) polystyrene microtiter plates. Then 100 μl of a 1% horse erythrocyte solution was added to each well. To ensure thorough mixing of the bacteria and erythrocytes, the total volume of each well was pipetted in and out with a micropipette. Incubation was at room temperature for 2 H, and

hemagglutination titters were evaluated macroscopically. All experiments were done in duplicate with 3 repeats.

2.2. Results

2.2.1. Biofilm formation

Table 2.1 presents the amount of biofilm formed in the 3 conditions assayed in the study described in this chapter. The PNAG-negative control strain 9142-M10 hardly formed any biofilm, whereas the parental PNAG-positive control strain, 9142, formed biofilms in all conditions assayed. In batch mode, for all 4 isolates, there was a slight increase in the dry weight of the biofilm after 72 H compared with 24 H ($p<0.05$, paired t-test). With this method, no significant differences ($p>0.05$, ANOVA and Tukey's multiple comparison test) were found in the abilities of the 4 strains to form biofilms. However, when the fed-batch approach was used, in addition to producing more biofilm, significant differences ($p<0.05$, ANOVA and Tukey's multiple comparison test) were found among the isolates, with both strains JI6 and PE9 producing more biofilm than strains FJ6 and LE7, as did the positive control strain 9142.

Table 2.1. Biofilm formation on acrylic under the different conditions used, in μg biofilm mass/mm^2 of acrylic.

Strain	24 H batch	72 H batch	72 H fed-batch
9142	1.5 (± 0.4)*	4.9 (± 1.4)*	16.8 (± 4.5) **
9142 – M10	0.2 (± 0.1)	0.5 (± 0.2)	1.2 (± 0.5)
FJ6	2.6 (± 0.4)*	4.2 (± 1.2)*	5.6 (± 2.2)
JI6	2.1 (± 0.4)*	3.6 (± 1.4)*	10.2 (± 2.3) **
LE7	1.9 (± 0.4)*	3.8 (± 1.3)*	4.2 (± 2.3)
PE9	2.5 (± 0.4)*	5.6 (± 1.0)*	12.4 (± 4.8) **

(* 24 H batch is significantly different from 72 H batch ($p<0.05$, paired t-test); ** significantly higher biofilm formation compared with other strains grown under the same conditions, ($p<0.05$, ANOVA and Tukey's multiple comparison test).

2.2.2. Hemagglutination titter

Table 2.2 presents the hemagglutination titters of the 4 *S. epidermidis* isolates and also the 2 control strains. The biofilm positive control strain had a hemagglutination titter of 1:8, indicating that 3.7×10^8 cell/ml caused visible agglutination of horse erythrocytes. On the other hand, the biofilm negative control strain was not able to agglutinate horse erythrocytes.

All 4 *S. epidermidis* isolates were able to cause hemagglutination. PE9 was most efficient at causing hemagglutination, since only 3.7×10^8 cell/ml were needed to agglutinate horse erythrocytes. Conversely, strain LE7 and JI6 were the least efficient strains at causing hemagglutination since at least 3.0×10^9 cell/ml were needed to agglutinate horse erythrocytes.

A linear regression analysis was undertaken to compare the amount of biofilm formed under different growth conditions and the hemagglutination titters. The correlation coefficient

(r) between hemagglutination titer and biofilm mass for biofilms formed in batch mode and grown for 24 or 72 H were 0.28 and 0.78, respectively, whereas the correlation between hemagglutination and biofilm mass for fed-batch biofilms was 0.94.

Table 2.2. Hemagglutination titers of the *S. epidermidis* strains.

Strain	Hemagglutination titters
9142	1:8
9142-M10	No hemagglutination
FJ6	1:1
JI6	1:8
LE7	1:1
PE9	1:8

2.3. Discussion

Results from some investigations into the ability of *S. epidermidis* strains to form biofilms on inert surfaces, and correlations with production of surface factors have been published [51,98]. However, there is not always agreement among the conclusions regarding biofilm formation, likely because of use of different systems by different investigators to form biofilms [98,162,185]. Thus, in order to make meaningful comparisons among different studies, it is important to determine which methodological differences can account for apparently disparate results.

In the study described in this chapter, the amount of biofilm formed on acrylic using distinct growth conditions was compared and these findings were correlated with the hemagglutination titer, a measure of the production of PNAG [136]. Since biofilms formed *in vivo* in an infected host develop over a long period of time, and biofilm properties change with age [162], it was hypothesized that changes in availability of nutrients over time could influence the amount of a *S. epidermidis* biofilm. When biofilms were formed under batch mode, the amount of biofilm slightly increased with the biofilm age. However no statistically significant differences were found between the amount of biofilm formed among the isolates strains. Also, the correlation between biofilm biomass and hemagglutination titer was low. Conversely, in the fed-batch systems, there was a higher amount of biofilm formed compared with the batch mode and clear differences in the amount of biofilm produced among strains were obtained ($p<0.05$, ANOVA and Tukey's multiple comparison test). Thus, the fed-batch system revealed differences in biofilm formation that were not apparent with the standard batch system. A strong linear relation was found between fed-batch biofilm formation and hemagglutination titers, indicating in this system PNAG may have made more of a contribution to formation of the biofilm compared with its contribution in the standard batch system.

Overall, in comparing biofilm biomass production by *S. epidermidis* in a standard batch system to a fed-batch system, produced by adding fresh medium, biofilm formation occurred

to a greater extent in the latter system and correlated with the amount of PNAG produced. These findings indicate that attention must be taken in choosing the growth method used to measure biofilm production by *S. epidermidis* in order to make meaningful comparisons among different investigations. Biofilm formation by medically relevant *S. epidermidis* is used in many studies, including those looking for molecular and cellular correlates of biofilm formation [51,75,88] concerning prevention of biofilm formation by antimicrobial agents [196] or to evaluate some host immune factors [156]. Since many of these studies attempt to evaluate the role of PNAG in the pathogenesis of infection and in biofilm-formation properties, the use of static-batch systems may not be suitable. Alternately, a fed-batch system for making comparisons among strains in their abilities to form biofilms may be more relevant to studies evaluating a role of PNAG in this process. Most importantly, studies reporting differences in a role of PNAG in biofilm formation, occurrence and role in pathogenesis may be strongly influenced by several factors such as those related to growth medium and availability of nutrients. Careful attention and standardization of the biofilm formation mode will be highly useful for making proper comparisons among different investigations evaluating a role for PNAG and biofilm in the pathogenesis of *S. epidermidis* infection.

Chapter 3

Quantitative analysis of adhesion and biofilm formation on hydrophilic and hydrophobic surfaces of clinical isolates of S. epidermidis

Summary

While is has been proposed that biofilm formation has 2 distinct phases, it was not well established if adherence and biofilm formation were closely linked phenotypes for clinical isolates. This current chapter describes the results of the initial adhesion to different materials (acrylic and glass) of 9 clinical isolates of S. epidermidis, along with biofilm positive and biofilm negative control strains. Furthermore, the maturation of biofilms of the same 11 strains both on glass and acrylic was also tested. The methodology used to assess adhesion and biofilm formation was described in the 2 previous chapters. The clinical isolates exhibited different cell surface physico-chemical properties, resulting in different abilities to adhere to inert surfaces. The adhesion to hydrophobic substrata, for all strains, occurred to a larger extent compared with hydrophilic surfaces. Bacterial cell hydrophobicity seemed to have little or no influence on adhesion. No direct relationship was found between the amount of biofilm formed and the initial adhesion level. All strains forming biofilms were able to agglutinate erythrocytes, indicating a relationship between biofilm maturation and PNAG production. These results indicate that high levels of initial adherence do not necessarily lead to thick biofilm formation.

Part of the work described in this chapter was published in 2005, in Research in Microbiology, 156:506-514

3.1. Materials and Methods

3.1.1. Bacterial strains

The *S. epidermidis* strains used in this work were: 9142, 9142-M10, IE75, IE186, IE214, M129, M187, FJ6, JI6, LE7 and PE9. Detailed information about these strains is presented in the supplements section, page 179.

3.1.2. Media and Growth conditions

TSB and TSA were prepared according to the manufacturer's instructions. All strains were grown for 24 (± 2) H at 37ºC in a shaker rotating at 130 rpm in 15 ml of TSB using bacteria grown on TSA plates not older than 2 days as inocula. Then, 50 μl of each cell suspension was transferred to 30 ml of fresh TSB, which was incubated for 18 (± 2) H at 37ºC at 130 rpm. After being harvested by centrifugation (for 5 min at 10,500 g and 4ºC), cells were washed twice and resuspended in saline (0.9 % NaCl prepared in distilled water) at a concentration of approximately 1×10^9 cells/ml, determined by the OD_{640nm}. These cell suspensions were used in the subsequent adhesion and surface characterization assays.

3.1.3. Substrate preparation

Glass was obtained by slicing microscope slides into 2 cm x 2 cm squares. Acrylic was also cut into 2 cm x 2 cm squares. These substrates were immersed in a 0.2% solution of a commercial detergent overnight, after which they were transferred to a new solution of 0.2% of the commercial detergent and washed in warm water with strong agitation for 5 min. The squares were then well rinsed with distilled water, and finally each individual square was well rinsed with ultra-pure water and dried at 60ºC, overnight.

3.1.4. Physico-chemical characterization of surfaces

3.1.4.1. Bacterial hydrophobicity assay

The method used for measuring contact angles on bacterial lawns has been described by Busscher *et al.* [33]. Briefly a suspension of *S. epidermidis* cells in saline solution was deposited onto a 0.45 μm cellulose filter by first washing the filter with 10 ml of distilled water for wetting, and then 20 ml of the cell suspension was added, obtaining a thick lawn of cells after filtration. The lawn of cells was then air dried for at least 3.5 H, until the so call "dried-plateau" was obtained. The hydrophobicity parameters were obtained using the sessile-drop contact angle technique, using an automated contact angle device [33]. Contact angles (see figure 3.1) were standardized using as reference liquids: water, formamide and α-bromonaphtalene. Contact angles were related to the surface hydrophobicity as reviewed by Azeredo and Oliveira [11]. All experiments were done in duplicates, and with 4 repeats.

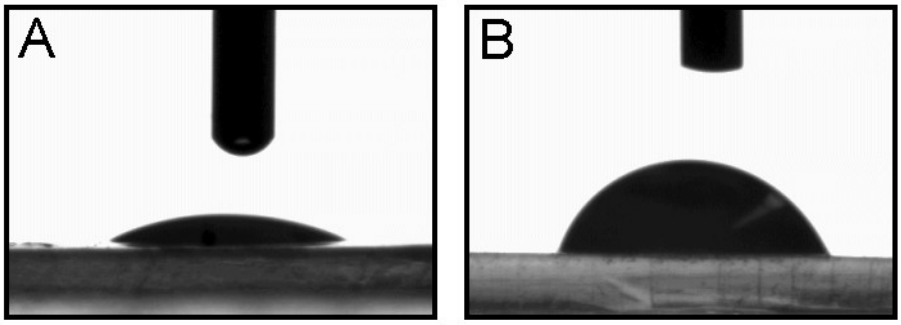

Figure 3.1. Image of a drop of water (A) and α-bromonaphtalene (B) on a glass surface.

3.1.4.2. Cell preparation for XPS analysis of the bacteria surface

X-Ray Photo Electron Spectroscopy (XPS) analysis of the elemental composition of the bacterial cells was performed as described by van der Mei *et al.* [228]. Briefly, fresh cells in TSB (18 ± 2H) were harvested and centrifuged for 5 min at 10,500 g, 4ºC. Cells were then resuspended in physiological serum at a density of approximately 1×10^9 cells/ml, and 20 ml of that suspension was filtered through a cellulose filter previously wetted with 10 ml of distilled water. After filtering, the cellulose filter covered with bacteria was sliced into small 1 cm^2 squares and quickly frozen in liquid nitrogen. Frozen filters were stored at –80ºC for 1 to 2 H, followed by 24 H of lyophilization.

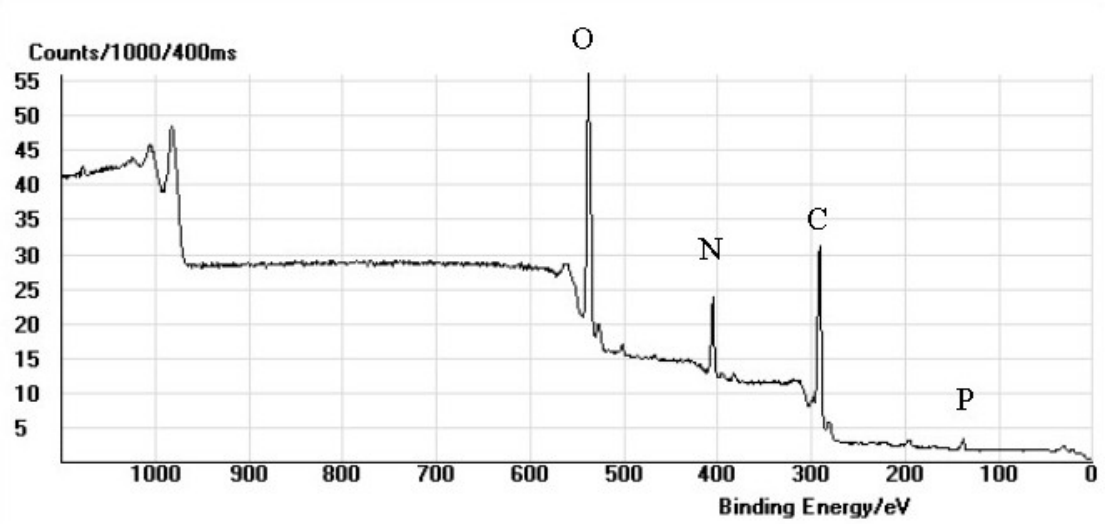

Figure 3.2. XPS spectrum of *S. epidermidis* 9142, showing the presence of oxygen, nitrogen, calcium and phosphorous.

The XPS analysis was performed using an ESCALAB 200A apparatus, with a VG5250 software and data analysis. The spectrometer used monochromatized Mg (Ka) X-ray radiation (15000 eV). The constant pass energy of the analyzer was 20 eV and it was calibrated with

reference to Ag 3d5/2 (368.27 eV). The pressure during analysis was under 1×10^{-6} Pa. The spectra were recorded following the sequence C_{1s}, O_{1s}, N_{1s}, P_{2p}. The elemental composition was defined as the ratio between oxygen and carbon (O/C), nitrogen and carbon (N/C), or phosphorous and carbon (P/C). An example of a XPS spectrum of the strain 9142 is presented in figure 3.2.

3.1.4.3. Substratum surface hydrophobicity

Cleaned and dried substratum surfaces were used for determining the hydrophobicity parameters of the surface. The hydrophobicity parameters were obtained using the sessile-drop contact angle technique, using an automated contact angle measurement apparatus [33]. Contact angles (see figure 3.1.) were standardized using as reference liquids: water, formamide and α-bromonaphtalene. Contact angles were related to the surface hydrophobicity as reviewed by Azeredo and Oliveira [11]. All experiments were done in triplicate, and with 4 repeats.

3.1.5. Adhesion assays

3.1.5.1. Initial adhesion to substrates

Initial adhesion was performed in a static system as described in chapter 1.

3.1.5.2. Image analysis

Image analysis was performed as described in chapter 1.

3.1.6. Biofilm assays

3.1.6.1. Biofilm formation on surfaces

Biofilm formation was preformed in a fed-batch system, for 72 H, as described in chapter 2.

3.2.6.2. Biofilm dry-weight determination

Biofilm dry-weight determinations were performed as described in chapter 2.

3.1.7 Hemagglutination assays

The hemagglutination assay was performed as described in chapter 2, but using planktonic populations, instead of biofilms.

3.2. Results

3.2.1. Surface physico-chemical analysis

Bacterial cell surface physico-chemical characteristics are presented in table 3.1. Water contact angles formed on bacterial lawns can be used as a qualitative indication of cell surface hydrophobicity, with lower values indicating a more hydrophilic surface.

Table 3.1. Water contact angle (in degrees) of *S. epidermidis* strains, and cell surface hydrophobicity parameters (in mJ/m^2).

Strain	Water contact angle (± SD)	γ_S^{LW}	γ_S^+	γ_S^-	ΔG_{lwl}^{TOT}
9142	26.1 (1.6)	29.07	4.32	43.79	17.59
9142-M10	19.9 (1.5)	28.82	4.66	47.09	19.97
IE75	26.8 (2.8)	26.63	5.06	43.83	17.10
IE186	19.6 (2.0)	27.53	5.12	47.37	19.75
IE214	18.7 (0,9)	19.51	8.96	48.44	15.58
M129	28.5 (2.6)	28.67	4.73	41.16	14.76
M187	33.7 (1.6)	27.63	4.93	37.49	11.45
FJ6	30.1 (3.8)	30.15	3.73	41.42	15.94
JI6	28.8 (5.1)	28.43	4.86	40.84	14.36
LE7	25.1 (3.8)	31.21	3.45	45.04	19.52
PE9	29.7 (1.2)	30.29	3.72	41.61	16.08

(SD means standard deviation; γ_S^{LW} represents the apolar Lifshitz-van der Waals surface free energy component; γ_S^+ represents the electron acceptor surface free energy component; γ_S^- represents the electron donator surface free energy component; ΔG_{lwl}^{TOT} represents the hydrophobicity measured in terms of the free energy of adhesion between 2 molecules immersed in water).

The values obtained for all the strains assayed were quite similar, ranging from contact angles of 19.9º (strain 9142-M10) to 33.7º (strain M187), indicating that these different bacterial strains have comparable levels of cell surface hydrophobicity. All of the clinical *S. epidermidis* strains examined here can be considered hydrophilic. From table 3.1 it can also be observed that all strains had surfaces that were predominantly electron donors (higher values of γ_S^-), with a low electron acceptor parameter (γ_S^+). The exception was strain IE214 that had the greatest electron acceptor parameter.

Table 3.2. Water contact angle (in degrees) of the substratum, and surface hydrophobicity parameters (in mJ/m2).

Surface	Water contact angle (± SD)	γ_S^{LW}	γ_S^+	γ_S^-	ΔG_{lwl}^{TOT}
Glass	23.0 (2.2)	34.53	2.72	45.46	19.98
Acrylic	85.5 (2.2)	38.06	0	7.59	-50.82

(SD means standard deviation; γ_S^{LW} represents the apolar Lifshitz-van der Waals surface free energy component; γ_S^+ represents the electron acceptor surface free energy component; γ_S^- represents the electron donator surface free energy component; ΔG_{lwl}^{TOT} represents the adhesion free energy).

Substrate surface physico-chemical characteristics are presented in table 3.2. Water contact angles of the 2 materials used clearly differed, with glass being hydrophilic, as

expected (water contact angle of 23.0º and ΔG_{lwl}^{TOT} >0) and acrylic being hydrophobic (water contact angle of 85.5º and ΔG_{lwl}^{TOT} <0).

The elemental composition of the surface of the bacterial strains, determined by XPS, is given in table 3.3. All strains used in the study described in this chapter exhibited high O/C values, ranging from 0.408 (strain M187) to 0.570 (strain JI6). On the other hand, P/C values were low, ranging from only 0.028 (strain IE214) to 0.055 (strain JI6).

Table 3.3. Bacterial surface elemental composition of cells grown in TSB during 18 H at 37ºC.

Strain	N/C	O/C	P/C
9142	0.203	0.479	0.042
9142-M10	0.189	0.530	0.046
IE75	0.195	0.408	0.038
IE186	0.193	0.463	0.041
IE214	0.197	0.420	0.028
M129	0.187	0.502	0.050
M187	0.200	0.408	0.030
FJ6	0.171	0.539	0.054
JI6	0.173	0.570	0.055
LE7	0.202	0.513	0.048
PE9	0.192	0.473	0.041

3.2.2. Initial adhesion to substratum

Initial adhesion of bacteria to both substrate surfaces is presented in figure 3.3. A wide range in the number of adhered cells was obtained, ranging from 3.19×10^5 cells/cm^2 (strain LE7 on glass) to 7.55×10^6 cells/cm^2 (strain FJ6 on acrylic). For 8 of 11 strains the number of bacterial cells initially adhered to glass was lower when compared to acrylic ($p<0.05$, paired-t-test). Strains 9142-M10, M129 and JI6 were the exceptions, with the latter not showing a significant difference in adhesion to the 2 substrates ($p<0.05$, paired-t-test).

Strain 9142-M10 had the highest initial adhesion to glass (7.4×10^6 cells/cm^2) whereas strains LE7 and IE75 had low initial adhesion to glass (3.2×10^5 cells/cm^2 and 7.0×10^5 cells/cm^2 respectively) making these phenotypes markedly different from the remaining strains ($p<0.05$, ANOVA and Tukey's multiple comparison test). As far as adhesion to acrylic is concerned, strain M129 can be considered a low adherent strain (5.6×10^5 cells/cm^2) being markedly different from most of the remaining strains ($p<0.05$, ANOVA and Tukey's multiple comparison test).

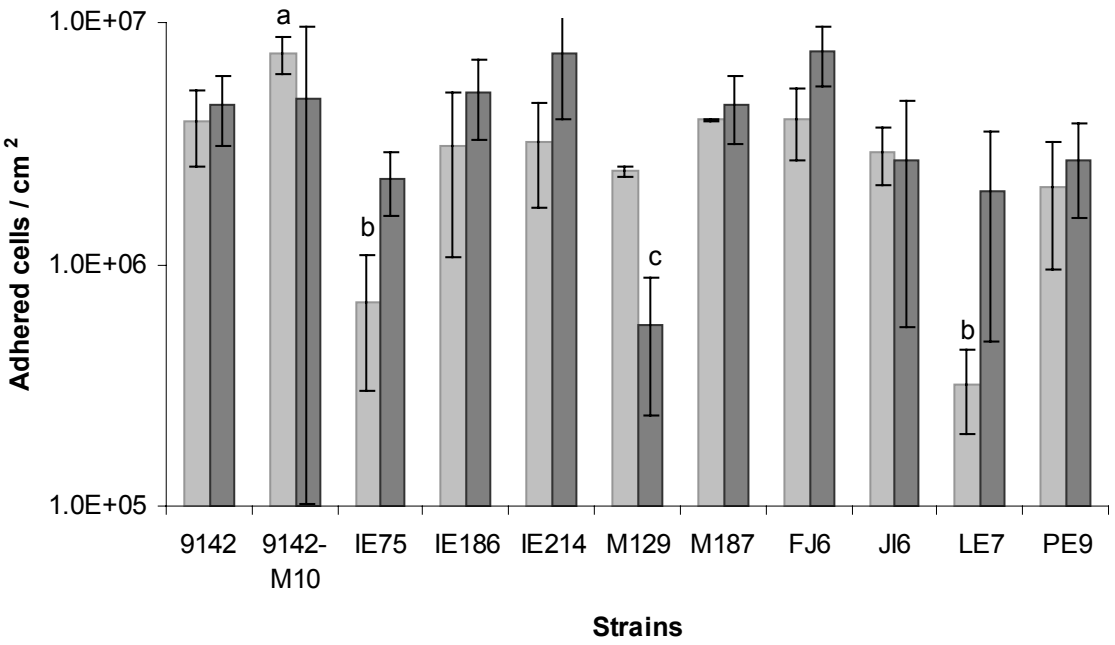

Figure 3.3. Differences in adhesion of *S. epidermidis* strains to glass (light bars) and acrylic (dark bars).(a) high adherent strains to glass ($p<0.05$); (b) low adherent strains to glass ($p<0.05$); (c) low adherent strains to acrylic ($p<0.05$)

3.2.3. Hemagglutination assays

Most strains were able to agglutinate human erythrocytes (table 3.4), however as can be seen by the titers, the overall degree of hemagglutination activities was relatively weak. Bacterial dilutions from a standardized initial amount that causes hemagglutination ranged from 1:1 (strain LE7) to 1:16 (strain IE214). Strains 9142-M10 and IE75 didn't cause any agglutination of human erythrocytes. For those strains, microscopic observations of the suspension containing bacterial cells and erythrocytes were performed. With this observation, strain IE75 microagglutinated the erythrocytes whereas the *ica*-interrupted strain 9142-M10 did not induce any hemagglutination.

Table 3.4. Macroscopic and microscopic hemagglutination titers of the *S. epidermidis* strains.

Strain	Hemagglutination titters	Microscopic observation
9142	1:2	-
9142-M10	No hemagglutination	No hemagglutination
IE75	No hemagglutination	Hemagglutination observed
IE186	1:4	-
IE214	1:16	-
M129	1:2	-
M187	1:4	-
FJ6	1:2	-
JI6	1:8	-
LE7	1:1	-
PE9	1:8	-

3.2.4. Biofilm formation

The amount of biofilm formed on both the glass and acrylic substrate surfaces is presented in figure 3.4. Most of the strains were able to form biofilms on both materials tested, except the ica-interrupted strain 9142-M10, which was used as a negative control for biofilm formation. It was observed that only a small amount of biofilm was formed by strain IE75 on both materials. The amount of biofilm produced by almost all of the other strains on acrylic surfaces was greater than on glass. The only exception was strain PE9. Therefore, a hydrophobic surface appears to promote biofilm formation by most clinical isolates of *S. epidermidis*.

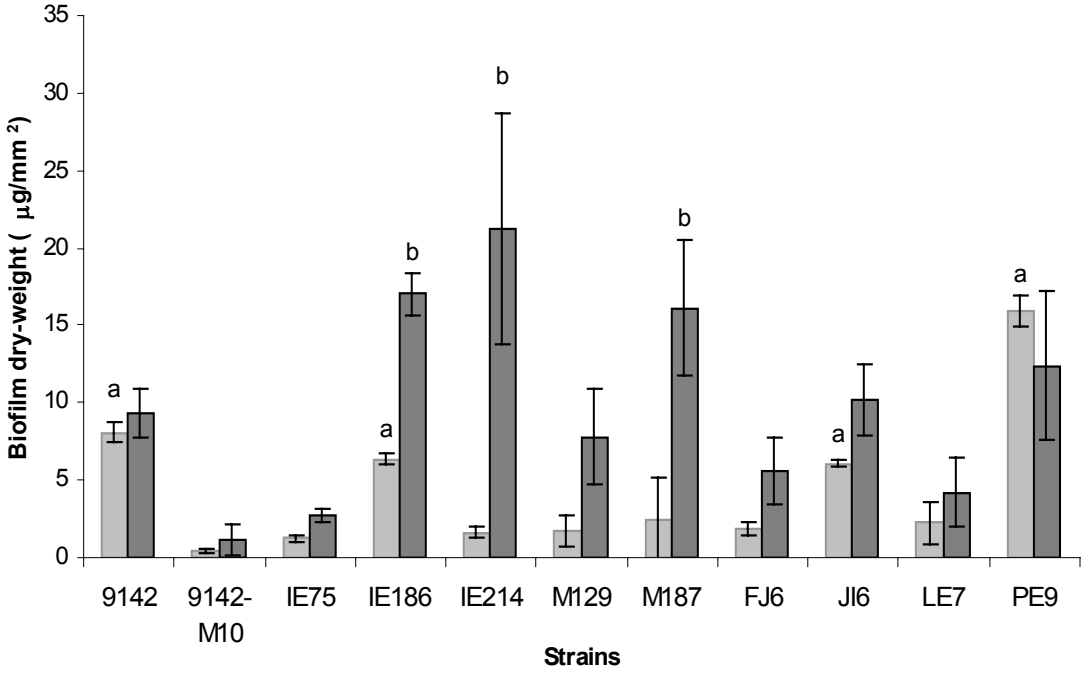

Figure 3.4. Biofilm formation of *S. epidermidis* strains on glass (light bars) and acrylic (dark bars).(a) high biofilms producers on glass ($p<0.05$); (b) high biofilms producers on acrylic ($p<0.05$).

Strains 9142, IE186, JI6 and PE9 showed significantly different abilities from the remaining strains to form biofilms on glass (8.2 mg/mm^2, 6.4 mg/mm^2, 6.0 mg/mm^2 and 15.0 mg/mm^2 respectively) being considered high biofilms producers on glass ($p<0.05$, ANOVA and Tukey's multiple comparison test). On acrylic, strains IE186, IE214 and M187 were the highest biofilms producers (16.9 mg/mm^2, 20.9 mg/mm^2 and 16.1 mg/mm^2 respectively) being markedly different from most of the remaining strains ($p<0.05$, ANOVA and Tukey's multiple comparison test). Since only 1 strain, IE186, was a high biofilm producer on both surfaces it appears that different clinical isolates have differing abilities to form biofilms on hydrophobic vs. hydrophilic surfaces.

3.3. Discussion

S. epidermidis is now recognized to be one of the most common causes of serious nosocomial infection [231], and this is related to the organism's ability to adhere to indwelling medical devices and form biofilms on them [236]. Bacterial adhesion is thought to be the first of 2 steps of biofilm formation [41,236], the second stage being accumulation of the bacterial cells into the biofilm mass. Biofilms play an important role in implant infections such as catheters [232], voice prostheses [31] and also bone-cement implants, intraocular artificial lens and cranioploastic implants [53].

In the study described in this chapter, the adherence of 9 clinical *S. epidermidis* strains, along with an isogenic pair of strains with 1 lacking an intact *ica* locus, to 2 different substrata using a static adhesion assay was evaluated. This methodology of assessing adherence has been controversial due to the use of washing steps necessary to remove non adherent and loosely adherent cells [18]. However, the methodology employed was optimized in order to minimize the problems related to the washing steps, as described in chapter 1.

The clinical isolates exhibited different abilities to adhere to the substrate surfaces and form biofilms. For all the strains used in the study described in this chapter, the highest level of initial adhesion occurred when the hydrophobic acrylic (ΔG_{lwl}^{TOT} = -50.82 mJ/m^2) was used as a substratum whereas a lower level of initial adhesion was generally obtained with the hydrophilic glass (ΔG_{lwl}^{TOT} = 19.98 mJ/m^2). Clearly, substratum hydrophobicity greatly influences the initial adhesion of *S. epidermidis*, a result implicated in other studies but never fully examined with a range of clinical isolates of this organism. However, no relationship was found between the bacterial strain's surface hydrophobicity and the extent of initial adhesion to either a hydrophilic or hydrophobic substrate. For instance, strain FJ6 exhibited one of the lowest hydrophilic surfaces (water contact angle of 30.1º) but was also one of the strains with high initial adhesion to the substrata. Conversely, strain IE214 had the highest hydrophilic surface (water contact angle of 18.7º) and was also one of the strains with high initial adhesion to the substrata. These findings are similar to those of other authors [30,52,156].

Strain IE214 had the greatest electron acceptor parameter (table 1). Interestingly, under the growth conditions used in the study described in this chapter this strain grew as highly aggregated cells, forming a flocculent suspension in the growth medium. This can be explained by both higher electron acceptor and donor parameters, meaning that this strain can establish a greater number of acid-base interactions between one cell and another [229].

Many prior studies suggested that hydrophobic interactions contribute to the initial adhesion of pathogens to tissues, leading to colonization, invasion or tissue destruction [61]. A microorganism may adhere to a substratum via the hydrophobic effect if the associating sites possess sufficiently high densities of apolar areas [61]. Compared to glass, acrylic has such

high densities of apolar areas, as can be seen by γ_S^- and γ_S^+ values presented in table 2, and the bacteria adhered better to this substrate compared to glass. Thus, *S. epidermidis* microorganisms may be more prone to adhere to hydrophobic surfaces such as acrylic.

It is generally accepted that the outermost cell surface plays a crucial role in bacterial adhesion to surfaces, as it interacts directly with the substratum surface [22,228]. In an attempt to correlate the adhesion results with the surface elemental composition, XPS analysis of the cell surface was performed. The ratios O/C, N/C and P/C of the various strains studied were in the same range of the values reported by Van der Mei *et al*. [228]. In their study, a cluster analysis of 210 microbial strains, including 33 staphylococci, revealed that O/C values for staphylococci are very high, ranging from 0.355 to 0.638 [228]. It has been suggested that high O/C may be an indicator of capsular polysaccharide material on the outer membrane [228]. No relation was found between the extent of adhesion and XPS data. Nevertheless, N/C values can be correlated with cell surface hydrophobicity: less hydrophobic cells exhibited lower N/C.

In order to determine if the initial adhesion event was a determinant of the subsequent amount of biofilm formed, biofilm dry weights were obtained on the same substrates used in the initial adhesion experiments. Several prior studies evaluated biofilm formation on the bottom of U-shaped polystyrene microtiter plates [41,88,90,136,151] but such studies did not consider the influence of different substrates on biofilm formation [151]. Furthermore, by weighing the dried biofilm mass a direct quantitative comparison of biomass formation by different strains could be made. In the present study, no direct relation between the ability of strains to initially adhere and subsequently form biofilms was found. For instance, strains IE75, M129 and JI6 had comparable initial adhesion levels; however, while the last 2 formed relatively thick biofilms, IE75 hardly formed more than a monolayer. This result indicates that biofilm formation is not dependent on the extent of initial adherence of bacteria to the substrate. In a study with 54 clinical isolates, a qualitative analysis of biofilm formation was performed and similar conclusions were drawn [75]. However, the study described here provides more detailed information because it is based on a quantitative analysis of biofilm formation and thus it makes it possible to obtain a better evaluation of the relationship between initial adhesion and biofilm formation. Heilmann *et al.* demonstrated in 1996, that biofilm formation and initial adhesion were 2 distinct phenomena, using 1 mutant *S. epidermidis* strain [90]. However, a recent study by Maira-Litran *et al.* [142] demonstrated that the original conclusions from Heilmann *et al.* [90] relating adherence and biofilm formation on polystyrene plates, was dependent on the manufacturer of the plates, since different results were obtained with the exact same strains and using the exact same methodology using plates made in the U.S. compared with those made in Germany.

Biofilm formation is more likely to be dependent on cell-to-cell adhesion rather than on the amount of cells initially attached to the surface. As no relationship between cell surface properties and biofilm formation was found, cell-to-cell adhesion is probably promoted by specific interactions and not influenced by the physico-chemical interactions of the bacteria and the attachment substrate. Likely, adherence is a complex phenomenon involving a variety of surface factors on the bacterium. One such factor, that has been proposed is the *S. epidermidis* autolysin encoded by the *atlE* gene [89]. However, while an *atlE* mutant was deficient in attachment to polystyrene, and this was restored in a complemented strain, it was never definitively shown in this study that it was the *atlE* protein itself, and not a secondary effect of the *atlE* mutation that caused the defect in adherence.

PNAG can agglutinate erythrocytes [195] and a direct relation was found between the ability of a strain of *S. epidermidis* to agglutinate erythrocytes and to form a biofilm. For 9 of the 11 strains, a linear relation was derived describing the relationship between biofilm formation (B) and hemagglutination (T) : B = 1.0807 X T + 3.6025, r = 0.9054. For instance, strain IE214 formed the greatest amount of biofilm (21.2 mg/mm^2 on acrylic) and exhibited the highest hemagglutination titer (1:16). Conversely, strain IE75 formed small amounts of biofilm on both surfaces (1.2 mg/mm^2 on glass and 2.7 mg/mm^2 on acrylic) and no macroscopic hemagglutination was observed, for this strain. However, via microscopic examination it was possible to verify that strain IE75 could adhere to human erythrocytes and cause some degree of agglutination. As expected, strain 9142-M10, the biofilm negative control strain, did not agglutinate human erythrocytes because this strain cannot express PNAG [136]. Probably the clinical isolate IE75 expressed small amounts of PNAG giving rise to both low biofilm formation and small hemagglutination capabilities, but the amount of PNAG produced by this strain was not formally quantified. Taken together, the hemagglutination data reflect the level of expression of PNAG, and although it may not be entirely quantitative, it is possible to conclude that PNAG is a clear determinant for biofilm formation, but not for initial adhesion of *S. epidermidis*, under the conditions studied.

Overall, it appears from these results that there is a wide range of variation in adherence and biofilm formation among clinical *S. epidermidis* strains. For instance, the number of adherent cells of clinical strain LE7 was 23 times lower than that of ica-interrupted strain 9142-M10 (on glass) and the number of adherent cells of clinical strain M129 was 13 times lower than that of clinical strain FJ6 (on acrylic). Strain IE214 formed a biofilm almost 8 times greater than that of strain IE75 and 5 times greater than that of strain LE7 (on acrylic). Thus, initial adhesion and biofilm formation on inert surfaces, which are considered to be manifestations of one of the major virulence factors of *S. epidermidis*, are strain dependent and not a consistent phenotypic characteristic of the species or of clinical isolates. This means that when

evaluating either bacterial adherence or biofilm formation it is important to take into account that the relative levels of these phenotypes do not reflect the potential of the organism to cause a clinically significant infection. Obviously host factors associated with susceptibility to infection make a major contribution to the outcome of an infectious process, and this cannot be determined by measuring bacterial phenotypes. Therefore, it might be important to consider that properties of PNAG unrelated to bacterial adherence and biofilm formation, such as providing resistance of the bacteria to host immune effectors [204,237] may be important in the outcome of an *S. epidermidis* infection, as will be discussed in sections III and IV.

Section II

Biofilms and resistance to antimicrobial agents

Section II cover image represents the rate of penetration (in minutes) of vancomycin (green) in S. aureus biofilm (red), determined by confocal microscopy analysis. This image was a kind gift from K. Jefferson, Virginia Commonwealth University, Richmond, USA.

Introduction

A major complication with the long-term use of medical devices is the development of biofilm infection [15]. This is an important component of *S. epidermidis* infections, since biofilm formation is one of the major virulence factors of these organisms [236], often leading to persistent infections [49].

The fact that biofilm bacteria are able to tolerate significantly higher levels of antibiotics than planktonic bacteria has been well-established in susceptibility assays, and the clinical relevance of this phenomenon is underscored by the occurrence of medical device-related infections that are refractory to antibiotic therapy [7,157]. Often, the antibiotic concentration needed to eradicate the biofilm is above the peak serum concentration of the antibiotic [157], rendering it ineffective in treating biofilm infections. Despite concerted efforts to treat biofilm infections with antibiotic therapy, the physical removal of an infected medical device is often necessary [100], which carries an additional economic and health cost. The resistance of bacterial cells in a biofilm to antibiotics does not seem to depend on traditional mechanisms of antibiotic resistance [5,211]. Although it is not yet clear how biofilms resist antimicrobial agents, a possible explanation has been suggested by several authors who assume that biofilms present a diffusional barrier to antibiotics [57,95,215]. However, it seems that this mechanism can only partially explain the increased resistance phenotype generally present in clinically-relevant biofilms [64]. Other mechanisms have been suggested (see figure II.A), including slow growth of the cells within the biofilm [227], activation of the general stress response [21], emergence of a biofilm-specific phenotype [140] and persister cells [208]. Resistance is reportedly up to 1000-fold greater in bacterial cells in biofilms, but a reliable method to compare the antibiotic sensitivities of planktonic bacteria to cells in biofilms is lacking [43]. A critical first step in understanding mechanisms of antibiotic resistance of cells in biofilms is to have a method to accurately determine the level of resistance relative to planktonic populations.

With the current inability to treat most biofilm infections, there is great interest in finding methods or strategies to inhibit biofilm formation. Several strategies have been proposed to inhibit biofilm formation on medical devices, including the administration of sub-minimal inhibitory concentrations (sub-MIC) of antibiotics [36,74,110], use of furanone compounds [15], anti-inflammatory drugs [8], bacterial extracts [80], development of new, anti-adhesive medical surfaces [44,176] or coating medical devices with several different compounds, including antibiotics [100,175,202]. It has been demonstrated that sub-MIC of antibiotics are able to modify the physicochemical properties and the architecture of the outer surface of *S. epidermidis*, affecting overall virulence [189]. Sub-MIC concentrations of antibiotics have been successfully used to inhibit bacterial initial adhesion to abiotic substrates [110] and it was

suggested that these studies could provide insights into preventing biofilm formation on medical devices [74]. However, as discussed in chapter 3, initial adherence to a surface and subsequent biofilm formation can be 2 independent phenomena [243], and so conclusions drawn regarding an effect of sub-MIC antibiotics on initial bacterial adherence may not be directly extrapolated to biofilm formation.

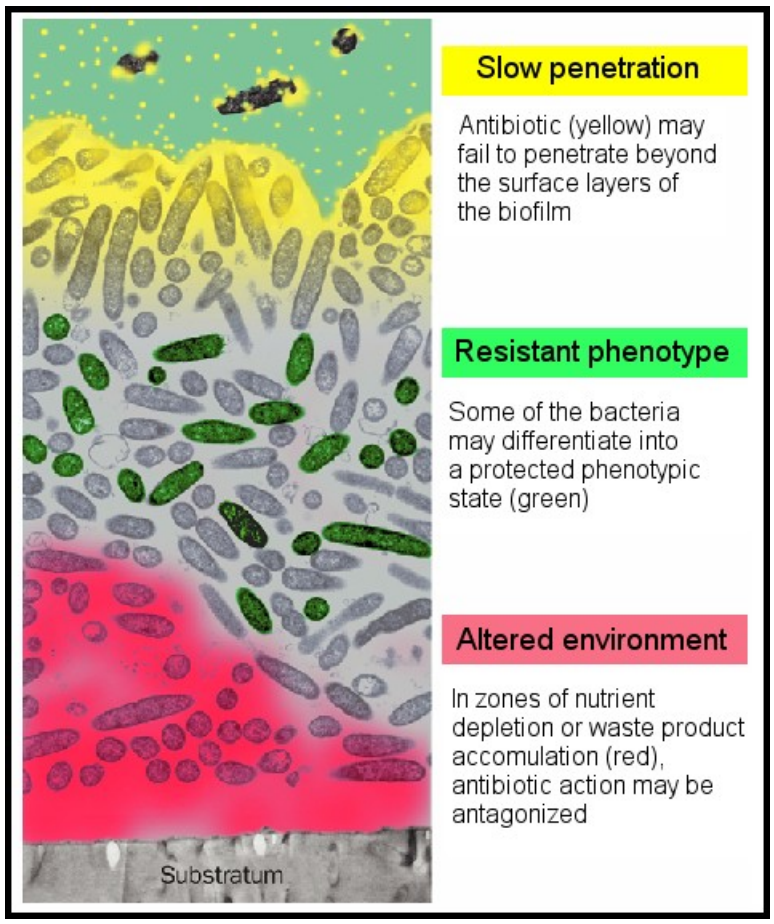

Figure II.A. Some of the most discussed hypothesis for biofilm resistance to antibiotics. Adapted from Lancet (2001), 258:135-138

Moreover, besides the reduced capability of biofilm formation by the bacteria, little is known about other changes implicated in the virulence of CoNS that might occur due to the presence of low concentrations of antibiotics. Factors such as biofilm spatial structure, cell surface properties, production of specific molecules responsible for biofilm formation (such as PNAG), constitution and distribution of the biofilm matrix and increased resistance to antibiotics should be addressed when studying the effect of sub-MIC concentrations of antibiotics in biofilm formation.

In the work described in this section, to test biofilm susceptibility to antibiotics, a range of antibiotics with different molecular weights and different mechanisms of action were selected:

inhibitors of cell wall synthesis (cefazolin, vancomycin and dicloxacillin), inhibitors of proteins synthesis (tetracycline) and inhibitors of RNA synthesis (rifampicin).

Although the drug companies are still investing in new antibiotics development, the rate at which microorganisms are acquiring resistance to these new drugs is concerning [223]. One possible alternative to antibiotic therapy would be the use of bacteriophages (phages). Phages are viruses that infect and kill bacteria [45], are ubiquous [1] and mostly harmless to humans [25]. The lytic phage life cycle is represented in figure II.B.

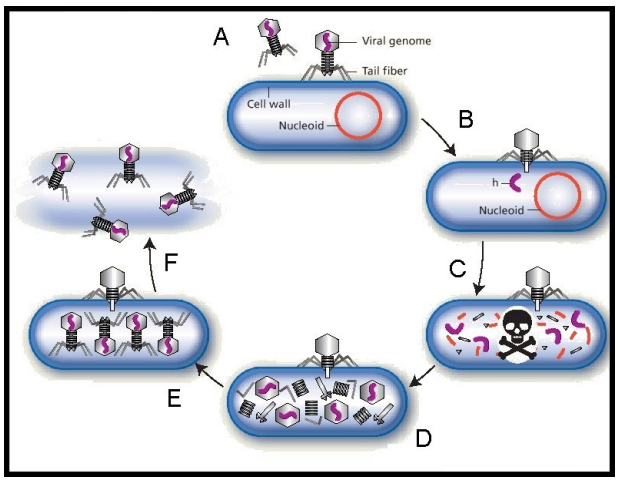

Figure II.B. The phage lytic life cycle: Phages attaches to a specific host bacterium (A), inject their nucleic acid (B) disrupting the bacterial genome and killing the bacterium (C) taking over the bacterial protein synthesis machinery to make phage parts (D). The phage is then assembled, and due to lysis of the bacterial cell wall hundreds of new phages are released into the environment (F). Adapted from Nat Biotechnol. (2004) 22:31-36.

The first records of phage therapy came from World War II Soviet and German armies [23]. Back in the 1960's the first report of a clinical trial using phages came from Georgia, in the old Soviet Union [12]. With the advent of antibiotics, phage biology research came to a halt, but more recently, probably due to the increase in antibiotic resistance, some new studies on phage therapy had been published, mainly using animal models [28,97,207]. While some studies have evaluated phage therapy against *S. aureus* [149,171], information is still lacking on *S. epidermidis*, especially on biofilm infections. Recently it has been shown that *Pseudomonas fluorescens* biofilms had similar susceptibility to phages as do planktonic cells [206]. This suggested that phages have the potential to be an useful therapy against biofilms, although more studies are necessary to support this conclusion [216].

In the work described in this section, antibiotics and phages were used to test susceptibility of planktonic or biofilm-grown bacteria to these agents, evaluating possible differences between these 2 modes of growth phenotypes.

Chapter 4

Comparative assessment of antibiotic susceptibility of coagulase-negative Staphylococci in biofilm vs. planktonic culture as assessed by bacterial enumeration or rapid XTT colorimetry

Summary

In this chapter, the phenomenon of biofilm resistance to antibiotics was addressed. Several CoNS strains were grown planktonically or as biofilms to determine the effect of the mode of growth on the level of susceptibility to antibiotics with different mechanisms of action. The utility of a new, rapid colorimetric method that is based on the reduction of a tetrazolium salt (XTT) to measure cell viability was tested by comparison with standard bacterial enumeration techniques. While the biofilm phenotype shown a high resistance to antibiotics that target cell wall synthesis, it was fairly susceptible to antibiotics that target RNA and protein synthesis. The study described in this chapter provides a more accurate comparison between the antibiotic sensitivities of planktonic vs. biofilm populations, because the cell densities in the 2 populations were similar and because the concentration required to reduce the global bacterial metabolism rather than to eradicate the entire bacterial population was measured.

Part of the work described in this chapter has was published in 2005, in Journal of Antimicrobial Chemotherapy, 56:331-336

4.1. Material and Methods

4.1.1. Antibiotics

The antibiotics and respective concentrations used in the study described in this chapter were 63 μg cefazolin per ml, 40 μg vancomycin per ml, 59 μg dicloxacillin per ml, 16 μg tetracycline per ml and 10 μg rifampicin per ml. The main characteristics of these antibiotics are described in table 4.1, and figure 4.1 presents the structure of the antibiotics used. The antibiotic concentration used in all assays was the peak concentration in human serum (PS).

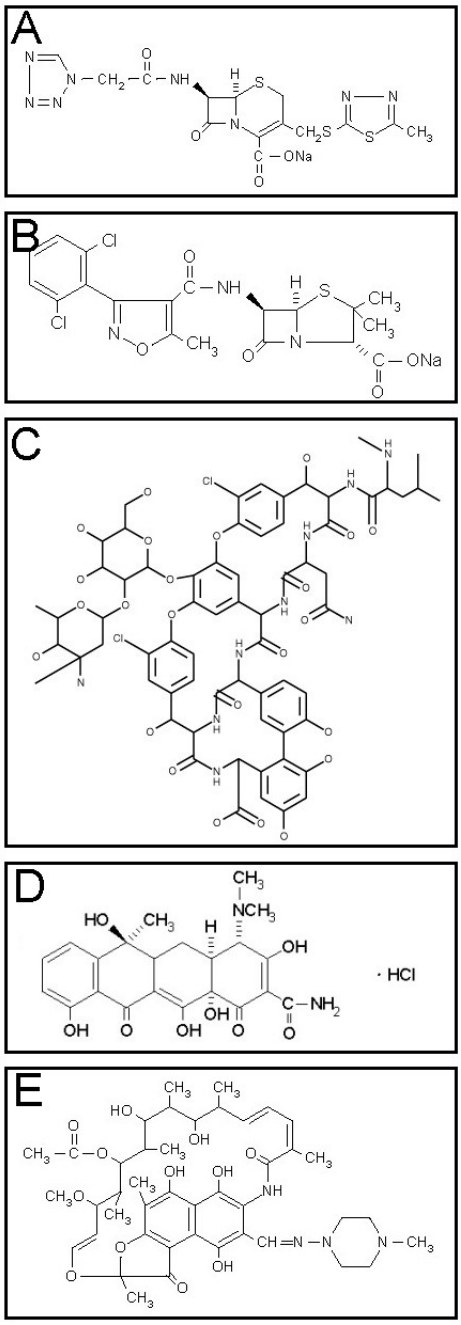

Figure 4.1. Structure of the antibiotics used in the study described in this chapter: (A) cefazolin, (B) dicloxacillin, (C) vancomycin, (D) tetracycline and (E) rifampicin.

Table 4.1. Characteristics of the antibiotics used in the study described in this chapter.

Antibiotic	Mechanism of action [(a)]	PS [(b)]	MW [(a)]
Cefazolin	Cell wall synthesis inhibitor	63	477
Vancomycin	Cell wall synthesis inhibitor	40	1,485
Dicloxacillin	Cell wall synthesis inhibitor	59	481
Tetracycline	Protein synthesis inhibitor	16	823
Rifampicin	RNA synthesis inhibitor	10	492

(a) The mechanism of action and the molecular weight (MW) in g/mol of the antibiotics were provided by the manufacturer.
(b) The peak serum concentration (PS) in μg/ml of cefazolin, vancomycin, tetracycline and rifampicin were obtained according to NCCLS [161] and for dicloxacillin according to Friberg *et al*.[72].

4.1.2. Bacterial strains and growth conditions

A total of 6 biofilm producing CoNS strains were used in the study described in this chapter: *S. epidermidis* 9142, IE186, M129, M187 [40,41], *S. haemolyticus* IE246 and M176 [38]. Detailed information about these strains is presented in the supplements section, page 179.

TSB and TSA were prepared according to the manufacturer's instructions. All strains were incubated in 15 ml of TSB inoculated with bacterial cultures less than 2 days old and grown on TSA plates, for 24 (± 2) H at 37ºC in a shaker rotator at 130 rpm. Cells were harvested by centrifugation (for 5 min at 10,500 g and 4ºC), and resuspended in a saline solution (0.9% NaCl prepared in distilled water) adjusted to an OD_{640nm} equivalent to 1×10^9 cells/ml, and then used in the subsequent assays.

4.1.3. Biofilm formation

Biofilms were produced as described previously [41]. Briefly, for each strain, 10 μl of a cell suspension adjusted to 1×10^9 cells/ml in 0.9% NaCl was added to a 96 well polystyrene microtiter plate containing 240 μl of TSB supplemented with 0.25% of glucose per well to promote biofilm formation. Plates were incubated at 37ºC with shaking at 150 rpm, for 24 (±4) H. The planktonic cells were removed carefully, and the biofilm was washed twice with 200 μl of 0.9% NaCl. This procedure yielded a biofilm containing approximately 2×10^8 cells/ml. This was determined as previously described [42] by disrupting the biofilm and resuspending the cells in TSB + 0.05% Tween, followed by 20 s of sonication at 20 W to homogenize the suspension. This procedure disrupted the cell clumps without impairing cell viability [42]. This was determined by comparing sonicated and non-sonicated suspensions by gram-staining and cell viability tests. Serial dilutions were made and plated on TSA plates that were incubated overnight at 37ºC.

4.1.4. Antibiotic susceptibility of planktonic cultures assessed by cfu plating

For each strain, 200 μl of a cell suspension adjusted to 1×10^9 cells/ml in 0.9% NaCl was added to 30 ml of TSB, and incubated at 37ºC with shaking at 130 rpm, until a cell density of 1×10^9 cells/ml was reached. Then, a 5-fold dilution was made in TSB containing each antibiotic at the respective PS concentration in order to obtain a cell suspension of 2×10^8 cells/ml, and growth was allowed to proceed for 6 H. A control was obtained by diluting the suspension in fresh TSB without adding antibiotic. Each hour a 1 ml sample was collected and centrifuged for 8 min at 9,000 g, and the pellet resuspended in 0.9% NaCl. Two washing steps were performed, followed by 20 s of sonication at 20 W. The viable cells were determined by performing 10-fold serial dilutions of this suspension, and 100 μl were plated on TSA plates. The plates were then incubated for 20 H at 37ºC. This experiment was repeated 3 times, in triplicate.

4.1.5. Antibiotic susceptibility of biofilms assessed by cfu plating

Biofilms were prepared in 96 well polystyrene microtiter plates as described above yielding an initial cell concentration of about 2×10^8 cells/ml. To each well containing the biofilm, 200 μl of TSB supplemented with 0.25% of glucose and 1 of the antibiotics at the PS concentration were added. Growth was allowed to occur during 6 H. A control was obtained by adding TSB with 0.25% of glucose but without any antibiotic to the biofilm cultures. At 2 hour time intervals, the planktonic cells of 4 random wells were removed carefully and the biofilm was washed twice with 200 μl of 0.9% NaCl. The 4 wells were thoroughly scraped until >93% (±5%) of the biofilm was removed (as determined by crystal violet spectrophotometric readings) [50] and resuspended in 1 ml of 0.9% NaCl, followed by centrifugation during 8 min at 9,000 g. The pellet was resuspended in 0.9% NaCl and washed twice, followed by 20 s of sonication at 20 W. The viable cells were determined by performing 10-fold serial dilutions of this suspension and plating 100 μL of the dilutions in triplicate on TSA plates that were then incubated for 20 H at 37ºC. This experiment was repeated 3 times, with individual samples evaluated in triplicate.

4.1.6. Antibiotic susceptibility of planktonic cultures assessed by XTT

The XTT colorimetric method was applied to determine antibiotic susceptibility as described previously [131], with some modifications. Briefly, after 3 H of exposure of 200 μl of a bacterial suspension to the antibiotics, cells were washed twice with 200 μl of 0.9% NaCl and transferred to individual wells of a 96-well polystyrene microtiter plate. Then, 50 μl of a solution containing 200 mg/l of XTT and 20 mg/l PMS (phenazine methosulfate) were added

to each well. The microtiter plates were incubated for 3 H at 37ºC in the dark. After that, 200 μl of the liquid medium in each well were transferred to a 1.5 ml tube and centrifuged for 5 min at 9,500 g. For the spectrophotometric readings, 100 μl of the supernatant were transferred to a new microtiter plate, and the absorbance was measured at 490 nm. A control was obtained with a cell suspension not exposed to the antibiotics. All samples were done in quadruplicate, and each experiment was repeated 3 times.

4.1.7. Antibiotic susceptibility of biofilms assessed by XTT

The XTT colorimetric method was applied to determine the antibiotic susceptibility as described previously [131], with some modifications. Briefly, biofilms exposed to the antibiotics were gently washed twice with 200 μl of 0.9% NaCl, then 250 μl of a solution containing 200 mg/l of XTT and 20 mg/l of PMS were added to each well. Microtiter plates were incubated for 3 H at 37ºC in the dark. Then, 200 μl of each well were transferred to a 1.5 ml tube, and centrifuged for 5 min at 9,500 g. For the spectrophotometric readings, 100 μl of the supernatant was transferred to a new microtiter plate, and the absorbance was measured at 490 nm. Controls were biofilms not exposed to the antibiotics. All samples were done in quadruplicate, and the experiment was repeated 3 times.

4.2. Results

4.2.1. Kinetics study

Figure 4.2 presents the time-kill curves for the tested antibiotics (see table 4.1) at the PS concentration against both planktonic and biofilm cells of *S. epidermidis* 9142. The growth profiles of *S. epidermidis* 9142 cells not exposed to antibiotics in planktonic cultures vs. biofilm cultures were significantly different ($p<0.05$, ANOVA and Tukey multiple comparisation test).

Non-antibiotic treated planktonic cells had significant growth over 6 H, whereas only a slight increase in cfu/ml was noted in cells growing in biofilms. All 3 cell-wall synthesis inhibitors (cefazolin, vancomycin, and dicloxacillin) were highly effective against planktonic cells, showing nearly a 1-log decrease in viable cells in the first hour, and a near 3-log difference after 6 H of exposure. Tetracycline was the least effective antibiotic on planktonic cells, whereas rifampicin exhibited intermediate efficacy. The activity of cell-wall synthesis inhibitors on cells growing in biofilms was markedly less than their activity on planktonic cells: the decrease in viable bacterial cells was less than 0.5-log even after 6 H of exposure to these antibiotics. It is interesting to note that in contrast to planktonic cells, tetracycline and rifampicin were the most effective antibiotics in terms of reducing viability of cells in biofilms.

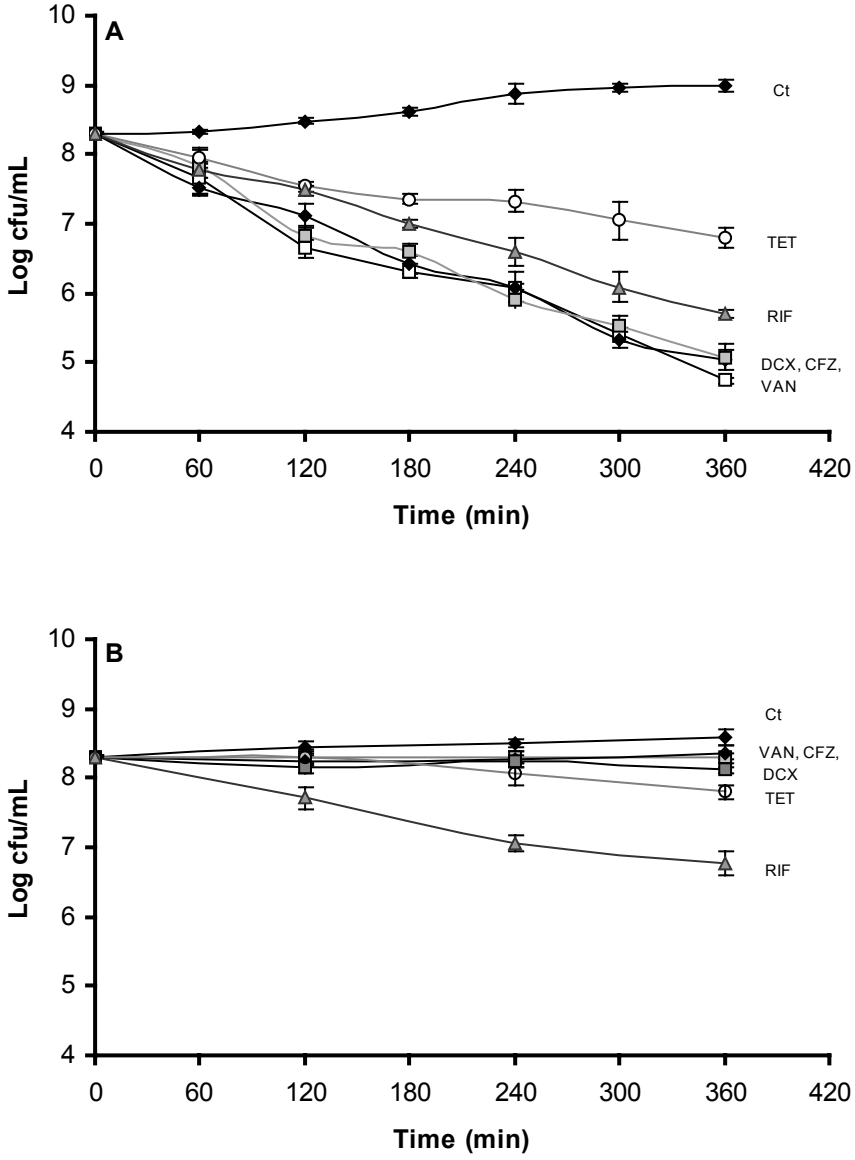

Figure 4.2. Control growth curves (Ct) and kill plots of the effect of cefazolin (CFZ); vancomycin (VAN); dicloxacillin (DCX); tetracycline (TET) or rifampicin (RIF) on *S. epidermidis* 9142 planktonic cells (A) and biofilm (B). Points represent means and error bars the SD.

4.2.2. Antibiotic susceptibility assessed by cfu plating

Figure 4.3 shows the mean reduction in bacterial cell viability for 6 different CoNS strains after exposure of planktonic cultures or cells in biofilms to antibiotics. As expected, for all *S. epidermidis* and *S. haemolyticus* strains, planktonic cells were more susceptible to all cell wall synthesis inhibitors used, compared to cells in biofilms. The differences in cellular survival detected between planktonic cells and biofilm cells with protein and RNA synthesis inhibitors were lower. In fact, for 50% of the strains there was no significant difference in the susceptibility of planktonic cells and biofilms to rifampicin ($p>0.05$, paired t test). The same

was observed for *S. epidermidis* with tetracycline but not for *S. haemolyticus* since cells in biofilms or planktonic cultures had significantly different susceptibilities.

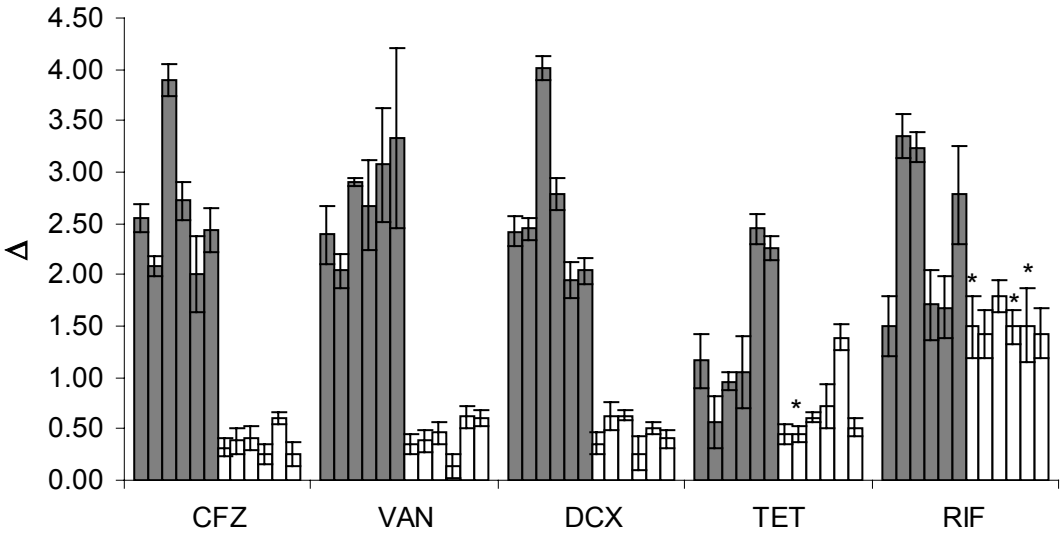

Figure 4.3. Mean fold reduction of cellular viability after 3 H of exposure to antibiotics. The y axis indicates the difference of the log10 cfu/ml between strains without antibiotic (controls) and strains treated with antibiotics (CFZ-cefazolin; VAN-vancomycin; DCX-dicloxacillin; TET-tetracycline; RIF-rifampicin), in planktonic cells (dark bars) and biofilm (white bars). Different bars represent different strains, from left to right: *S. epidermidis* 9142, IE186, M129, M187, *S. haemolyticus* IE246 and M176. * indicates values that are not significative different ($p>0.05$, paired t-test) when comparing between planktonic vs. biofilm cells of the same strain.

When analyzing the average differences in susceptibilities between planktonic cells and those in biofilms, for each antibiotic, a ratio can be calculated between the susceptibility of planktonic cells and biofilm cells: 7.0 for cefazolin, 6.4 for vancomycin, 5.6 for dicloxacillin, 2.0 for tetracycline and 1.6 for rifampicin. This shows that rifampicin and tetracycline are less affected by the biofilm phenotype, since the ratios of their activities are close to 1 when comparing effects in planktonic and biofilm cells. In contrast, all 3 cell wall inhibitors were highly affected by the biofilm phenotype, as demonstrated by the high ratios of their activities.

4.2.3. Antibiotic susceptibility assessed by XTT

Figure 4.4 presents the mean reduction in metabolic activity after exposure of planktonic cultures and cells in biofilms to antibiotics, as measured by the decrease in metabolic activity using the XTT reagent. The findings were very similar to the results obtained by measuring the decrease in viability by cfu platting: the major reductions in metabolic activity were primarily found with planktonic cells, and the differences between cells in biofilms and planktonic cells were greater for cell wall synthesis inhibitors.

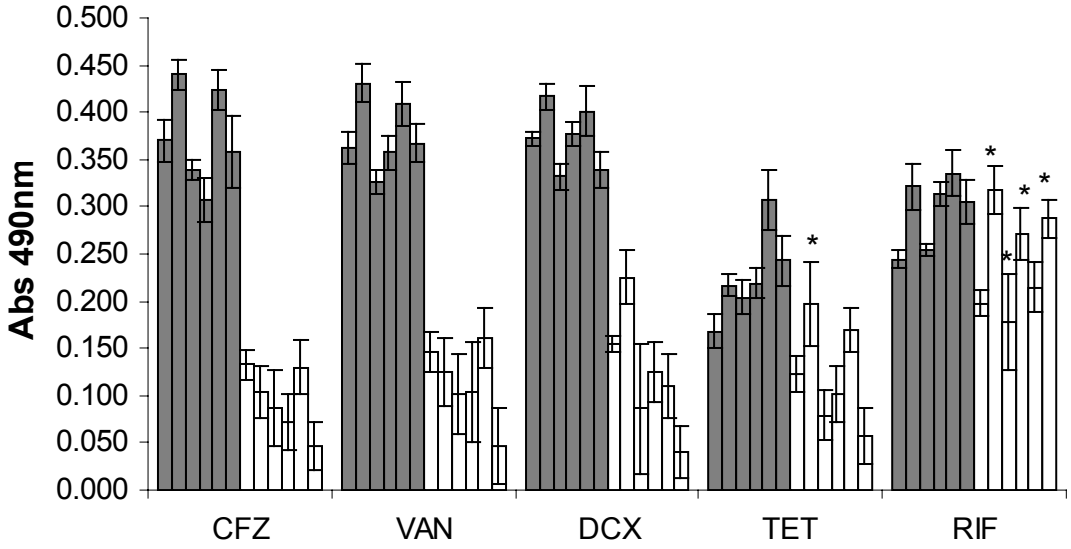

Figure 4.4. Mean reduction of cellular activity, measured by XTT, after 3 H of exposure to the antibiotics, expressed as the difference of absorbance readings at 490 nm between control without antibiotic and antibiotic treated strains (CFZ-cefazolin; VAN-vancomycin; DCX-dicloxacillin; TET-tetracycline; RIF-rifampicin) per μg of antibiotic used (Δ/PS), in planktonic cells (dark bars) and biofilm (white bars). Different bars represent different strains, from left to right: *S. epidermidis* 9142, IE186, M129, M187, *S. haemolyticus* IE246 and M176. * indicates values that are not significative different (P>0.05, paired t-test) when comparing between planktonic vs. biofilm cells of the same strain.

4.3. Discussion

Antibiotic resistance is a serious problem encountered with many human pathogens [93], and is particularly notable with *S. epidermidis*, since many clinical isolates of this organism are resistant to up to 8 different antibiotics [70]. Adding to this problem is the fact that the major virulence factor of *S. epidermidis* and other CoNS is biofilm formation [172] and that cells in biofilms are normally more resistant to antibiotics than planktonic cells [211], making drug resistance in a CoNS infection an even more serious problem.

A number of assays have been developed to quantify the level of susceptibility of cells in biofilms but such assays do not provide a fair comparison with the standard MIC assay for planktonic bacteria [3,43,119]. This is because NCCLS standards stipulate the use of low inocula of the planktonic bacteria [161], whereas bacteria are at a high cell density in established biofilms. This difference affects antibiotic susceptibility assays in a number of ways. First, certain antibiotics such as vancomycin exhibit a cell density-dependent effect and are much less effective against high bacterial inocula. Second, most antibiotic susceptibility assays for cells in biofilms measure the minimum biofilm eradication concentration (MBEC) rather than the minimum inhibitory concentration (MIC) [43]. It has been established that in any bacterial population, be it planktonic or sessile cells in biofilms, there exists a certain

percentage of persister cells, which are extremely tolerant to antibiotics [116,208]. For this reason it takes a high concentration of a given antibiotic to completely eradicate even a planktonic population of bacteria. Overall, comparing the MICs of planktonic bacteria to the MBEC of biofilm bacteria may result in exaggerated differences between the susceptibility levels. Indeed, comparisons between MIC's for planktonic cells and MBEC's for cells in biofilms suggests there may be a 1,000-fold difference in the susceptibility of the biofilm cells to certain antibiotics. In the study described in this chapter it was found that the killing efficacy of achievable peak serum concentrations of cefazolin, vancomycin, dicloxacillin, tetracycline, and rifampicin was less than 10-fold higher against *S. epidermidis* cells in biofilms (figure 4.5). This decrease in efficacy is still quite significant however, and could account for frequent therapeutic failure of these drugs against biofilm infections.

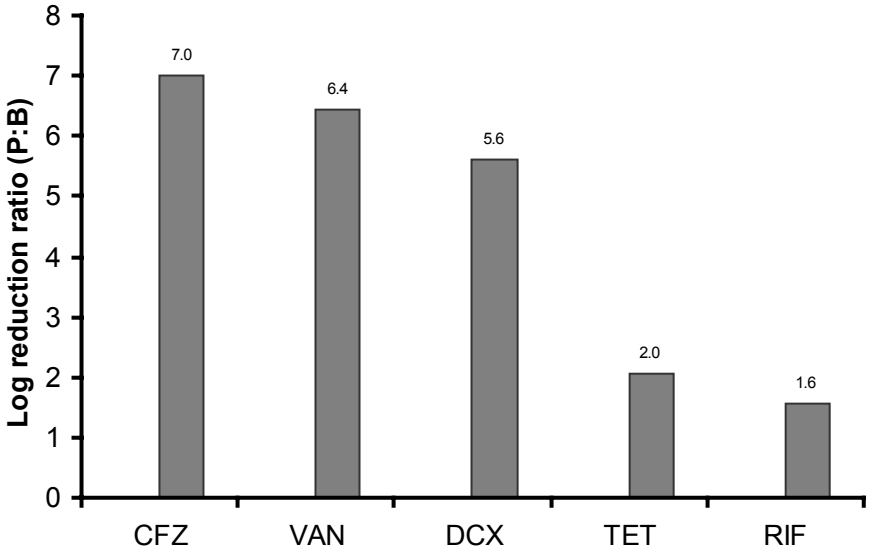

Figure 4.5. Resistance of the biofilms to the antibiotics, expressed by the log reduction of the antibiotic activity planktonic bacteria (P) compared to biofilms (B).

A critical first step in understanding mechanisms of antibiotic resistance of cells in biofilms is to have a method to accurately determine the level of resistance relative to planktonic populations. Besides determination of viable cells by classic cfu plating, the effects of antibiotics on metabolic activity by colorimetrically measuring XTT reduction were also evaluated [226]. This method has started to become widely used and several comparisons with NCCLS standard susceptibility tests have already demonstrated it's reliability [87,131]. One of the major advantages of this method it is the short time necessary to obtain results. Measuring antibiotic sensitivities of cells in biofilms can be laborious and the application of a reliable and rapid method is desirable in a clinical laboratory. Kuhn *et al.* described the lower

sensitivity as one disadvantage of the XTT method [122]. The results presented in the study described in this chapter also demonstrated that cfu platting method has a higher sensitivity, when compared to XTT.

The assay described in this chapter provides a more consistent comparison between the antibiotic sensitivities of planktonic *vs.* biofilm populations. Furthermore, since the antibiotics were used at the PS concentration, the relative differences in the effects of antibiotics on planktonic *vs.* biofilm cells can be considered to have potential clinical relevance. The present results demonstrate that rifampicin was the most effective antibiotic against *S. epidermidis* or *S. haemolyticus* cells in biofilms as assessed by both cfu plating and XTT measurements. As the pathogenesis of CoNS is often dependent upon colonization of implanted surfaces and subsequent biofilm formation, it is of utmost importance to assess the susceptibility of cells in biofilms to antibiotics rather than the susceptibility of planktonic cells. Many clinical practices still rely on MIC determinations performed with microbial suspensions [73,91,94], however, as the present results demonstrate, the susceptibility levels of planktonic cells does not reflect the correspondent susceptibility of the cells in biofilms.

The differences in cfu following antibiotic treatment demonstrated that on average, for all strains tested, the susceptibility to tetracycline and rifampicin were less affected by the biofilm phenotype. In fact, for some strains there was no significant difference in the cfu achieved comparing planktonic cells and biofilm cells in regard to their susceptibility to antibiotics (the ratio was almost 1).

Low growth rates have been considered as an antibiotic resistance mechanism that has been observed in *E. coli* biofilms [66]. In the present analysis, growth rates of cells in biofilms were lower than that of planktonic cells (figure 4.2), which could partially explain the higher resistance of biofilms to antibiotics, particularly for cell wall synthesis inhibitors whose efficiency is very much dependent of the growth rate of the cells. However, RNA synthesis inhibitors are also dependent on the growth rate of the cell and the results showed that both planktonic cells and cells in biofilms were comparably susceptible to these agents. It has also been suggested that the biofilm matrix itself could pose a barrier to the penetration of the antibiotics [57,95,215]. However, other studies indicate that diffusion through the biofilm matrix is roughly equivalent to water [212] and the results obtained indicate that antibiotics with the same mechanism of action but having different molecular weights did not differ in their efficacy against cells in biofilms.

The results presented in this chapter demonstrated that antibiotics that target cell wall synthesis have a reduced activity in biofilms, independent of the size of the antibiotic molecule, but antibiotics that target RNA and protein synthesis have similar activities on planktonic cells as they do on cells in biofilms, suggesting that the phenotypic resistance of

cells in biofilms to antibiotics is affected primarily by the mechanism of action of the antibiotic. Several different resistance mechanisms in biofilms have been suggested, and although each one can partially explain some cases of antibiotic resistance of cells in biofilms, an overall understanding of antibiotic resistance of this phenotype is still yet to be elucidated. Considering that biofilm formation is one of the major virulence factors involved in CoNS infections [236], susceptibility testing of CoNS should not rely on MIC determinations. XTT activity measurements could provide a quick and reliable methodology to assess the susceptibility of CoNS cells growing in biofilms to antibiotics.

Chapter 5

The relationship between inhibition of bacterial adhesion to a solid surface by sub-mic concentrations of antibiotics and the subsequent development of a biofilm

Summary

Antibiotics are often ineffective against biofilm infections, as discussed in the previous chapter. Some studies suggest that low concentrations of antibiotics could inhibit biofilm formation, by showing that sub-mic concentrations of antibiotics could inhibit initial microbial adherence to medical-device surfaces. However, since initial adherence and subsequent biofilm formation can be 2 distinct phenomena, as discussed in chapter 3, conclusions regarding effects of sub-mic antibiotics on initial adhesion cannot be extrapolated to biofilm formation. In this chapter, the effect of sub-mic concentrations of several antibiotics in inhibiting initial adherence to inert surfaces and also biofilm maturation is described. Most of the antibiotics used resulted i*n effective reduction of bacterial adherence to acrylic, in some cases reaching over 70% inhibition of adherence. When strains with a high biofilm forming capacity were grown in sub-mic concentrations of those antibiotics there were combinations of the drugs that significantly inhibited biofilm formation. However the correlation between inhibition of initial adherence and biofilm maturation was low. The results discussed in this chapter demonstrate that assays evaluating the inhibition of initial adherence to medical surfaces cannot fully predict the effect on inhibition of biofilm formation.*

Part of the work described in this chapter was published in 2005, in Research in Microbiology, 156:650-655

5.1. Materials and Methods

5.1.1. Bacterial strains

A total of 7 CoNS biofilm producing strains were used in the study described in this chapter: *S. epidermidis* 9142, IE75, IE186, M129, M187, *S. haemolyticus* IE246 and M176. Detailed information about these strains is present in the supplements section, page 179.

5.1.2. Substrate preparation

Acrylic was prepared as described in chapter 2.

5.1.3. Antibiotics and determination of the MIC value

The antibiotics used in the study described in this chapter were cefazolin, vancomycin and dicloxacillin, which act as inhibitors of cell wall synthesis and are routinely used to treat staphylococcal infections [69,123,180]. Determination of the MIC range for each strain was carried out according to NCCLS standards [161]. The sub-MIC concentration used was ½ of the lowest MIC value, whenever just 1 antibiotic was added to the bacterial cell suspension, and ¼ of the MIC value, whenever combinations of 2 antibiotics were added to the bacterial cell suspension. These concentrations were not high enough to inhibit bacterial growth, except in a few specific cases of synergism that are indicated in the results section.

5.1.4. Inhibition of initial adhesion

5.1.4.1. Growth conditions

TSB and TSA were prepared according to the manufacturer's instructions. All strains were inoculated into 15 ml of TSB from TSA plates not older than 2 days. Liquid cultures were grown for 24 (± 2) H at 37ºC in an orbital shaker at 130 rpm. The cells were harvested by centrifugation (for 5 min at 10,500 g at 4ºC) then washed and resuspended in a saline solution (0.9% NaCl prepared in distilled water) to an OD_{640nm} equivalent to 1×10^9 cells/ml. This suspension was used in the biofilm assays. For adherence assays, 1 ml of this cell suspension was transferred to 30 ml of fresh TSB containing sub-mic concentrations of antibiotics, and incubated for 18 (± 2) H at 37ºC with shaking at 130 rpm. After being harvested by centrifugation (for 5 min at 10,500 g at 4ºC), cells were washed twice and resuspended in a saline solution (0.9% NaCl prepared in distilled water) and adjusted to an OD_{640nm} equivalent to 1×10^9 cells/ml and used in the adherence assays.

5.1.4.2. Static adherence

Static adherence was performed as described in chapter 1.

5.1.4.3. Image analysis

Image analysis was performed as described in chapter 1.

5.1.5. Biofilm formation

5.1.5.1. Biofilm assays

Formation of bacterial biofilms was performed in a fed-batch system, as described in chapter 2.

5.1.5.2. Biofilm quantification

Biofilms were quantified by dry-weight determinations, as described in chapter 2.

5.2. Results

5.2.1. Determination of the sub-MIC value of antibiotics

The results from the antimicrobial susceptibility testing of all CoNS strains are summarized in table 5.1. MIC values were generally higher when using cefazolin or dicloxacillin, compared to vancomycin. *S. epidermidis* 9142, M187 and *S. haemolyticus* M176 were found to be the more antibiotic-resistant strains. Table 5.1 also presents the concentration of antibiotics used in the assays employing sub-MIC of antibiotics.

Table 5.1. MIC values and sub-mic concentrations used in the adherence and biofilm formation assays (in μg/ml)

Strain	MIC range			Sub-MIC		
	CFZ	VAN	DCX	CFZ	VAN	DCX
S. epidermidis 9142	64 - 128	8 - 16	64 - 128	32	4	32
S. epidermidis IE75	8 - 32	4 - 8	0.5 - 16	4	2	0.25
S. epidermidis IE186	2 - 16	8	0.5 - 4	1	4	0.25
S. epidermidis M129	4 - 32	8	4 - 16	2	4	2
S. epidermidis M187	64 - 128	8	16 - 64	32	4	8
S. haemolyticus IE246	0.5 - 2	2 – 4	0.25 - 2	0.25	1	0.125
S. haemolyticus M176	32 - 128	2 - 4	16 - 128	16	1	8

CFZ, Cefazolin; VAN, Vancomycin; DCX, Dicloxacillin.

5.2.2. Inhibition of adherence

Results from studying the effects of growth with sub-MICs of antibiotics on bacterial adherence to acrylic are presented in table 5.2. Dicloxacillin was the antibiotic that prevented initial adherence to the greatest extent when only 1 antibiotic at ½ of the MIC was used (average reduction per strain of 54 ± 11%). Vancomycin was the least effective antibiotic in this regard (average reduction per strain of 25 ± 7%). When using combinations of 2 antibiotics, each at ¼ of the MIC, the combinations where dicloxacillin was present generally gave the highest inhibition, reaching in some cases near 80% inhibition (*S. epidermidis* IE186

with dicloxacillin and vancomycin or *S. epidermidis* M129 with dicloxacillin and cefazolin). Some combinations of antibiotics, even at the lowest concentrations tested, could inhibit initial adhesion at fairly high percentages. Some of the combinations had a synergistic effect and were able to inhibit bacterial growth, as in the case of *S. epidermidis* M187 and *S. haemolyticus* IE246 when grown in the presence of cefazolin and dicloxacillin.

Table 5.2. Inhibition of initial adhesion (in percentage) to acrylic due to growth in sub-mic concentrations of antibiotics

Strain	CFX	VAN	DCX	½CFX + ½VAN	½VAN + ½DCX	½CFX + ½DCX
S. epidermidis 9142	49 (±8)	34 (±4)	66 (±3)	36 (±9)	44 (±3)	40 (±3)
S. epidermidis IE75	13 (±6)	20 (±6)	36 (±9)	10 (±6)	16 (±7)	46 (±6)
S. epidermidis IE186	44 (±11)	30 (±9)	66 (±6)	58 (±4)	79 (±3)	66 (±8)
S. epidermidis M129	42 (±10)	29 (±3)	48 (±4)	23 (±9)	52 (±9)	77 (±3)
S. epidermidis M187	2 (±5)	26 (±5)	58 (±4)	42 (±4)	*	*
S. haemolyticus IE246	21 (±3)	17 (±4)	46 (±9)	*	55 (±5)	*
S. haemolyticus M176	28 (±6)	19 (±3)	59 (±3)	16 (±4)	19 (±3)	12 (±4)

(CFX) Cefazolin, (VAN) Vancomycin and (DCX) Dicloxacillin at the sub-mic concentration (½ of MIC).
* these combinations of antibiotics didn't allow the cells to grow, working as a bactericidal concentration and demonstrating synergistic effect.

5.2.3. Inhibition of biofilm formation

Results from testing the effects of growth in the presence of sub-MIC of antibiotics on biofilm formation on acrylic are presented in table 5.3. When using only 1 antibiotic at ½ of the MIC, vancomycin was the antibiotic that was least effective in preventing biofilm formation (average reduction per strain of 21 ±10%). Dicloxacillin and cefazolin were more effective than vancomycin (average reduction per strain of 51 ± 12% and 44 ± 9%, respectively).

Table 5.3. Inhibition of biofilm formation (in percentage) on acrylic, under sub-mic concentrations of antibiotics

Strain	CFX	VAN	DCX	½CFX + ½VAN	½VAN + ½DCX	½CFX + ½DCX
S. epidermidis 9142	43 (±7)	24 (±9)	54 (±9)	13 (±2)	30 (±3)	10 (±2)
S. epidermidis IE186	55 (±4)	24 (±11)	32 (±2)	40 (±3)	40 (±14)	21 (±4)
S. epidermidis M187	32 (±3)	8 (±3)	60 (±4)	67 (±5)	*	*

(CFX) Cefazolin, (VAN) Vancomycin and (DCX) Dicloxacillin at the sub-mic concentration (½ of MIC).
* these combinations of antibiotics didn't allow the cells to grow, working as a bactericidal concentration and demonstrating synergistic effect.

When using combinations of 2 antibiotics, each at ¼ of the MIC, in most cases the inhibition of biofilm formation was less effective compared with use of only 1 antibiotic at ½ of the MIC. The only exception found was for strain *S. epidermidis* M187, for which most

combinations of antibiotics had a synergistic effect and were also able to inhibit bacterial growth.

Figure 5.1 presents the correlation found between adhesion and biofilm formation inhibition. The correlation coefficient obtained (R) was only 0.48 meaning that these 2 properties are not very linearly dependent. The main differences were found when using combinations of antibiotics. For instance, when using combinations of vancomycin and dicloxacillin, inhibition of adherence of *S. epidermidis* IE186 was 79% but only 40% of the biofilm formation was inhibited.

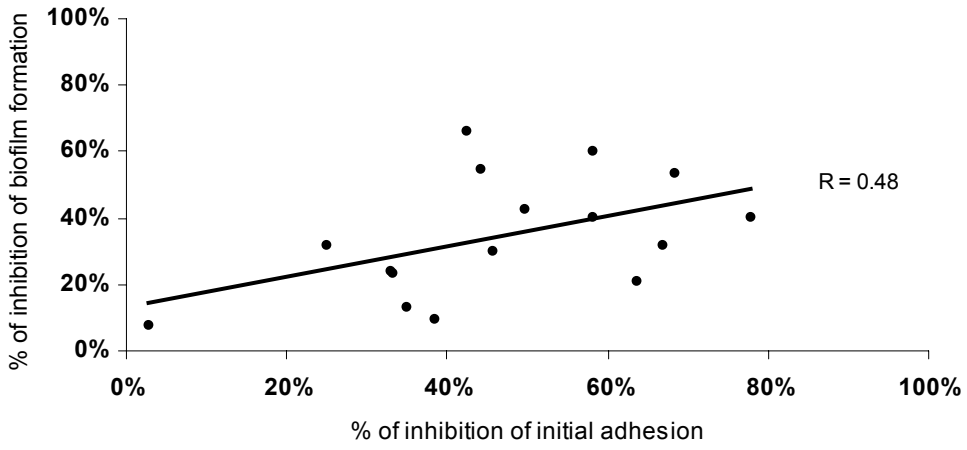

Figure 5.1. Correlation between inhibition of adhesion and inhibition of biofilm formation.

5.3. Discussion

It has been suggested that if a low concentration of antibiotics or other drugs are able to prevent initial adherence of bacteria to surfaces, the subsequent step of biofilm formation would also be inhibited [74]. A similar conclusion might be drawn for other possible interventions being considered to reduce the incidence of device-related infections, such as use of biomaterials with low intrinsic binding of microbes. However, it has previously been demonstrated, and corroborated by the work presented in chapter 3, that the initial adherence and subsequent biofilm formation by staphylococcal strains are 2 distinct phenomena [51]. Accordingly, it was important to determine if growth of CoNS strains in the presence of sub-MICs of antibiotics was equally effective at preventing initial adherence and subsequent biofilm formation on acrylic surfaces. Such results could be relevant to determining the usefulness of an approach targeted at inhibiting bacterial adherence in preventing a biofilm-related infection. Therefore, antibiotics commonly used for staphylococcal infections were chosen and the effect on either initial adhesion or biofilm formation was evaluated using

bacteria grown in low concentrations of such antibiotics. Acrylic was the selected surface because it's a very common polymer used in biomedical applications [53].

All strains were able to strongly adhere to acrylic in the absence of antibiotics. The most effective antibiotic in preventing initial adhesion was dicloxacillin (mean inhibition of 54 ± 11%), and the least effective was vancomycin (mean inhibition of 25 ± 7%). However, for each antibiotic used, a wide variation on inhibition of adherence was found. For instance, when using cefazolin 49% of the adherence of *S. epidermidis* 9142 was inhibited whereas only 13% of the adherence of *S. epidermidis* IE75 was achieved with this drug. Dicloxacillin inhibited 66% of the initial adherence of *S. epidermidis* 9142, while the effect on *S. epidermidis* IE75 was only 36% inhibition of adherence.

Since the clinical strains used in the study described in this chapter had different susceptibilities to antibiotics, the concentration of each antibiotic used in the inhibition assays varied for each strain (see table 5.1). In order to determine if the variation in inhibition of adherence for the different strains was due to the variable antibiotic concentrations used, a linear regression plot was derived for each sub-mic antibiotic concentration used and the respective percentage of inhibition. The correlation coefficients obtained (R) were 0.13 for cefazolin, 0.92 for vancomycin and 0.54 for dicloxacillin. This means that although a good relation was found between drug concentration and percentage of inhibition for vancomycin, for the remaining antibiotics, difference in inhibition could not be attributed to the differences in drug concentration. Probably, other factors intrinsic to an individual strain could contribute to decrease the susceptibility to the sub-MICs of the antibiotics, such as the expression of surface antigens [51].

When sub-MIC combinations of antibiotics were used, a wide variation in inhibition of CoNS adherence to acrylic was observed. Notably, combinations where dicloxacillin was present were always more effective than when dicloxacillin was absent. As expected, some synergistic effects on inhibition of growth were found with a combination of the antibiotics used. For instance, when ¼ of the MIC of cefazolin plus ¼ of the MIC of dicloxacillin were used, *S. epidermidis* M187 and *S. haemolyticus* IE246 were not able to grow.

Some of the CoNS strains used in the adherence assays had a low ability to form biofilms (chapter 3). Thus, only high biofilm forming bacteria were selected for the assays of biofilm inhibition by sub-mic antibiotics. As was seen for the adherence assays, dicloxacillin was the most effective antibiotic at preventing biofilm formation on acrylic. However, when cefazolin or vancomycin was used the percentage of inhibition of biofilm formation was generally lower. The difference between adhesion and biofilm inhibition was even higher, when combinations of the antibiotics at ¼ of the MIC value were used.

Although it has been suggested that by preventing initial adherence, subsequent microbial biofilm formation could be prevented, experimental support for this conclusion is minimal. It has been reported that when testing several antibiotics with different mechanisms of action, after the initial adherence of CoNS to either acrylic or silicone, the bacteria became more resistant to some antibiotics compared with non-adherent, planktonic cells [7]. In a different study, it was suggested that attached bacteria would have a slower metabolic rate, and that could partially explain the increase in resistance to antibiotics [245]. Pagano *et al.* have evaluated the differences between a prophylactic and therapeutic approach to the CoNS biofilm problem. These authors verified that by adding low concentrations of linezolid or vancomycin before the bacteria could reach the surface, they could inhibit biofilm formation. However, if the application of the drug was delayed for just 6 hours after initial adherence occurred, the inhibition of biofilm formation was less effective [179]. Rupp and Hamer assessed the inhibition capabilities of some antibiotics on adherence and biofilm formation using a few *S. epidermidis* strains. Although these authors didn't search for a relation between inhibition of adherence and inhibition of biofilm formation, some differences were found between the ability of a given antibiotic to inhibit adherence and subsequent biofilm formation [196].

In summary, despite some similarities in the results of the adherence and biofilm inhibition assays, adherence inhibition assays cannot fully predict the outcome of biofilm formation. Even so, it seems that dicloxacillin has a significant effect in preventing CoNS adhesion and also biofilm formation to acrylic. Interestingly, standard bacterial susceptibility tests (with planktonic cells) demonstrated higher susceptibility of CoNS to vancomycin, but this antibiotic was the least effective for preventing initial adhesion and biofilm formation. Clearly, standard bacterial susceptibility tests do not reveal the potential of an antibiotic to inhibit biofilm formation.

How growth in sub-inhibitory concentrations of dicloxacillin affects S. epidermidis and S. haemolyticus biofilms

Summary

As discussed in the previous chapter, low concentrations of antibiotics can inhibit microbial adherence to medical-device surfaces. However, little is known about the changes that occur in the physiology of bacteria within biofilms formed in the presence of sub-MIC concentrations of antibiotics. In this chapter, these issues were addressed. Biofilms formed in the presence of sub-MIC concentrations of dicloxacillin contained less biomass and exhibited notable changes in the composition of the biofilm matrix. Changes in the spatial structure were also verified by confocal scanning laser microscopy, indicating that biofilms grown in the presence of a sub-MIC of dicloxacillin contained a lower cell density. Physiologic alterations in the bacteria within biofilms grown in the presence of sub-inhibitory concentrations of the antibiotic were also evaluated. The results showed differences in bacterial surface characteristics when grown in sub-MIC antibiotics, including decreased hydrophobicity and decreased expression of the exo-polysaccharide PNAG. The elemental composition of the cell surface was also analyzed and whereas S. epidermidis exhibited a decrease in oxygen and nitrogen content, S. haemolyticus exhibited an increase of these 2 elements. Additionally, an increase in resistance to several antibiotics was observed in the cells within biofilms formed in the presence of dicloxacillin.

Part of the work described in this chapter was published in 2005, in Applied and Environmental Microbiology, 71:8677-8682

6.1. Materials and Methods

6.1.1. Strains

In this work, 2 biofilm forming CoNS clinical strains were used: *S. epidermidis* M187 and *S. haemolyticus* M176. Detailed information about these strains is present in the supplements section, page 179.

6.1.2. Media and Growth conditions

TSB and TSA plates were prepared according to the manufacturer's instructions. All strains were grown for 24 (± 2) H at 37ºC in a shaker rotating at 130 rpm in 15 ml of TSB, using bacteria grown on TSA plates not older than 2 days as inoculum. After being harvested by centrifugation (for 5 minutes at 10,500 g and 4ºC), cells were washed twice and resuspended in saline (0.9% NaCl prepared in distilled water) at a concentration of approximately 1×10^9 cells/ml, determined by the OD_{640nm}. These cell suspensions were used in the subsequent biofilm assays.

6.1.3. Determination of growth parameters under the effect of sub-MIC concentrations of dicloxacillin

The concentration of dicloxacillin used in the study described in this chapter was 8 μg/ml, which is a sub-MIC concentration as determined in a previous study (chapter 5). Bacterial growth parameters were obtained by following the increase in the OD_{640nm} of cell suspensions grown in TSB in the presence or absence of dicloxacillin. At the stationary growth phase the number of cells was determined by making 1:10 serial dilutions in TSB and plating 100 μl per dilution on TSA, followed by 24 H incubation at 37ºC.

6.1.4. Biofilm formation

Biofilm formation was induced as described previously [41]. Briefly 50 μl of a cell suspension of 1×10^9 cells/ml prepared in a 0.9% NaCl solution was added to 96 or 6 well polystyrene plates containing TSB + 0.25% glucose. Biofilm formation was allowed to occur during 48 H at 37ºC with cultures rotating at 120 rpm. Every 12 H the TSB medium containing suspended cells was removed and fresh TSB + 0.25% glucose was added. These biofilms were considered the controls (CT). To evaluate the effect of sub-MIC concentrations of dicloxacillin in biofilm formation, biofilms were formed in culture media (TSB + 0.25% glucose) supplemented with 8 μg/ml of dicloxacillin (DCX).

6.1.5. Biofilm mass quantification

Biofilm mass was quantified determined as described previously [90] with some modifications. Briefly, bacteria grown in 96 well polystyrene plates were washed twice with 0.9% NaCl solution, dried in an inverted position, and stained with 0.4% safranin for 10 min. The plates were washed with distilled water, and dried over-night. To each well, 100 μl of 0.9% NaCl solution was added, and the absorbance was measured in an ELISA plate reader at OD_{490nm}. For each condition studied, 3 separate experiments were done.

6.1.6. Confocal scanning laser microscopy analysis

Biofilm staining was performed as previously described [163], with some modifications. Briefly, biofilms formed on 6 well polystyrene plates were washed twice with 0.9% NaCl. Wheat germ agglutinin (WGA) conjugated to Oregan green at 10 μg/ml was added to the biofilms, and incubated for 20 min at room temperature, in the dark. After staining, the biofilms were gently rinsed with 0.9% NaCl.

Confocal scanning laser microscopy (CSLM) analysis was performed with an LSM 510 Meta attached to an Axioplan II microscope, as previously described [125], with some modifications. Biofilms were observed using a 63X water immersion objective. The bacterial cells were detected by the refraction of light in the red spectrum and WGA was detected by fluorescence in the green spectrum, using a single channel analysis. Excitation wavelengths were set at 633 nm, with output power of 70%, for detection of bacterial cells, and 488 nm, with output power of 10%, for detection of WGA. The excitation beam splitter used was HFT UV/488/543/633. The filters used to detect the refracted light by bacterial cell were LP650 and to detect emitted light by WGA was BP 505-530. The beam splitter used was NFT 545. For each condition, 3 independent biofilms were used and in each biofilm, 4 different regions of the surface were analyzed and the thickness of the biofilm was measured. The 3D projections were made with LSM 510 software.

6.1.7. Contact angle measurements

Contact angles measurement of bacterial lawns was performed as described in chapter 3.

6.1.8. XPS analysis of the bacteria surface

The elemental composition of bacterial cell surfaces was assessed by XPS analysis as described in chapter 3.

6.1.9. Biofilm matrix composition

The biofilm matrix was extracted as previously described [9] with some modifications. Briefly, biofilms were scraped from the substratum surfaces, resuspended in 0.9% NaCl and sonicated for 30 s, 20 W, then vortexed for 2 min. The resultant bacterial suspensions were adjusted to approximately 1×10^9 cells/ml and centrifuged at 10,500 g, 6 min, 4ºC. The supernatants were filtered through a 0.2 μm nitrocellulose filter and stored at -20ºC before being used in the quantification assays. Proteins and polysaccharides of the biofilm matrix were determined by the Lowry [132] and Dubois [62] methods.

6.1.10. PNAG immunological detection

PNAG production by biofilms was detected as previously described [51] with some modifications. Briefly, biofilms were scraped from the substratum surfaces, resuspended in TSB, sonicated for 30 s, 20 W, then vortexed for 2 min. The resultant bacterial suspensions were adjusted to approximately 1×10^9 cells/ml. An equal volume of each suspension was resuspended in 300 µl of 0.5 M EDTA (pH 8.0) and incubated for 5 min at 100°C. Cells were harvested by centrifugation at 10,500 g, 6 min and 100 µl of the supernatant was incubated with 10 µl of proteinase K for 60 min at 60°C. Then, proteinase K was heat inactivated by incubating 30 min at 80°C. This solution was then diluted 4-fold into 500 μl of Tris-buffered saline (20 mM Tris-HCl, 150 mM NaCl [pH 7.4]) and 100 μl of each dilution were immobilized on a nitrocellulose filter that was then blocked with 1% bovine serum albumin, and incubated for 2 H with a rabbit antibody raised to *S. aureus* PNAG (kindly provided by T. Maira-Litran) [141] absorbed and diluted 1:5,000 as described by Gerke *et al.* [77]. The secondary antibody used was a horseradish peroxidase-conjugated anti-rabbit IgG antibody diluted 1:6,000 and detected with the Amersham ECL (enhanced chemiluminescence) Western blotting system.

6.1.11. Resistance to antibiotics

The MIC of bacterial cells in biofilms formed in the presence or absence of sub-inhibitory concentrations of dicloxacillin was determined using NCCLS protocol [161] with some modifications. Briefly, biofilms were scraped from the substratum surface, resuspended in TSB, sonicated for 10 s at 20 W, adjusted to a standard cell inoculum, and incubated in 96-well polystyrene microtiter plates with several 2-fold dilutions of dicloxacillin, tetracycline and rifampicin, for 24 H at 37ºC in TSB.

6.1.12. Detection of *icaC* gene by PCR

Genomic DNA from the CoNS strains was extracted using a DNeasy Tissue kit. For the detection of *icaC* gene the following primers were used: 5'- ATAGTGAATCACTTATCACCGC-3' and 5'- GAGAATCTAAGATAATTGGGTGC-3'. Both primers were custom synthesized by Qiagen Operon. For the PCR reaction 25 μl of PCR supermix high fidelity was added to 0.5 μl of each primer and 2 μl of DNA. PCR conditions comprised an initial 5 min denaturation step at 94ºC, followed by 32 cycles of 30 s at 94ºC, 30 s at 50ºC and 45 s at 72ºC, and a final extension step of 5 min at 72ºC.

6.2. Results

6.2.1. Growth rate in the presence of sub-MIC dicloxacillin

Table 6.1 summarizes the effect of dicloxacillin on the doubling time in log phase and also the bacterial concentration reached at the stationary phase. When grown in the presence of dicloxacillin, both strains presented a slightly longer doubling time in the log phase, with statistical difference ($p<0.05$, paired t-test). However, in the stationary growth phase, no significant difference was observed between growth in the presence or absence of dicloxacillin ($p>0.05$, paired t-test).

Table 6.1. Growth parameters of planktonic cells grown in the presence (DCX) or absence (CT) of sub-MIC concentrations of dicloxacillin.

Strain	Doubling time in log phase (min)	Stationary phase concentration (10^9 cfu/ml)
M187 CT	60 (± 8)	8.2 (± 0.9)
M187 DCX	66 (± 10)	7.2 (± 1.4)
M176 CT	59 (± 8)	4.6 (± 0.8)
M176 DCX	67 (± 5)	5.1 (± 1.4)

(± represents the SD).

6.2.2. Amount of biofilm formed

The amount of biofilm formed by *S. haemolyticus* M176 in TSB supplemented with glucose was significantly lower ($p<0.05$, ANOVA and Tukey multiple-comparisons test) than the biofilm mass of *S. epidermidis* M187, formed in the same conditions. The use of dicloxacillin at a low concentration (8 μg/ml=½MIC) significantly reduced ($p<0.05$, paired t-test) the amount of biofilm formed by both strains (figure 6.1).

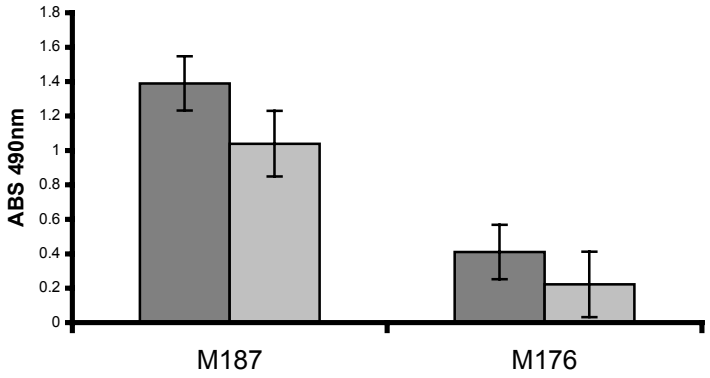

Figure 6.1. Amount of biofilm formed by *S. epidermidis* M187 and *S. haemolyticus* M176 in the absence (dark bars), and presence of sub-MIC concentration of dicloxacillin (light bars), evaluated by the safranin colorimetric assay. (Error bars represent the SD).

6.2.3. Biofilm structure

The CSLM observations clearly demonstrated differences in the structure of biofilms formed in the presence of dicloxacillin (figure 6.2).

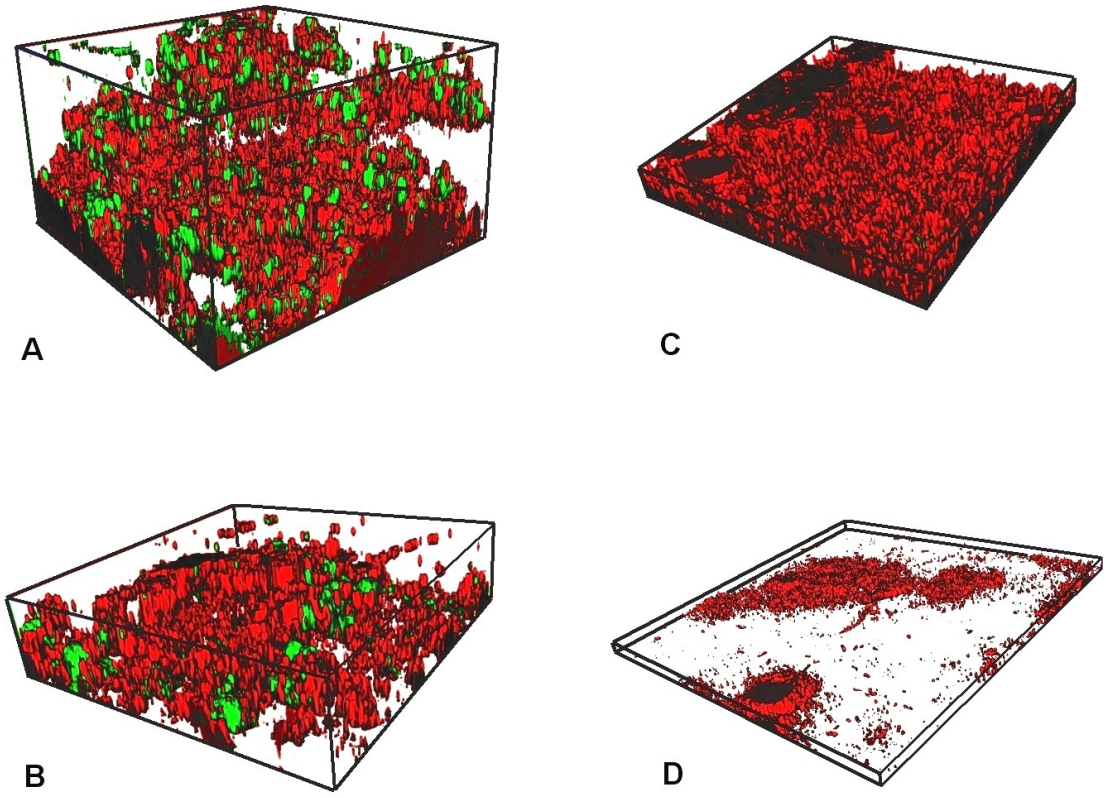

Figure 6.2. 3D representation of the biofilms using confocal microscopy analysis. Green represents the PNAG, asymmetrically distributed in the biofilm, and red represents the bacterial cells. A) M187 CT; B) M187 DCX; C) M176 CT and D) M176 DCX.

First, biofilms formed in the presence of sub-MIC concentrations of dicloxacillin were less thick than control biofilms grown without the antibiotic. *S. epidermidis* M187 biofilms were 100 ± 28 μm thick when formed without antibiotic and 49 ± 14 μm when sub-MIC concentrations of dicloxacillin were present. In *S. haemolyticus* M176 biofilms, the reduction of thickness was from 30 ± 13 μm to 8 ± 3 μm. These reductions were both statistically significant ($p<0.05$, paired t-test).

Besides the difference in the biofilm thickness, sub-inhibitory concentrations of dicloxacillin also influenced the surface area covered. The CSLM images of *S. epidermidis* M187 and *S. haemolyticus* M176 biofilms show that control biofilms covered the entire abiotic surface (figure 6.2A and 2C) whereas biofilms formed in sub-MIC of dicloxacillin exhibited only a partial degree of surface coverage (figure 6.2B and 2D). This reduction is more accentuated in *S. haemolyticus* biofilms.

The presence of PNAG as a major component of the biofilm matrix, as measured by WGA binding, was only detected in *S. epidermidis* M187 biofilms, and was more abundant in the control compared to biofilms grown in the sub-MIC of dicloxacillin.

6.2.4. Cell surface properties

Table 6.2 summarizes the effect of dicloxacillin on some bacterial cell surface properties. Cells entrapped in biofilms formed in sub-inhibitory concentrations of dicloxacillin had significantly lower ($p<0.05$, paired t-test) water contact angles, reflecting a decrease in hydrophobicity [18].

Table 6.2. Bacterial cell surface properties of the biofilms of *S. epidermidis* M187 and *S. haemolyticus* M176 formed in the presence (DCX) and absence (CT) of sub-MIC concentration of dicloxacillin (± represents the SD).

Strain	Contact angle	Surface elemental composition		
		N/C	O/C	P/C
M187 CT	28.0 (± 1.1)	0.192 (± 0.009)	0.480 (± 0.037)	0.032 (± 0.004)
M187 DCX	22.9 (± 1.6)	0.145 (± 0.025)	0.399 (± 0.001)	0.038 (± 0.005)
M176 CT	36.4 (± 2.2)	0.152 (± 0.045)	0.397 (± 0.011)	0.031 (± 0.004)
M176 DCX	31.8 (± 1.7)	0.191 (± 0.041)	0.441 (± 0.052)	0.027 (± 0.005)

XPS analysis also revealed differences in the surface elemental composition of the biofilm cells. The high O/C ratio observed is a common CoNS characteristic and can be related to the presence of a slime layer surrounding the cell wall [228] suggesting that *S. epidermidis* cells formed on sub-MIC concentration of dicloxacillin may elaborate less slime than the control biofilm cells. The opposite was found for *S. haemolyticus* biofilm cells, whereby the O/C ratio was higher in the presence of dicloxacillin, suggesting that the control biofilms had less slime layer surrounding the cells.

6.2.5. Biofilm matrix

Figure 6.3 presents the detection and relative quantification of the PNAG present in the biofilm matrix. PNAG was only detected in *S. epidermidis* biofilms, being absent from *S. haemolyticus* biofilms. The amount of PNAG per cell produced in *S. epidermidis* biofilms was slightly lower in biofilms formed under sub-MIC concentrations of dicloxacillin.

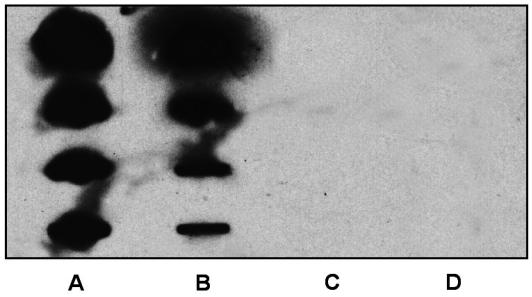

Figure 6.3. Immunological detection and relative quantification of PNAG extracted from the biofilm matrix: M187 CT (A), M187 DCX (B), M176 DCX (C); M176 CT (D). Rows 1-4 represents serial 4-fold dilutions of cell-surface extract.

Table 6.3 presents the composition of the biofilm matrix formed in the presence or absence of sub-MIC concentrations of dicloxacillin. In both CoNS species, each biofilm matrix presented a significantly lower ($p<0.05$, paired t-test) protein content per number of cells in the biofilm, when formed in the presence of dicloxacillin.

Table 6.3. Composition of the biofilm matrix, expressed in $\mu g/10^8$ cell, of biofilms of *S. epidermidis* M187 and *S. haemolyticus* M176 formed in the presence (DCX) or absence (CT) of sub-MIC concentration of dicloxacillin ($\pm$ represents the SD).

Strain	Proteins	Polysaccharides
M187 CT	3.39($\pm$ 0.20)	1.52($\pm$ 0.32)
M187 DCX	2.81($\pm$ 0.74)	0.99($\pm$ 0.39)
M176 CT	3.26($\pm$ 0.35)	0.98($\pm$ 0.48)
M176 DCX	1.37($\pm$ 0.38)	1.77($\pm$ 0.59)

With respect to polysaccharide production, *S. epidermidis* biofilms formed in sub-MIC of dicloxacillin produced significantly lower amounts ($p<0.05$, paired t-test) than the control. Conversely, *S. haemolyticus* control biofilm matrix presented a significantly higher ($p<0.05$, paired t-test) polysaccharide content, per cell in the biofilm, compared to the biofilm matrix formed in sub-MIC of dicloxacillin.

6.2.6. Antibiotic resistance

The growth in sub-MIC concentrations of dicloxacillin induced an increase in the resistance of the biofilm cells to dicloxacillin as well as antibiotics with different mechanisms of action including tetracycline and rifampicin. The most pronounced increase in resistance was to dicloxacillin (figure 6.4).

6.3. Discussion

CoNS biofilm infections have become a serious problem in the last few years [231,232]. Several strategies have been evaluated to inhibit biofilm formation. Previous reports suggested that the use of sub-MICs of antibiotics could increase biofilm formation [189]. However, more recent studies demonstrate that sub-MICs of some antibiotics are effective in reducing the amount of biofilm formed [38,79,181,247], which may have some clinical interest. However, other changes that can occur in the physiology of biofilm cells might compromise the general use of this strategy to prevent biofilm formation. Several studies have reported an increase in antibiotic resistance due to bacterial growth in sub-MIC concentrations of antibiotics [79,219]. Even so, the prophylactic use of antibiotics to prevent CoNS infections is widely used [86]. In the study described in this chapter, changes in the biofilm structure and matrix composition and also in antimicrobial resistance were observed when sub-MIC concentrations of dicloxacillin were used. It must be stressed that the concentration of dicloxacillin used was low enough not to inhibit the growth of bacteria (table 6.1).

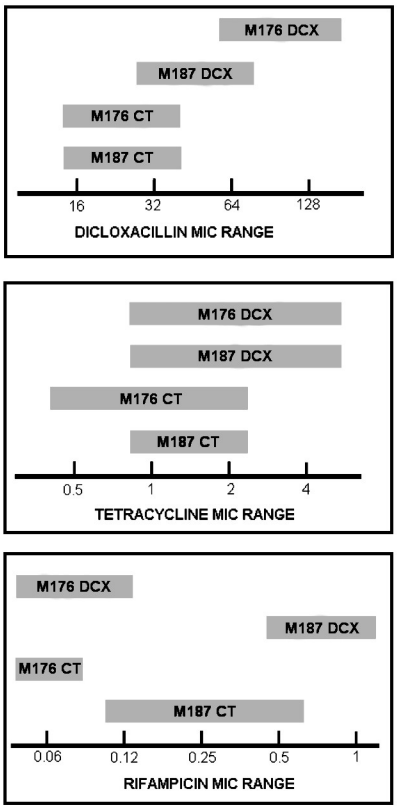

Figure 6.4. Shift in the MIC range of dicloxacillin, tetracycline and rifampicin, of the biofilm cells formed in the presence (DCX) or absence (CT) of sub-MIC concentrations of dicloxacillin.

Bacterial adhesion to surfaces is the first step in biofilm formation [236]. Hydrophobic interactions play an important role in initial adhesion to inert surfaces [61]. Cells from both biofilms formed in the presence of sub-MIC of dicloxacillin presented lower water contact angles, indicating a decrease in hydrophobicity [18]. This lower cell surface hydrophobicity could have had an impact in the initial adhesion to the surface. CSLM observations revealed that a reduced extent of surface coverage by the biofilms exposed to sub-MIC levels of dicloxacillin compared to the controls. While control biofilms formed in the absence of dicloxacillin covered the entire substratum, biofilms exposed to sub-MICs of dicloxacillin were

not able to colonize the entire available surface. These data suggest that sub-MIC concentrations of dicloxacillin probably inhibit initial adhesion by diminishing cell surface hydrophobicity. Nevertheless, the reduction of cell surface hydrophobicity cannot fully account for the decrease in the amount and thickness of biofilms formed in the presence of sub-MICs of dicloxacillin. As demonstrated in chapter 3, initial adhesion and biofilm formation are not always directly related [42]. Cell-to-cell adhesion, which is associated with the production of an intercellular adhesin (PNAG) in *Staphylococci spp*., plays a critical role in biofilm formation and maturation [236].

PNAG production was semi-quantitatively evaluated by means of an immunological detection assay, and also by CSLM observations of biofilms treated with the lectin, WGA. CSLM has been successfully used in a wide range of assays as a tool to determine the composition and structure of biofilms [106,130]. In the present study, besides evaluating the spatial structure of biofilms, this technique also enabled the detection of PNAG in the matrix of the biofilm. PNAG production was only detected in *S. epidermidis* biofilms. In these biofilms, the amount of PNAG produced per cell was slightly reduced in the sub-MIC formed biofilms. Since PNAG production is related to biofilm formation in *Staphylococci* [88,151] these results can explain the reduction on biofilm formation. Interestingly, in *S. haemolyticus* biofilms no PNAG was detectable. This could mean that: 1) either *S. haemolyticus* produces levels of PNAG that are below the level of detection of both methods; or 2) the exo-polysaccharide of *S. haemolyticus* is structurally different and the probes used, which are very specific, were not able to detect it; or 3) *S. haemolyticus* does not produce PNAG. To address this questions, the presence of the *icaC* gene in both species by PCR amplification was assessed, and while *S. epidermidis* was positive for the *icaC* gene, *S. haemolyticus* was *icaC* negative. Absence of the *ica* locus seems to be common in CoNS species. De Silva *et al.* [58] probed for the presence of the *ica* locus in 180 CoNS strains and found that the prevalence of *ica* genes in *S. epidermidis* was around 50% and that those genes were absent in *S. haemolyticus* strains. According to the present study, biofilm quantification assays clearly demonstrate that *S. haemolyticus* does not form a biofilm as thick as *S. epidermidis*. Since PNAG has been described as the molecule responsible for biofilm formation in many strains of staphylococci, the data obtained seem to suggest that *S. haemolyticus* M176 does not produce PNAG and therefore can not form a thick biofilm.

Interestingly, *S. haemolyticus* was very aggregative, especially in the presence of sub-MIC of dicloxacillin. However, these cell aggregates were not firmly attached to the surface. The results provided by the XPS analysis revealed that cells of *S. haemolyticus* biofilms formed in the presence of sub-MIC dicloxacillin have a higher O/C ratio. This characteristic

can be associated with an increase in the slime layer content of the outer cell surface [228] that can explain the more aggregative appearance of *S. haemolyticus* cells.

Biofilm formation in sub-MICs of dicloxacillin also influenced the composition of the biofilm matrix. It has been suggested that the matrix of biofilms can be responsible for the increased resistance to antibiotics by acting as a diffusion barrier [57,215]. Changes in the biofilm matrix can therefore influence susceptibility of the biofilm cells to antibiotics. In both species studied, the matrix composition was clearly different between the control biofilm and the sub-MIC biofilm. Biofilm cells, after growing 1 day in the presence of sub-MIC concentrations of dicloxacillin, developed a slightly increased resistance to several antibiotics with different mechanisms of action. This shift in the MIC range was more drastic when dicloxacillin was used in the MIC assay. Similar results have been reported by other authors [79].

The rise of antimicrobial resistance can compromise the use of the sub-MIC approach to prevent biofilm formation. New approaches are being developed based on the same principle of sub-MIC alterations in growth, but using other molecules like non steroidal anti-inflammatory drugs [7], or specific enzymes that target biofilm formation [99,238] which are not associated with the problem of antimicrobial resistance. However, new studies should also provide more information regarding other changes on the biofilm physiology, like the results reported here leading to a better understanding of the biofilm formation and treatment processes, rather than just focusing on the inhibition of biofilm formation.

Chapter 7

Susceptibility of S. epidermidis planktonic cells and biofilms to the lytic action of staphylococcus bacteriophage K

Summary

In this chapter the activity of bacteriophage K against S. epidermidis planktonic and biofilm cells was tested, to evaluate phenotypic resistance to phage K, and to determine its potential role as an antimicrobial agent against S. epidermidis biofilm infections. Planktonic or biofilm cultures were infected with phage K and bacterial viability was evaluated by standard bacterial enumeration techniques. Phage K could infect and kill most of the S. epidermidis strains. When infecting biofilm cultures, phage K was also efficient at reducing the number of viable cells, suggesting that this agent can be used to treat biofilm infections.

7.1. Materials and Methods

7.1.1. Bacteria, Phage and growth conditions

Phage K and its host propagating strain *S. aureus* DPC5246 were a kind gift from A. Cofey (Cork, Ireland). All 11 *S. epidermidis* strains were used to test the phage host range. More information about these *S. epidermidis* strains is presented in the supplements section, page 179.

TSB and TSA were prepared according to the manufacturer's instructions. Top agar was prepared by adding 0.6% agar to TSB medium. All strains were incubated in 15 ml of TSB inoculated with bacteria grown on TSA plates not older than 2 days, and grown overnight at 37ºC in a shaker rotator at 130 rpm. Bacteria were then harvested by centrifugation (for 5 min at 10,500 g and 4ºC), washed twice and resuspended in a saline solution (0.9% NaCl prepared in distilled water) to a concentration of 1×10^9 cells/ml.

7.1.2. Phage propagation

Phage propagation was performed as described previously [206] with some modifications. Briefly, 90 ml of top agar, 1 ml of bacteria and 1 ml of phage K containing 1×10^9 plaque forming units (pfu) were added to a T-flask containing a thin layer of TSA. The T-flask was incubated for 18 H at 37ºC. Phage K was removed by elution from the top agar by adding 90 ml of SM buffer (5.8 g/l NaCl, 2 g/l $MgSO_4.7H_2O$, 50 ml/l 1M Tris pH 7.5) to the T-flask and incubated for 24 H at 4ºC with rotation at 50 rpm. SM buffer was recovered and centrifuged at 10,000 g during 10 min at 4ºC. Then, 4 volumes of the supernatant were added to 1 volume of chloroform followed by 30 s of vortexing. The organic and aqueous phases were separated by centrifugation at 4,000 g during 10 min at 4ºC. The aqueous phase, containing the phages, was stored at 4ºC until required.

7.1.3. Phage enumeration

Phage enumeration was performed as described previously [206]. Briefly, the phage sample was diluted 10 fold in SM buffer. Then, 100 µl of each phage dilution was added to 100 µl of *S. aureus* DPC5246 resuspended in 0.9% NaCl. This suspension was mixed with 3 ml of top agar and poured onto the surface of a TSA plate. The plates were incubated for 18 H at 37ºC and the number of plaques (PFU's) were counted. All experiments were done in duplicate with 3 repeats.

7.1.4. Phage host range

The ability of phage K to infect and kill *S. epidermidis* strains was performed in a plaque assay as described previously [171]. Briefly, for each *S. epidermidis* strain, 100 µl of an

overnight culture resuspended in 0.9% NaCl was mixed with top agar and poured in a Petri dish with a thin layer of TSA. After the overlay had solidified, 20 μl of phage containing 8×10^9 pfu's was spotted onto the surface. Plates were air-dried and incubated at 37ºC for 18 H. No clearance of the cell lawn indicated resistance to phage K; an opaque clearing indicated low susceptibility and a transparent clearing indicated high susceptibility to phage K.

7.1.5. Susceptibility of planktonic cultures to Phage K

For each strain susceptible to phage K, 200 μL of a cell suspension adjusted to 1×10^9 cells/ml in 0.9% NaCl was added to 20 ml of TSB, and incubated at 37ºC with shaking at 130 rpm, until a cell density of 2×10^8 cells/ml was reached. Then, phage K was added at different multiplicities of infection (MOI) (0, 0.1, 0.5, 1 and 5) and growth was allowed to occur during 5 H. Samples were collected at different time points, and the OD_{640nm} was determined. The sample was also diluted 10 fold and plated in triplicate in TSA. Plates were then incubated overnight at 37ºC.This experiment was repeated 3 times.

To determine the concentration of phage in suspension, during bacterial growth, a sample was collected every hour and phage was quantified as described above (7.1.3).

7.1.6. Biofilm formation

Biofilm formation was performed for 24 H in a batch system, as described in chapter 2, using 96 well polystyrene microtiter plates.

7.1.7. Susceptibility of biofilms to Phage K

For each strain susceptible to phage K, biofilms were formed, as described above, for 24 H in TSBG. Then, each biofilm was washed twice in 0.9% NaCl to remove planktonic cells. Next, 2×10^8 pfu of phage K diluted in 0.9% NaCl was added to half of the wells, and as negative controls, 0.9% NaCl was added to the remaining half of the wells. The microtiter plates were incubated for 24 H at 37ºC and 130 rpm. The biofilms were washed twice in 0.9% NaCl, and the total biomass of the biofilms was determined by crystal violet staining, as described in chapter 6. This experiment was repeated 3 times.

7.1.8. Susceptibility to phage K of biofilm-grown cells *vs*. planktonic cultures

S. epidermidis M187 was selected for this study. Biofilms were formed for 24 H in TSBG as described above. The biofilms were then scraped from the surface and resuspended in 0.9% NaCl, as described in chapter 4. Resuspended biofilms were then vortexed for 20 s and sonicated during 20 s at 20 W, to solubilize the bacteria. Planktonic bacteria were grown for 24 H in TSB, in order to obtain cells in the stationary growth phase. The suspension was

centrifuged at 10,000 g for 5 min and resuspended in 0.9% NaCl by vortexing for 20 s and sonication during 20 s at 20 W. Both suspensions were then diluted in a poor medium (10% TSB diluted in 0.9% NaCl) to an OD_{640nm} of 0.4, that was equivalent to ~2×10^8 cells/ml, as determined by microscopic counting using a Neubaur chamber. Phage K at a MOI of 1 was added to each suspension, and the reduction of OD_{640nm} was monitored during 5 H, as compared to a control without phage. This experiment was repeated 3 times with triplicates.

7.2. Results

7.2.1. Host range of phage K

The results from the phage host range screening are summarized in table 7.1. Of the 11 strains used, only 1 was not susceptible to phage K. Considering the remaining strains, 4 were highly susceptible to phage K, as determined by the transparent clearance of the cell lawn, while the clearance of the cell lawn of the remaining 6 strains was not so evident (figure 7.1).

Table 7.1. Activity of phage K on *S. epidermidis* clinical isolates

Bacterial strain	Biofilm formation ability [47]	Phage sensitivity *
S. epidermidis 9142	+	+/-
S. epidermidis 9142-M10	-	+/-
S. epidermidis IE75	-	+/-
S. epidermidis IE186	+	+/-
S. epidermidis IE214	+	+/-
S. epidermidis M129	-	-
S. epidermidis M187	+	+
S. epidermidis FJ6	-	+
S. epidermidis JI6	+	+
S. epidermidis LE7	-	+
S. epidermidis PE9	+	+/-

* no clearance of cell lawn (-),some clearance of cell lawn but opaque (+/-),clearance of the cell lawn(+).

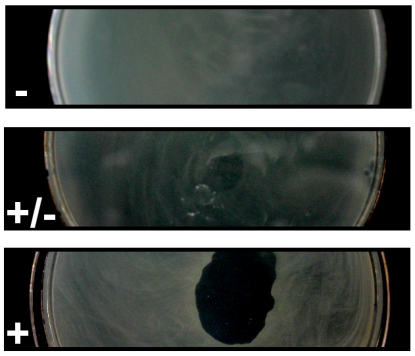

Figure 7.1. Aspect of *S. epidermidis* M129 (-), PE9 (+/-) and M187 (+) cell lawns challenged with phage K.

For further studies, 2 strains with different susceptibilities to phage K were selected: *S. epidermidis* M187, which is highly susceptible to phage K and *S. epidermidis* PE9 exhibiting a low susceptibility, as determined by the transparent clearance of the cell lawn, *S. epidermidis* PE9 only presented a low susceptibility (figure 7.1). The criterion used to select these 2 strains was also based in their ability to form biofilms in order to better compare the action of phage K on *S. epidermidis* biofilms. Accordingly, both strains have high (and similar) biofilm formation abilities, as described in section I.

7.2.2. Susceptibility of planktonic cultures to phage K

The lytic activity of phage K against planktonic cultures of *S. epidermidis M187* and *S. epidermidis PE9* in the exponential phase of growth is illustrated on figure 7.2. Bacteria were challenged with phage at MOI, from 0.1 to 5.

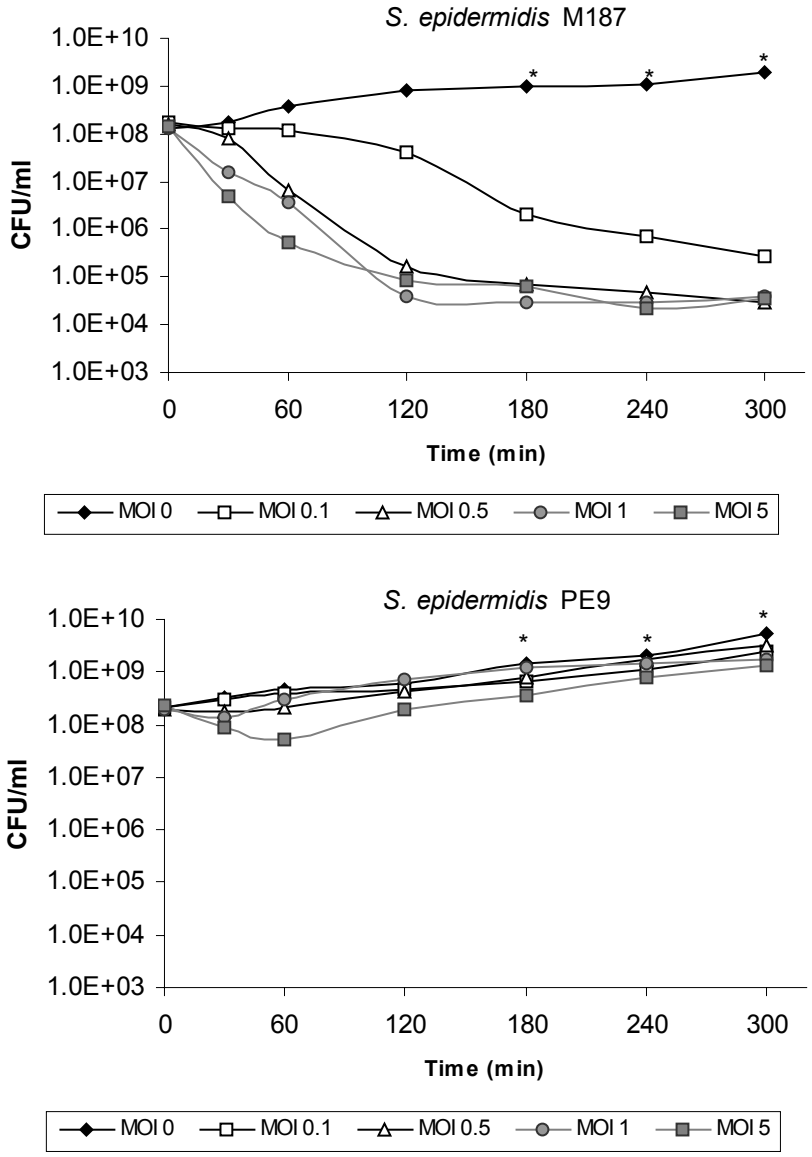

Figure 7.2. Susceptibility of *S. epidermidis* M187 and PE9 to phage K at different MOI.
* at these time points, macroscopic clusters of cells were observed, suggesting that there was more growth than as detected by plating aliquots of the suspension.

S. epidermidis M187, which was considered susceptible to phage K by the plaque assay, was killed more than 99.99% in less than 2 H, with a MOI of 5 or 1. Even with a MOI as low as 0.1, after 5 H 99.90% of *S. epidermidis* M187 cells were lysed. In a previous report using *S. aureus*, phage K demonstrated a similar high ability to lyse planktonic bacteria [20].

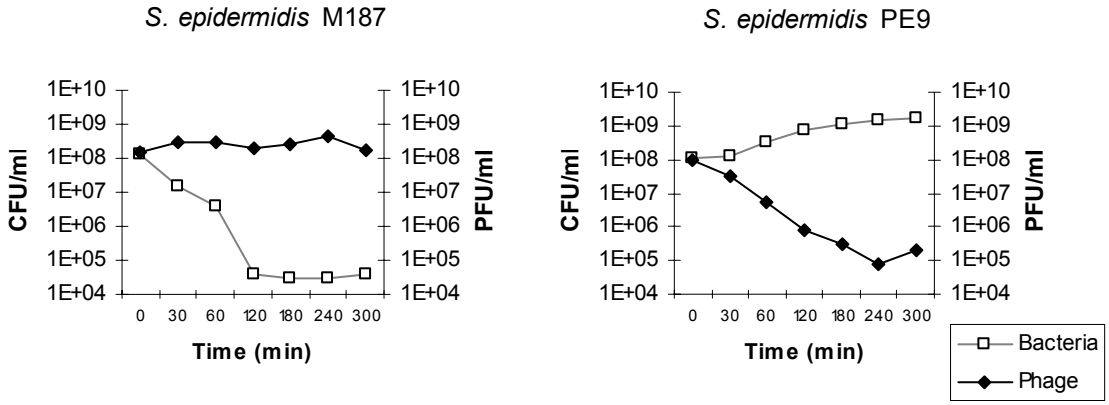

Figure 7.3. Evolution of the number of bacteria and phage after infection, for *S. epidermidis* M187 and PE9.

The lytic performance of phage K against the less susceptible strain *S. epidermidis* PE9 was not so high, except when using a MOI of 5. Nevertheless, at this high MOI and 1 H after phage challenging, bacteria started to grow again. The concentration of phage K present in suspension during the 5 H of the assay was also measured. Interestingly, while for strain M187 the concentration of phage K increased during the first hour and then remained constant, for strain PE9 the concentration of phage K decreased 1000 fold in 4 H, and then remained constant (figure 7.3).

7.2.3. Susceptibility of biofilms to phage K

To determine the action of phage K in *S. epidermidis* biofilms, strains M187 and PE9 were grown in TSBG in 96 well polystyrene microtiter plates for 24 H, after which the biofilms were challenged with phage K.

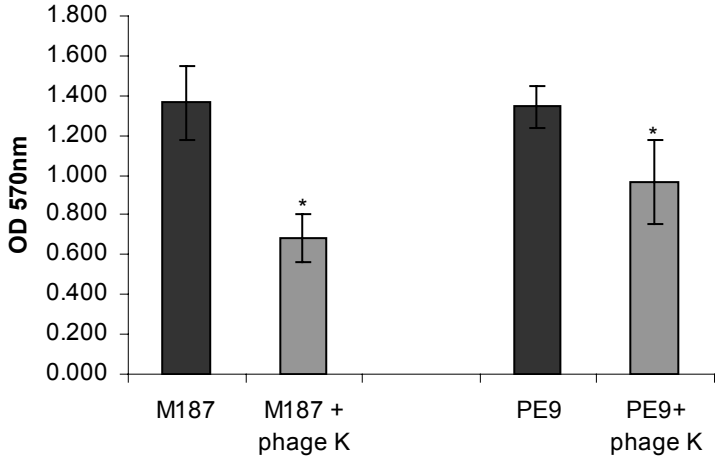

Figure 7.4. Reduction of biofilm biomass after 24 H of challenge with 2×10^8 pfu's of phage K. * significant reduction in biomass compared to control ($p<0.05$, paired samples t-test).

As illustrated on figure 7.4, 24 H after the challenge there was an evident reduction in the biomass of *S. epidermidis* M187 biofilm, as compared to the control. Interestingly, biofilms of PE9 were also significantly reduced (paired samples t-test, $p<0.05$) as compared to the controls, although not as much as with M187 biofilms.

7.2.4. Susceptibility to phage K. of biofilm-grown cells *vs.* planktonic cultures

To compare planktonic and biofilm-grown cell susceptibilities to phage K, the lytic assays were performed with *S. epidermidis* M187 planktonic cells at the stationary growth phase (after 24 H of growth) and 24 H biofilm-grown cells, in a low-nutrient medium in order to slow down the growth rate of cells and to preserve the biofilm phenotype for the maximum possible time.

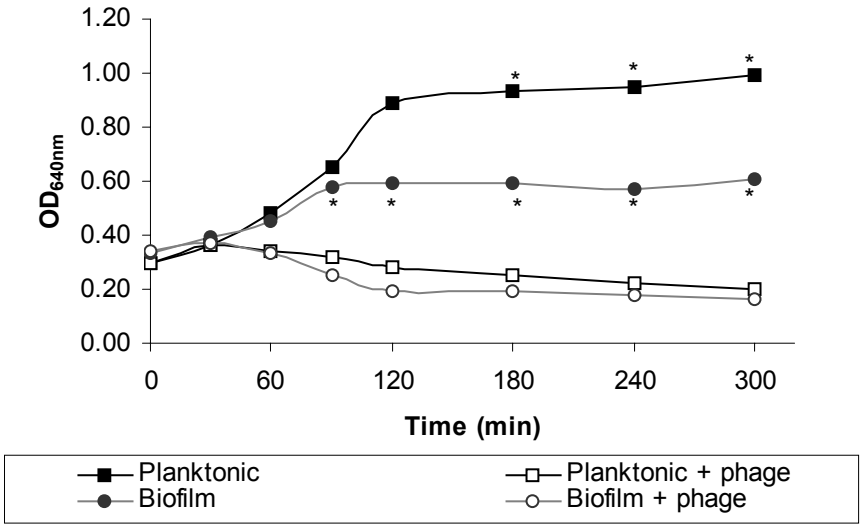

Figure 7.5. Comparison between planktonic and biofilm-grown cells susceptibility to phage K. * at these time points, macroscopic clusters of cells were observed, suggesting that there was some cell growth, even in the absence of the increase of OD.

Figure 7.5 illustrates the effect of phage K at a MOI of 1, in biofilm grown cells and also in planktonic stationary phase cells. Biofilm grown cells and stationary phase planktonic cells demonstrated similar susceptibility to phage K. It was interesting to notice that the biofilm-grown cells started to aggregate relatively quickly, and after 90 min of phage challenging, no more cell growth was detected in planktonic cells assay (as determined by no increase of the OD of the cell suspension), although macroscopic cells clusters were detected. Cell clusters were also detected in the planktonic culture, but only after 180 min of growth.

7.3. Discussion

With the emergence of antibiotic resistance in many of the main human bacterial pathogens, some attention has been directed to the potential of phages as antimicrobial

agents. Phages can be very specific, making them harmless to eukaryotic cells and even to other bacteria. This feature presents an advantage to broad-spectrum antibiotics, which, when they work, can also kill beneficial flora in the intestinal tract [223]. Phages can be divided into temperate or lytic types; while temperate phages have integrase enzymes, allowing them to recombine their DNA into the host DNA, coexisting with the host, lytic phages don't have this class of enzymes and will necessary kill the host [23]. Lytic phages are preferred in phage therapy, due to safety reasons, since the recombination of phage and host DNA could potentially be dangerous [24,35]. Bacteriophage K is a lytic phage [171], therefore being a possible candidate in future phage therapy.

Another major advantage of phages, regarding antibiotics, is that phages have the ability to replicate in the presence of the host bacteria, while the antibiotic concentration will decay after the initial administration. Previous studies performed by other authors demonstrated that after lethal intramuscular or intracerebral injection of *Escherichia coli*, a single dose of phage was more effective that multiple doses of tetracycline, ampicillin, choramphenicol or trimethoprim plus sulphafuraxole [207].

Phage K has been previously described as a polyvalent phage, with the ability to infect and kill 9 different species of Staphylococcus, including *S. epidermidis*. [171]. However, the host range of phage K in *S. epidermidis* clinical isolates was not previously evaluated. Phage K was found to be effective against most of the clinical isolates previously characterized in terms of biofilm formation abilities (chapter 3) and susceptibilities to antibiotic therapy (chapter 4). To better compare the efficacy of phage K against biofilm infections, kill experiments were performed only with two of the strains sensitive to phage K and having equal and high abilities to form biofilms on medical surfaces [42].

Although relatively large numbers of phage are found in biofilm-related environments, little information exists regarding the role of phages in biofilms [216]. An interesting study using *Pseudomonas fluorescens* demonstrated that both planktonic and biofilm bacteria were equally susceptible to phage killing [206]. It is already well established that biofilm bacteria are often refractory to antibiotic therapy [211]. The use of phages to control antibiotic-resistant biofilm infections can therefore be seen as another potential advantage of phage therapy. One of the drawbacks regarding phage therapy has to do with the possibility that bacteria will acquire phage resistance, in the same way observed for antibiotic resistance. However since phages are also living organisms, they also evolve and can adapt to new bacterial strains. Buckling and Rainey have demonstrated this principle using *P. fluorescens* and its phage [27]. As described in several other reports [16,206,222], a few hours after the bacterial population reached its minimum, some growth occured. This new bacterial population was tested to see if

they had acquired resistance to phage K, using the plaque assay. The results revealed that the bacteria were still susceptible to phage K (data not shown).

Planktonic cells of strain M187 were highly susceptible to phage K. A fast decrease in the number of viable cells was observed even when low concentrations of phage were used. Conversely, planktonic cells of PE9 were only susceptible to a very high phage concentration (figure 7.2). The release of new phages is expected after cell lysis in a normal lytic cycle, increasing the phage titre. This fact was only observed when M187 was the host strain. In the assays with PE9 (figure 7.3), there was a quick drop of the phage titre from ~2X10^8 pfu/ml to ~5X10^6 pfu/ml 1 H after the challenge, which could be due to phage adsorption to the host surfaces and/or phage inactivation. Since it has been found that some media can inhibit phage propagation [170], it was tested whether this quick drop in phage titter could be due the influence of the TSB medium, by incubating phage K at ~2×10^8 pfu/ml in TSB at 37ºC. After 5 H, the phage titter was only reduced ~30%, excluding the possibility that TSB alone was responsible for the fast decrease of the phage titter in the PE9 challenge (from ~2×10^8 pfu/ml to ~1×10^5 pfu/ml). The phage titter stabilized 4 H after the PE9 challenge. It seems that while in the M187 strain the rate of cell lysis and rate of phage release is very fast, in strain PE9 the rate of cell lysis and phage release is comparatively lower.

When phage K was applied to a 24 H biofilm of either the highly susceptible strain M187 or the poorly susceptible strain PE9, no biomass reduction was observed 5H after phage challenge (data not shown). However, 24 H after the phage challenge, a significant reduction of the biomass of both M187 and PE9 biofilms was detected, although less pronounced for PE9 biofilms. This result suggests that phage lytic action against biofilms is slower than against planktonic cultures. Sillankorva *et al.* also showed that phage action in biofilms was slower compared to planktonic cultures of *P. fluorescens* [206] but nevertheless the total biomass reduction was equivalent in both planktonic and biofilm cultures. Previous studies have demonstrated that phages are able to penetrate the biofilm matrix [216], therefore the slower lytic performance of phages against biofilms is probably due to the physiological state of biofilm cells, and not to diffusion barriers. In order to better compare the phage K lytic action against planktonic and biofilm cells of *S. epidermidis* M187, the same concentration of planktonic and biofilm cells were used in the assays. Moreover, the planktonic cells used were grown in a low nutrient medium and harvested at the stationary growth phase and the biofilms were dispersed and sonicated in order to achieve a suspension of biofilm-grown cells. Both planktonic and biofilm-grown cells demonstrated low rates of killing by phage K (figure 7.5). Also interesting was the fact that planktonic cells in exponential growth phase were much more sensitive to phage K lysis than stationary growth phase planktonic cells. This effect was previously demonstrated for *P. fluorescens* planktonic cultures [206]. It seems that biofilms are

slowly killed by phage K, not due to a specific biofilm phenotype, but probably due to the low metabolic activity of biofilms [17,48,208,217].

Section III

Immune response to biofilm infections

Section III cover image represents the immune response after 24 H of intraperotineal challenge with S. epidermidis 9142 biofilm-grown cells. Mario Arala-Chaves Immunology Laboratory, ICBAS, Porto University, Porto, Portugal.

Introduction

The human body is in constant contact with microorganisms: billions of bacteria are present in and on the human body, and most of these bacteria play beneficial and even essential roles for the human host [139]. However, some bacteria can sometimes cause disease and eventually kill their host. The human immune system is responsible for combating these pathogenic bacteria [146]. *S. epidermidis* and the rest of CoNS are considered opportunistic pathogens, since they normally inhabit host tissues without damage to the host and only in specific circumstances cause disease [239].

The human immune response can be divided in 2 different categories: the innate immune response or the adaptive immune response [146]. The latter may involve antibody production, the activation of specific immunologically competent cells, or both [138]. The differences between these 2 types of response is that the adaptive immune response is highly specific for a particular pathogen and improves with each successive encounter with the same pathogen, while the innate response is non specific and does not improve, even after repeated exposure to the same pathogen [146] (see figure III).

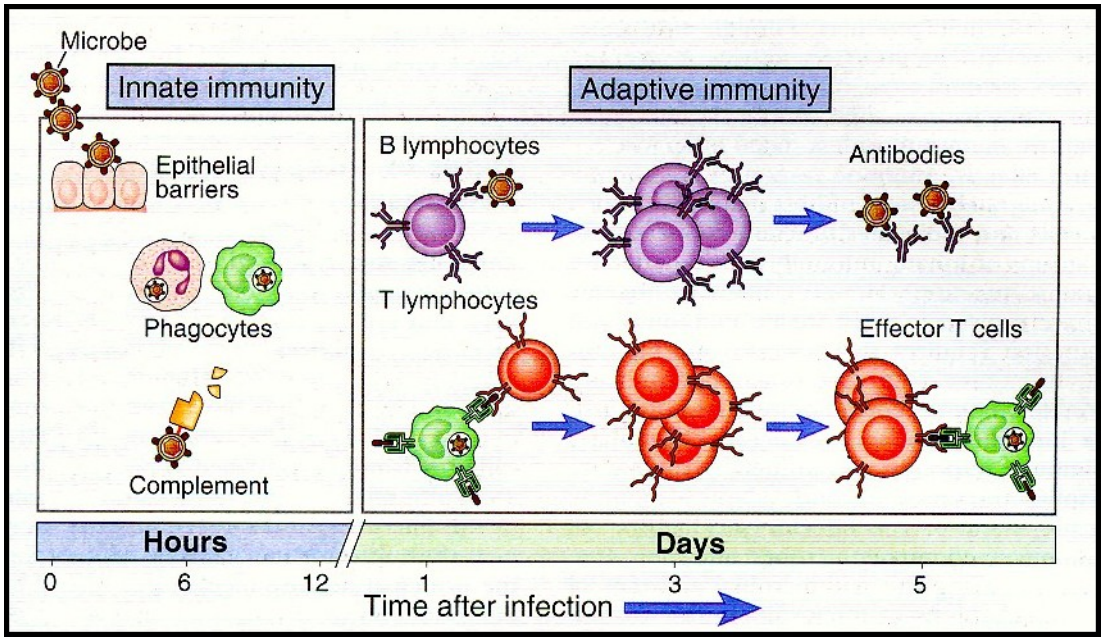

Figure III. Major group of cells involved in the innate and adaptive immune response. Adapted from Abbas and Lichtman, Cellular and Molecular Immunology,5th ed (2003), Elsevier Science.

The main cells involved in the innate response are generally called phagocytes, although other cells also play an important role such as NK cells, mast cells and eosinophils. Phagocytes can bind, internalize and then eventually kill the pathogens [133]. Neutrophils (also called PMN's) constitute the majority of the circulating phagocytes [146] and are short-lived cells (2-3 days) [138]. Macrophages are another group of phagocytes, but are long-lived

cells and have an interesting characteristic, absent in neutrophils: they can interact with cells of the adaptive immune response, in a process called antigen presentation [146]. Dendritic cells can also internalize pathogens and are much more important for antigen presentation to the cells involved in the adaptive immune response.

Responsible for the adaptive immune response are the lymphocytes. There are 2 major groups of lymphocytes: B cells and T cells [133]. B cells mainly interact with pathogens that reside in the tissue fluids or blood (extracellular pathogens) while T cells have a wider role: (a) they can kill host-infected cells, (b) they can help B cells in the production of antibodies against extracellular pathogens and (c) they can provide help for the activation of phagocytes [146]. The immune cells express a large number of different molecules on their surfaces and some of these molecules are present only on a specific type of cells. Many of these molecules have been identified using specific monoclonal antibodies [133]. This characteristic can be used to identify particular cells, by using specific antibodies coupled with fluorocromes, in a technique called fluorescence-activated cell sorting, also known as flow cytometry [210].

The major components of the host immune response to microorganisms on indwelling devices are part of the innate immune system, particularly phagocytosis by inflammatory cells [234]. Inflammation is one of the most important and ubiquitous aspects of host defense against invading microorganisms [145]. However, inflammation is also an important aspect of microbial pathogenesis since the inflammatory response elicited by an invading microorganism can result in considerable host damage [139]. B cells and IgM antibodies in particular play a role as the first class of Ig to be produced in a typical immune response to a bacterial infection [138].

When bacteria assume the biofilm phenotype, they present several characteristics different from planktonic growth [37,243], including enhanced resistance to antimicrobials (as described in section II) and also differential gene expression [190]. Biofilms also protect the resident bacteria from attack by the immune system [60,235]. However, the basis for this property is still far from well understood. While it has been shown than *P. aeruginosa* biofilms can pose a diffusion barrier to neutrophils [105], Leid *et al.* have shown that human leukocytes can easily penetrate *S. aureus* biofilms but fail to phagocytose the bacteria [128]. After a mature biofilm is formed, they can release antigens and stimulate the production of antibodies, but the bacteria resident within the biofilm are resistant to these defense mechanisms [49].

Recently it was been shown *in vivo* that PNAG protects planktonic *S. aureus* and *S. epidermidis* bacteria against antibody independent phagocytosis [121,238]. Phagocytosis of bacteria with a capsule, like *S. epidermidis* PNAG, is enhanced by a process called opsonization, that involves antibody and complement mediated phagocytosis [138,146]. However, these 2 studies were made with planktonic cells and did not address the biofilm

phenotype that is the major virulence characteristic of *S. epidermidis*. While there are a few studies addressing biofilm infection and immune response [105,154], recently, Leid *et al.* pointed out for the need to distinguish between the immune response of planktonic bacteria and biofilm-grown bacteria [129]. In this section, this issue is addressed evaluating possible differences of planktonic and biofilm bacteria in some *in vivo* and *in vitro* immunological studies.

Chapter 8

Comparative antibody-dependent phagocytosis of S. epidermidis biofilm and planktonic cells

Summary

The results described in this chapter address the in vitro opsonophagocytic ability against total biofilms (i.e. biofilm-grown cells and the surrounding biofilm matrix) and planktonic cells, using rabbit polyclonal antibody to PNAG. Fragmented biofilms were more resistant to opsonic killing than their planktonic counterparts and confocal microscopy analysis demonstrated that S. epidermidis biofilms do not pose a physical barrier to the penetration of antibody. PNAG was quantified on the cell surface and also in the extracelullar medium, and in both conditions, planktonic cells had significantly less PNAG than biofilms. It was hypothesized that PNAG protected biofilms from phagocytosis. To test this hypothesis purified PNAG was added to a planktonic culture and this reduced the opsonic killing of the bacteria, suggesting that the increased resistance of biofilm cells to opsonophagocytosis was due to excessive PNAG protection.

Part of the work described in this chapter has been published in 2006, in Infection and Immunity, 74:4849-4855

8.1. Experimental procedures

8.1.1.Growth conditions and bacteria strains.

For this study the strains that were *ica* positive, strong PNAG producers and formed thick biofilms were selected for use in the opsonophagocytic assays: *S. epidermidis* 9142, IE186, IE214 and M187. All *S. epidermidis* strains were grown at 37ºC on tryptic soy agar plates. Liquid cultures were grown overnight in TSBG, at 37ºC and 200 rpm. Detailed information about these strains is presented in the supplements section, page 179.

8.1.2. Opsonophagocytosis of planktonic and biofilm bacteria by serum raised to PNAG.

Opsonophagocytic assays were performed as described previously [154] with some modifications. Briefly, biofilms were formed in 6 well polystyrene plates, during 48 H in fed-batch system as described in chapter 2, with a constant rocking motion, at 37ºC, in TSBG. Biofilms were fragmented by scrapping from the surface and then sonicated twice for 5 s at 20 W to homogenize the suspension. Planktonic bacteria were grown overnight in TSBG, at 37ºC with shaking, and were sonicated as above. Both suspensions were then diluted in TSBG to a concentration of approximately 2×10^8 cells/ml as determined by the OD_{640nm} The opsonophagocytic assay was performed as described by Maira-Litran [141] using a rabbit polyclonal sera raised against a deacetylated staphylococcal PNAG [143] using a final bacteria concentration of approximately 1×10^6 cells/ml. The assay was done in triplicate and repeated 2 to 3 times.

8.1.3. Confocal scanning laser microscopy analysis

Biofilm preparation for CSLM analysis was performed as previously described [163], with some modifications. Briefly, biofilms formed on 6 well polystyrene plates were washed twice with 0.9% NaCl. The biofilms were then incubated for 2 H at room temperature with a rabbit antibody raised to *S. aureus* PNAG (kindly provided by T. Maira-Litran) produced as described [143] and affinity-column purified [115] as described previously and then washed 3 times for 5 min, with PBS. The secondary antibody used was an Alexa Green-conjugated goat anti-rabbit IgG at 2 μg/ml, and it was incubated with the biofilms for 1 H at room temperature, in the dark, and the biofilms were then washed 3 times for 5 min, with PBS. Some of the biofilms were then incubated with WGA conjugated to Texas Red at 10 μg/ml for 20 min at room temperature, in the dark. After staining, the biofilms were gently rinsed with PBS.

CSLM analysis was performed with an LSM 510 Meta attached to an Axioplan II microscope, as previously described [125], with some modifications. *S. epidermidis* 9142 biofilms were observed using a 63X water immersion objective, using a multiple track channel

analysis: The first channel excitation wavelength was set at 633 nm, with output power of 70%, for detection of the biofilm structure. A second channel, with excitation wavelength at 488 nm, with output power of 10%, was used to detect the antibodies. A third channel, with excitation wavelength at 543 nm, with output power of 70%, was used to detect WGA. The excitation beam splitter used was HFT UV/488/543/633. The filter used to detect the refracted light by the biofilm cells was NFT 635 VIS, BP 500-550 for the antibodies and LP650 for the WGA. The beam splitter used was NFT 545.

8.1.4. Relative quantification of PNAG in planktonic and biofilm cells

For relative evaluation of the concentration of PNAG in biofilms and in planktonic cells, biofilms and planktonic cells of *S. epidermidis* 9142 were selected. Biofilms were scraped and sonicated as described above, and then adjusted to a concentration of approximately 1×10^9 cells/ml as determined by OD_{640nm}. The same was done with the planktonic suspension. PNAG was then extracted and detected as described by Cramton *et al*. [50].

8.1.5. Inhibition of phagocytosis by the biofilm matrix and purified PNAG

Inhibition of phagocytosis was evaluated as described before [143], with some modifications. To obtain the biofilm matrix, a 24 H biofilm was disrupted by sonication, diluted in TSB to a concentration of approximately 1×10^9 cells/ml, and centrifuged at 10,000 rpm, for 10 min. The supernatant was boiled for 5 min, and then allowed to cool down at room temperature. For each ml of supernatant, 20 µl of proteinase K were added and incubated for 60 min at 60°C. Then, proteinase K was heat inactivated by incubating 30 min at 80°C. A solution of 100 µg/ml of purified PNAG that was kindly provided by T. Maira-Litran [141] was also used as a positive control inhibitor. As a negative control, a 24 H culture of *S. epidermidis* 9142-M10 was diluted to approximately 1×10^9 cells/ml and treated with EDTA to extract surface polysaccharides, as described previously [39]. A rabbit polyclonal sera raised against a deacetylated Staphylococcal PNAG [143] was incubated for 90 min at 4ºC diluted 1:1 in either a solution of biofilm supernatant, a solution of 100 µg/ml of PNAG, cell surface extract of 9142-M10 or in TSB. Subsequently, the antiserum was centrifuged, and the supernatant used in an opsophagocytic assay as described above.

8.2. Results

8.2.1. Antibody penetration in the biofilm

To determine whether the 3-dimensional structure of the biofilm acted as a physical barrier to the penetration of macromolecules, PNAG-specific rabbit antibodies were allowed to bind to *S. epidermidis* 9142 biofilms, and then a goat α-rabbit IgG coupled to a fluorescence

dye was added. Confocal microscope analysis of the mixture revealed that the antibodies were able to penetrate deep inside the biofilm, as visualized in the x and y cross-section (figure 8.1) demonstrating that *S. epidermidis* biofilms do not pose a permeability barrier to antibodies. *S. epidermidis* biofilms reached a thickness of approximately 100 μm as described in chapter 6.

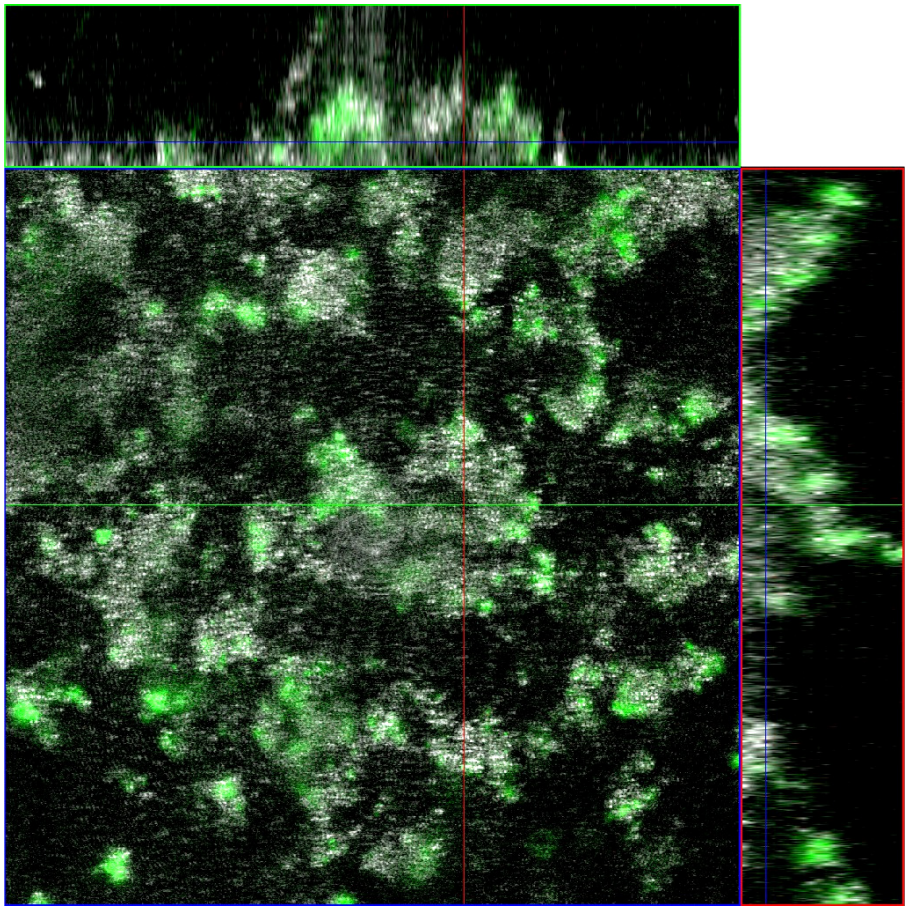

Figure 8.1. Confocal analysis of 9142 biofilm: x, y and z cross-sections of the biofilm, stained with Goat α-Rabbit IgG Alexa 488 conjugated (green).

8.2.2. Localization of the antibody in the biofilm matrix.

Figure 8.2 is a top view of the biofilm representing the result of a 3 distinct confocal microscope channels analysis: 8.2A shows the binding of the antibody; 8.2B shows the biofilm matrix (as result of the lectin binding); 8.2C shows the biofilm 3-dimensional structure and 2D is the combination of all channels. Interestingly, most of the antibody signal (green) overlaps the lectin signal (red) which can be observed as a yellow color that appears on figure 8.2D, meaning that the antibody is mainly bound to the biofilm matrix.

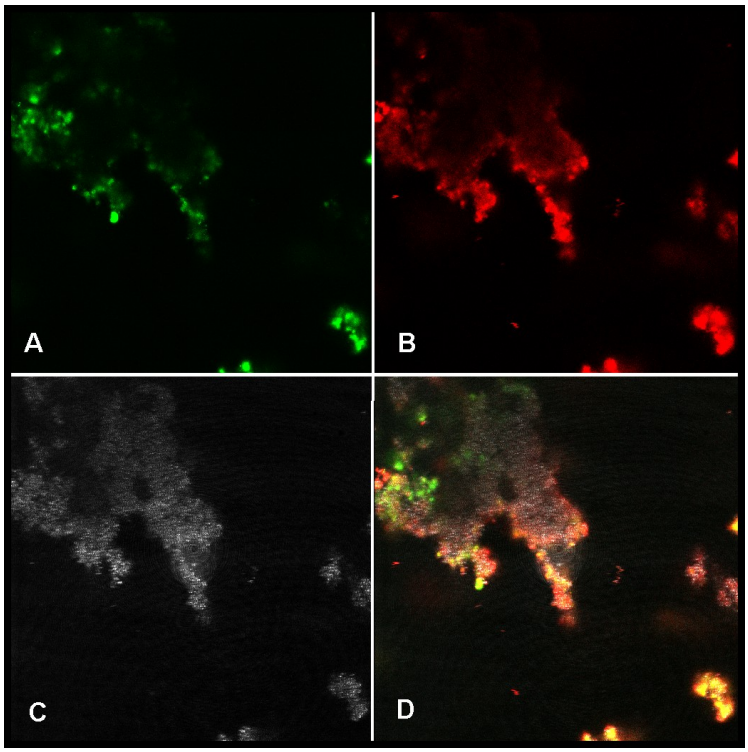

Figure 8.2. Confocal analysis of 9142 Biofilm: z-section of: A) Goat α-Rabbit IgG Alexa 488 conjugated; B) WGA Texas Red conjugated; C) Biofilm structure reflected by far red light; D) co-localization of antibody with WGA.

8.2.3. Opsonophagocytosis of planktonic and biofilm cells.

Figure 8.3 presents the results of the antibody-mediated phagocytosis of suspensions of planktonic and biofilm cells. Interestingly, planktonic cells were more easily killed in the phagocytic assay than biofilm cells. The average of the opsonic killing of the planktonic cell suspensions was ~60% while in biofilm cells suspension the average dropped to less than 20% (statistically significant, $p<0.05$, paired t-test).

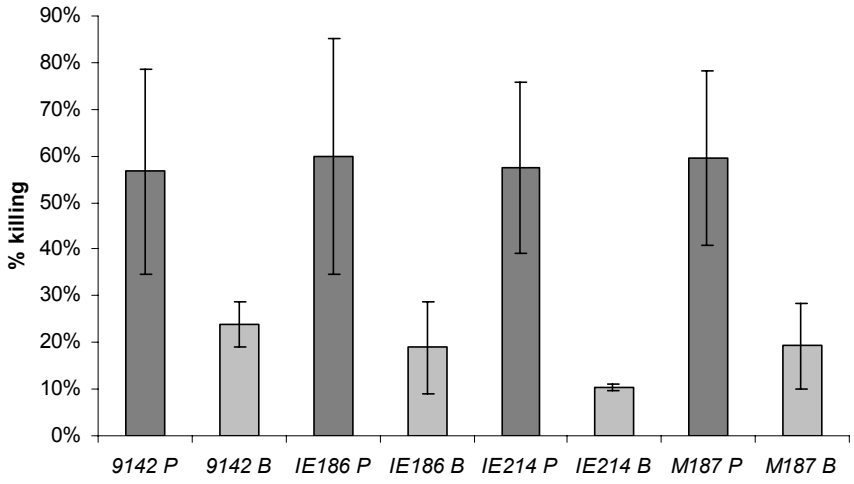

Figure 8.3. Opsonophagocytosis of planktonic (P) and biofilm (B) cells of CoNS mediated by a Rabbit α-dPNAG antibody.

8.2.4. Relative quantification of PNAG in planktonic and biofilm cells.

To compare the amounts of PNAG in biofilm and planktonic cells, secreted or cell surface-associated, suspensions of disrupted biofilms and planktonic cells of *S. epidermidis* 9142 with approximately 1×10^9 cells/ml were used.

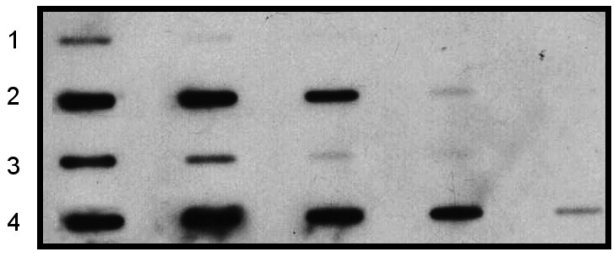

Figure 8.4. PNAG relative quantification with 1:10 fold dilution: 1st lane: supernatant of 9142 planktonic cells; 2nd lane: EDTA cell surface extract of 9142 planktonic cells; 3rd lane: supernatant of 9142 biofilm cells; 4th lane: EDTA cell surface extract of 9142 biofilm cells.

Figure 8.4 presents the relative quantification of PNAG. Both in biofilm and planktonic cells, most of the PNAG was cell surface associated (lane 2 and 4) having approximately 100x more PNAG on the cell surface than in solution. PNAG was also more abundant on the biofilm cells (~10x more) (as expected), and this difference was even more accentuated for the secreted polysaccharide (~100x more in biofilm supernatant than in planktonic supernatant).

8.2.5. Inhibition of phagocytosis by PNAG from the biofilm matrix.

Figure 8.5 demonstrates that previous treatment of the antibody with *S. epidermidis* 9142 biofilm matrix components decreased the antibody efficiency in promoting bacterial killing of planktonic cells.

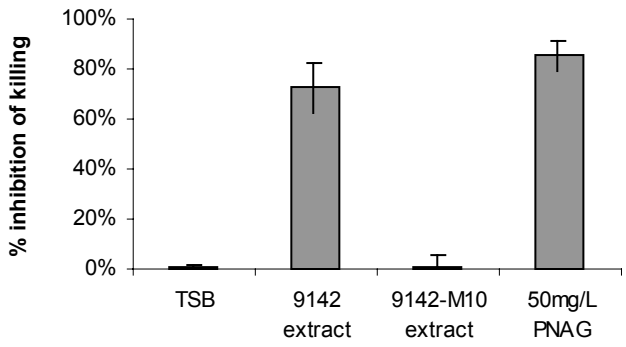

Figure 8.5. Inhibition of phagocytosis of *S. epidermidis* 9142 planktonic cells. Rabbit α-PNAG IgG was adsorbed with TSB (negative control) or with the biofilm matrix or purified PNAG before use in the opsonophagocytic assay.

As a positive control, purified PNAG was also used in the inhibition assay, and as a negative control, cell surface extract of strain 9142-M10 was used. The final concentration of PNAG was 50 μg/ml. Figure 8.5 demonstrates that addition of *S. epidermidis* 9142 biofilm matrix components to antibodies to PNAG decreased the opsonic killing of planktonic cells. While non-inhibited antibodies (simply diluted in fresh medium) would kill ~60% of the planktonic bacteria (as seen in figure 8.3), after incubation of the antibodies to PNAG with the biofilm matrix there was a ~75% inhibition of killing of an equivalent suspension of planktonic bacteria. PNAG at 50 μg/ml inhibited ~90% of the killing and the cell surface extract of strain 9142-M10 didn't inhibit the opsonic killing at all. These results suggest that the high-level synthesis of the PNAG component in the biofilm matrix can bind to the opsonic antibodies and subsequently inhibit the killing of otherwise susceptible bacteria.

8.3.Discussion

In the last few years several studies were published reporting the increased resistance of biofilms to effectors of the immune system [105,118,154,250]. However, it is still not clear if this resistance is associated with bacterial phenotypic alterations triggered by the sessile mode of life. Until now, there was no direct evaluation of the resistance of *S. epidermidis* planktonic or biofilms cells to the immune system. In order to better understand biofilm resistance to the immune system, such a comparison is necessary. Bacteria have a number of mechanisms to evade immune defenses that are unrelated to the biofilm phenotype such as capsule synthesis [158,203], surface protein modification, and molecular mimicry. However, little was known about biofilm-specific properties that confer resistance to the immune system.

Phagocytic assays have been widely used to test, *in vitro*, the resistance of bacteria to components of the immune system [121,141,238,240]. However application of this technique to biofilms poses a serious technical limitation. The assay is only functional with a low number of bacteria cells (normally bellow 10^6 cfu/ml, in order to maintain a balanced proportion between bacteria and leukocytes) and mature biofilms have a much higher number of bacteria. In order to be able to compare biofilm with planktonic bacteria phagocytosis, the biofilm was disrupted and diluted until the suspension achieved a lower concentration, the same as that used for planktonic bacteria, as described previously by Meluleni *et al.* [154]. Although it can be questionable that disrupted biofilms were used instead of their native 3-dimensional form, fragmented biofilms also present a relevant physiological state of a mature biofilm [239], which is thought to be the reason why some infections are persistent [49].

The levels of opsonic killing of planktonic cells were similar to previous studies reported for *S. aureus* planktonic cells [141]. It could be expected that both planktonic and biofilm cells would have similar susceptibility to the antibody mediated phagocytosis, since the antibody

used was specific to PNAG [143], which is present on the surface of both cell types. However, biofilm cells were clearly less susceptible to phagocytic killing. Accordingly, it can be hypothesized that the increased resistance of biofilm cells could be explained by the presence of some phagocytosis inhibitor in the biofilm matrix. This raises the hypothesis that the biofilm matrix, when disrupted, could inhibit phagocytosis. To test this hypothesis, the crude biofilm matrix was extracted and used in an inhibition assay following Maira-Litran's method [143]. Since it is already known that most of the biofilm matrix of *S. epidermidis* is composed of PNAG, purified PNAG was also used in the inhibition assay. The final concentration of PNAG was 50 μg/ml, which is in the range used previously by Maira-Litran *et al.* [143].

Although fragmentized biofilms were used in the study described in this chapter, it would be interesting to verify how the antibody would bind, once inside an intact biofilm. It was already demonstrated that the antibody could penetrate inside the biofilm structure (figure 8.1) but how the antibody would be distributed inside the biofilm matrix was unknown. To analyze the spatial distribution of the antibody, a lectin that could strongly bind to Staphylococcal biofilms matrices was used. The present results show that the biofilm matrix can protect bacteria from antibody-dependent phagocytosis, probably due to competition of the antibody binding site with the biofilm matrix or the bacterial cell. It is already known that PNAG protects planktonic bacteria against antibody-independent phagocytosis [121,240]. Furthermore, Leid *et al.* showed that human leukocytes can penetrate biofilms, but there was no evidence of internalization of the bacteria by the leukocytes [128]. From this study it can be concluded that biofilms have more PNAG per cell than planktonic bacteria. A possible explanation can be based on 2 reasons: biofilms can reach high cell densities, and PNAG production is stimulated under these conditions [59]; in most *S. epidermidis* biofilms, besides the surface associated PNAG there is also secreted PNAG that is a major constituent of the biofilm matrix [198]. It can be considered that the results obtained by Leid *et al.* can be explained by the high concentrations of PNAG inside the biofilm matrix. Considering the present results and in accordance with Leid *et al.* it can be hypothesized that, in *S. epidermidis* biofilms, resistance to the immune system is not a mechanism *per se*, but an enhancement of an already known evasion mechanism, in this case, the protection to phagocytosis is enhanced by the increased amount of PNAG in the biofilm. Kropec *et al.* recently demonstrated that PNAG protects bacteria from antibody-independent phagocytosis [121], thus it can be speculated that antibody-independent phagocytosis is also inhibited by the presence of the biofilm matrix.

In conclusion, this study shows that a rabbit immunoglobulin raised against PNAG can penetrate into *S. epidermidis* biofilms, showing that biofilms do not pose a diffusion barrier to components of the immune system. Furthermore, PNAG protects biofilms from antibody-

mediated phagocytosis. The distinct response between the planktonic and biofilm cells to the opsonophagocytic killing highlights different aspects of virulence of these 2 phenotypes.

Chapter 9

An in vivo study of the immune response against S. epidermidis planktonic or biofilm grown cells in BALB/c mice

Summary

The main goal of the work described in this chapter was to evaluate possible differences in the immune response to infections by S. epidermidis cells grown planktonically or in biofilms, using an in vivo murine model. Groups of male BALB/c mice were challenged intra-peritoneally with S. epidermidis, and then sacrificed 6 H, 24 H and 8 days after the challenge. Flow cytometric and qualitative cytospin analysis of cells recovered from peritoneal exudates and from the spleen, indicated that the bacterial cells obtained from the biofilm were less inflammatory and/or immunogenic than planktonic cells. The analysis of imunoglobulins present in the sera of each group of mice, 8 days after the challenge, indicated that less IgM and IgG were produced when the mice were challenged with biofilm cells. Overall, the results described in this chapter demonstrate that the phenotype of biofilm-grown cells is sufficiently different from planktonic cells to induce a distinct immune response.

9.1. Experimental procedures

9.1.1. Mice

Male BALB/c mice (6–8 weeks old) were purchased from the Gulbenkian Institute of Science (Oeiras, Portugal). Animals were kept at the animal facilities of the Institute Abel Salazar during the time of the experiments. Housing of mice was performed according to the European Convention for the Protection of Vertebrate Animals used for Experimental and Other Scientific Purposes (ETS 123).

9.1.2. Bacteria and growth conditions

For this study, biofilm-forming strain *S. epidermidis* 9142 was used. Cultures were grown at 37ºC on tryptic soy agar plates. Liquid cultures were grown over night in TSBG. Biofilms were formed in 6 well polystyrene plates for 48 H with rocking, at 37ºC, in TSBG. The growth medium was replaced by fresh TSBG after 24 and 36 H. Biofilms were then scrapped from the surface and sonicated twice for 5 s at 20 W to homogenize the suspension. Planktonic bacteria were grown overnight in TSB, at 37ºC with shaking, and then were also sonicated like the biofilm suspension. Both suspensions were then diluted in TSB to an OD_{640nm} of 1.5, centrifuged for 10 min at 5,000 g and resuspended in 0.9% NaCl.

9.1.3. Mice challenge with bacteria

Mice were challenged by intra-peritoneal (IP) inoculation with 0.5 ml PBS containing 2×10^8 bacteria from either a planktonic or biofilm culture. Alternatively, mice were similarly inoculated with 0.5 ml of PBS (negative control). Mice were sacrificed by cervical displacement 6 H, 24 H and 8 days after infection.

9.1.4. Quantification of total cells

The spleens of each mouse were removed and gently teased in 10 ml of BSS with 2% of fetal calf serum in order to be homogenized, and then filtered to remove macroscopic aggregates. The peritoneal cavity was washed with 7 ml of PBS using a 25 gauss needle, and then 4 ml were removed, and concentrated 8× by centrifugation at 1,200 g during 10 min for quantification and cytospins analysis. Total leukocytes in the spleen and the peritoneal exudates were quantified by microscopic analysis using a Neubauer chamber.

9.1.5. Cytospins

For cytospin analysis, peritoneal exudates cells were adjusted to a concentration of 3.5×10^5 cell per 0.3 ml. To each cytospin slide 0.3 ml of cells and 20 μl of BSA 30% were added. The slides were centrifuged at 1,000 g for 5 min, and then air-dried for 5-10 minutes.

Using a solution of 90% ethanol and 10% formaldehyde, cells were fixed during 1 min. Cells were then stained with hemacolour and air dried, prior to observation by microscopy. Images were acquired using a phase contrast microscope coupled to a 3CCD video camera.

9.1.6. Flow cytometric analysis

For cytometric analysis peritoneal exudates or spleen cells from BALB/c mice, were resuspended in BSS, supplemented with 10 mM of sodium azide and 1% BSA. The following monoclonal antibodies were used on previously titrated dilutions [233] for immunofluorescence cytometric analysis in a FACScan with the CellQuest software: goat anti-mouse IgM fluoroscein isothiocyanate (FITC) conjugate, rat anti-mouse, B220 phycoerythrin (PE) conjugate, rat anti-mouse CD8 FITC conjugate and rat GR-1 FITC conjugate. A number of 5×10^5 mononuclear cells were stained per sample. Dead cells were excluded by propidium iodide incorporation.

9.1.7. Quantification of serum immunoglobulins

Total and anti-*S. epidermidis* immunoglobulins in mouse sera were quantified by enzyme-linked immunosorbent assay (ELISA) as previously described [233], with some modifications. Briefly, polystyrene microtiter plates were coated with 4 μg/ml of goat anti-mouse immunoglobulin or with 1×10^8 *S. epidermidis* and incubated overnight at 4ºC. Wells were then saturated with 1% BSA in PBS for 1 H at room temperature. Serial dilutions of the serum samples were then plated and incubated for 2 H at room temperature. After washing, bound antibodies were detected by addition of alkaline phosphatase-coupled monoclonal goat anti-mouse-IgG isotypes (IgG1, IgG2a) and goat anti-mouse–IgM antibody for 30 min at room temperature. Substrate solution containing ρ-nitrophenyl phosphate was then added after washing and the reaction was stopped by addition of 0.1M EDTA pH 8 0. The absorbance was measured at $OD_{405\ nm}$. The ELISA antibody titres were expressed as the reciprocal of the highest dilution giving an absorbance of 0.1 above background.

9.2. Results and Discussion

9.2.1. Quantification of total number of cells in the spleen and peritoneal cavity

A quick, but crude evaluation of the total number of cells involved in the immune response to planktonic or biofilm-grown cells, was performed by homogenizing the spleen and counting the total number of leukocyte cells present. The total number of leukocyte cells was also quantified in the peritoneal cavity exudates. Table 9.1 summarizes the total number of cells in the spleen and peritoneal exudates in all the conditions studied.

Table 9.1. Total number of cells from the peritoneal exudates and from the spleen.

Time after Challenge	Group of mice	Peritoneal exudate (10^6)	Spleen (10^7)
6 H	Control	4.0 (±0.2)	15.7 (±5.9)
	Planktonic	7.4 (±0.8)*	22.7 (±0.5)**
	Biofilm	6.2 (±1.0)	20.3 (±0.6)**
24 H	Control	4.4 (±1.9)	21.8 (±2.8)
	Planktonic	11.1 (±1.0)**	26.7 (±3.9)*
	Biofilm	6.2 (±1.4)**	23.9 (±2.6)
8 days	Control	2.2 (±0.6)	19.3 (±0.7)
	Planktonic	2.8 (±1.1)	40.0 (±9.0)**
	Biofilm	3.8 (±1.8)	25.3 (±3.4)**

The peritoneal exudates counts are per 0.2 ml while the spleen is per 1 ml. * paired samples t-test with control, $p<0.05$, ** paired samples t-test between planktonic and biofilm, $p<0.05$

Mice challenged with planktonic or biofilm-grown bacteria showed some significant differences in the total number of cells present in the spleen (after 6 H and 8 days) and in the peritoneal cavity (after 24 H). However, in most cases, there was no statistically significant difference between these 2 groups. Nevertheless, comparing with PBS-treated controls, mice challenged with planktonic bacteria showed a statistically significant increase in the total number of cells in the peritoneal cavity (after 6 H) and in the spleen (after 24 H) while biofilm-grown bacteria did not. This could indicate that planktonic bacteria elicit a stronger innate immune response.

9.2.2. Cytospins

A cytospin image allows a quantitative and qualitative analysis of the cell diversity found in peritoneal cavity of mice challenged with either planktonic, biofilm-grown cells or PBS. Macrophages and PMN's were scarce in the control group, and more abundantly present in either of the mice challenged with planktonic or biofilm-grown cells (figure 9.1). Furthermore, mice challenged with planktonic suspensions presented more PMN's, 24 H after the challenge.

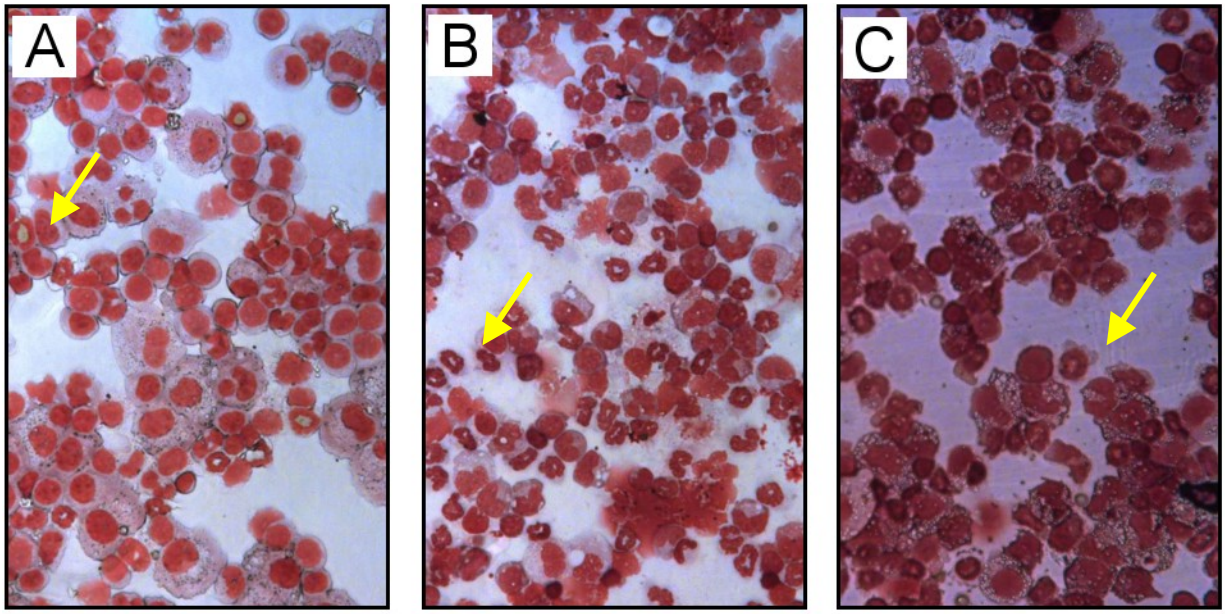

Figure 9.1. Cytospins of the peritoneal exudates of control mice (A), challenged with planktonic cultures (B) or challenged with biofilm-grown cells (C). Arrows indicate some PMN's.

In vivo phagocytosis of planktonic or biofilm-grown bacteria was also quantified by counting the number of internalized bacteria per peritoneal cavity PMN's using the cytospin slides (figure 9.2). The PMN's of mice challenged with planktonic bacteria had a higher number of internalized bacteria, as compared with PMN's from mice challenged with biofilm-grown bacteria (paired samples t-test, $p<0.05$). It seems, therefore, that biofilm-grown bacteria not only elicit a less intense innate immune response, but are also more resistant to phagocytosis. This evidence was already demonstrated *in vitro* in the previous chapter and confirmed here in an *in vivo* assay.

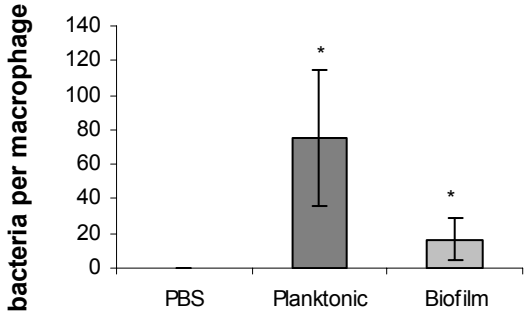

Figure 9.2. Quantification of phagocitised bacteria by the peritoneal cavity PMN's, 24H after the challenge (* paired samples t-test, $p<0.05$).

9.2.3. Flow cytometric analysis

As suggested by the peritoneal exudates cytospins (see figure 9.1), some differences were found regarding PMN's recruitment into the peritoneal cavity of mice challenged with a planktonic suspension (figure 9.1B) or with biofilm-grown bacteria (figure 9.1C). This was confirmed by flow cytometry. While 6 H after the challenge the difference between the mice challenged with the planktonic or biofilm suspension was not so obvious (data not shown), 24

H after the challenge the difference was clear and also statistically different (paired t-testes, $p<0.05$), as shown in figure 9.3.

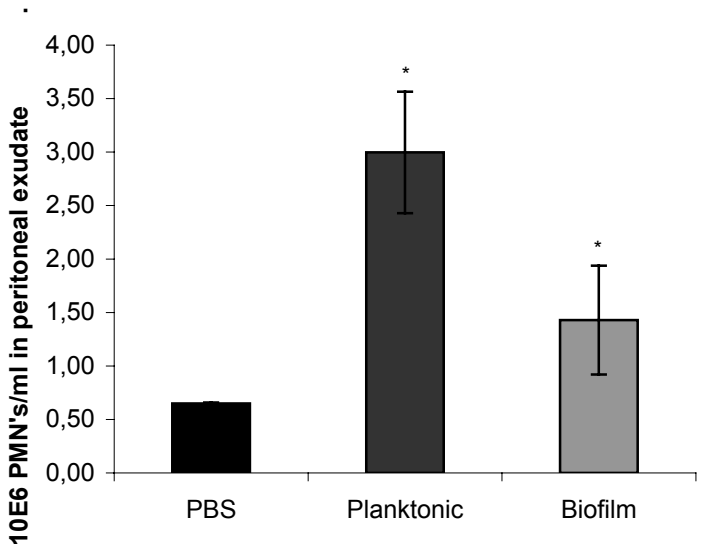

Figure 9.3. Recruitment of PMN's in the peritoneal exudates, 24 H after challenge. (* paired samples t-test, $p<0.05$)

The quantification of total number of cells in the spleen by microscopy also revealed an increase in their number when the mice were challenged with the planktonic population. The flow cytometry analysis confirmed this observation, as shown in figure 9.4. While 24 H after the bacterial challenge the differences in the number of B and T cells were not so obvious (data not shown), 8 days after the challenge with the planktonic population of *S. epidermidis*, both B and T cells numbers were increased in the spleen, as compared to those in control and also biofilm-grown cells challenged mice.

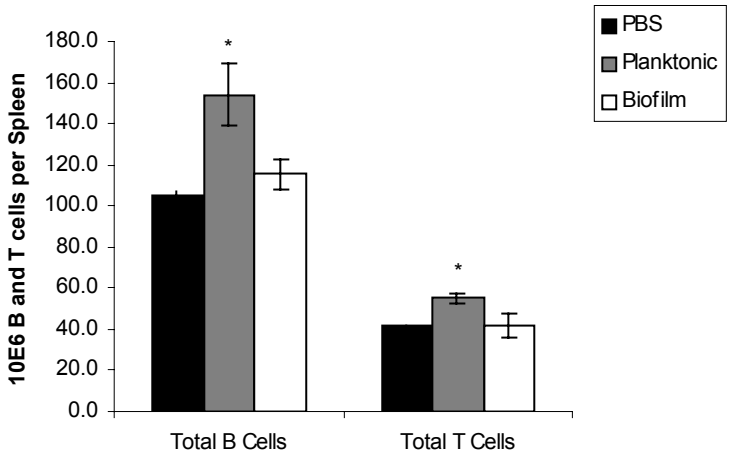

Figure 9.4. Total number of B and T cell in spleen, after 8 days of challenge. (* paired samples t-test, $p<0.05$)

9.2.4. Immunoglobulins production

Immunoglobulins in the mouse sera were detected 8 days after the challenge. Total Ig and *S. epidermidis*-specific Ig were quantified, as presented in figure 9.5. In both cases, challenge with planktonic bacteria induced higher serum antibody levels compared with biofilm-grown bacteria, and this difference was statistically different (paired samples t-test, $p<0.05$).

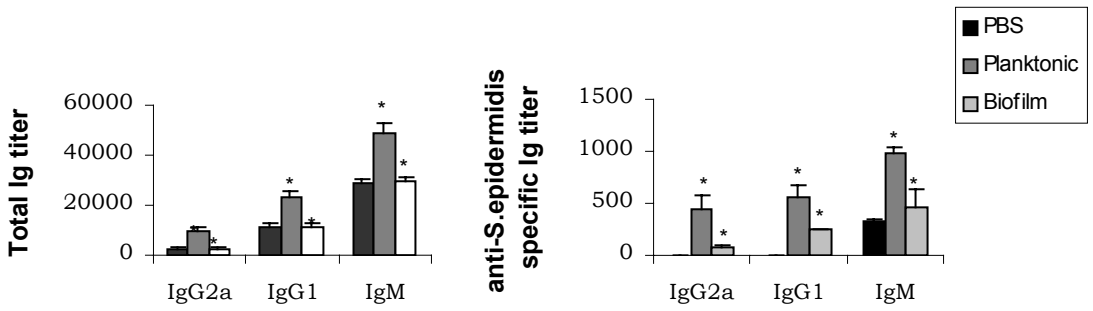

Figure 9.5. Mice serum total and anti-*S. epidermidis* IgG1, IgG2a and IgM, 8 days after challenge. (* paired samples t-test, $p<0.05$)

In conclusion, biofilm-grown bacteria were able to stimulate a less intense innate and adaptive immune response, as compared with planktonic bacteria: Phagocytes, T-cells, B-cells and antibodies elicited a lower response in the group of mice challenged with biofilm-grown bacteria. Furthermore, biofilm-grown bacteria were also more resistant to *in vivo* phagocytosis. As discussed in the previous chapter, the higher amounts of PNAG in the cell surface of biofilms cells can explain this resistance to phagocytosis [121,238] and probably also plays a role in the evasion of the adaptive immune response. Further studies should be conducted, using purified PNAG and evaluate its role in the activation and proliferation of components of the immune system.

Section IV

Molecular Biology of Staphylococcal PNAG

Section IV cover image represent the detection of PNAG in S. epidermidis M187 biofilm using confocal microscopy. The green signal results from the WGA-alexa green binding to extracelular PNAG. Center for Brain Imaging, Harvard Medical School, Boston, USA.

Introduction

The intercellular adhesin (*ica*) locus present in *S. epidermidis* [90] and *S. aureus* [51] encodes the proteins required to synthesize PNAG (see figure IV). *IcaA* is a trans-membrane glucosyltransferase and can synthesize short PNAG polymers *in vitro* using UDP-N-acetyl-glucosamine as a substrate [83]. *IcaD* increases the biosynthetic efficiency of *IcaA* [83]. *IcaC* is also a trans-membrane protein and appears to be involved in linking short polymers to make longer oligomers of PNAG [83]. *IcaB* was the last gene to have its function elucidated, exhibiting de-acetylase activity [238], being responsible for mediating attachment of PNAG to the cell surface, as will be described in chapter 10.

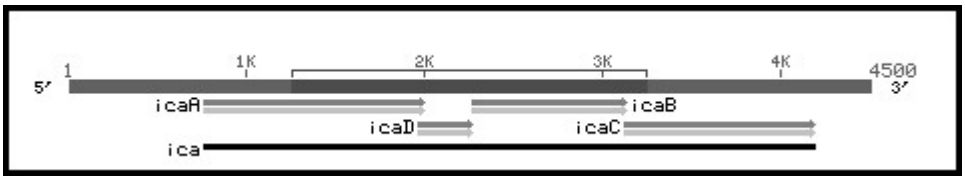

Figure IV. Structure of the *icaABCD* operon. Adapted from www.pubmed.com.

For a long time, it was thought that staphylococci biofilms contained 2 different polysaccharides: one responsible for initial adhesion to surfaces, called capsular polysaccharide adhesion (PS/A), first isolated by Tojo *et al.* [224], and another responsible for bacterial aggregation, called polysaccharide intercellular adhesion (PIA), first characterized by Mack *et al.* [134]. 2 years after the discovery of PS/A, Christensen *et al.* [46] isolated a similar molecule to PS/A but called it slime-associated antigen (SSA) since they claimed the glucose content was higher that in PS/A. However, latter, Baldassari *et al.* [14] suggested that SSA and PIA could be the same antigen. 2 years latter, McKenney *et al.* [151] isolated another antigen, identical to PS/A and "chemically related" to PIA, and they named it poly-N-succinyl-β(1-6)-glucosamine (PNSG). Subsequent studies demonstrated that the presence of the N-succinyl groups was an artifact, and indeed the staphylococcal polysaccharide is a poly-N-acetyl-β (1-6)-glucosamine (PNAG) [141]. Recently, analysis of PIA and PNAG determined that these 2 molecules are the same chemical identity [198].

While PIA was named due to its function as an intercellular adhesin, PNAG was named due to its chemical structure. Besides mediating intercellular adhesion, PIA/PNAG has more described functions, namely related with the immune evasion of *S. epidermidis* and *S. aureus* (see section III). Therefore, PIA/PNAG should be referred to its chemical name, since PIA/PNAG is no longer just an adhesin.

PNAG is a large MW polymer of β-1-6-linked N-acetyl-glucosamine and in its mature form, is a mixture of polymers such that about 10-20% of the amino groups are not acetylated,

which could give some of the polymers within the polysaccharide complex a net positive charge [141]. What is not known is whether PNAG consists of a minority of highly deacetylated molecules mixed in with a majority of fully acetylated molecules or if there is a range of acetyl substituents spread over individual molecules. In a recent study of PNAG synthesis in *S. epidermidis*, it was shown that IcaB induced partial de-acetylation of PNAG, and that was necessary for its association with the bacterial cell surface and also necessary for biofilm formation [178]. In addition, it was recently demonstrated that antibodies raised to highly acetylated (>90%) PNAG lacked protective efficacy against PNAG-positive *S. aureus* strains, and exhibited significantly lower opsonic killing relative to antibodies raised to chemically de-acetylated PNAG (~15% acetylation, dPNAG) [143].

Based on the findings that IcaB in *S. epidermidis* is a PNAG de-acetylase, and that antibodies raised to highly-acetylated PNAG are not protective in mice, it was hypothesized that the superior opsonic and protective activity of antibodies to the deacetylated form of PNAG was related to preferential surface retention of this form of the antigen. Such retention would obviously be essential for effective opsonic killing and protection mediated by this immune effector mechanism.

In this section, an experimental approach to test this hypothesis is presented. *S. aureus* was used as a model organism, instead of *S. epidermidis*, because of: (a) the availability of a set of *S. aureus* ica positive, ica negative and ica over-expressing strains already characterized that would reduce the amount of work necessary; (b) the molecular mechanisms of PNAG production in both species seems to be similar and (c) due to the already recently described role of *icaB* in the pathogenesis of *S. epidermidis*. Furthermore, a new method for detecting PNAG in staphylococcal strains is described, based on a classic antibody-based dot-blot, but using commercially available lectins.

Chapter 10

Molecular basis for preferential protective efficacy of antibodies directed to the poorly-acetylated form of staphylococcal PNAG

Summary

As described in sections I, II and III, PNAG has a major role in biofilm formation and in immune evasion of S. epidermidis. Other studies have also verified these properties in S. aureus. Due to the fact that PNAG is a major staphylococcal surface antigen, this is a target for vaccine development. Antibodies specific for epitopes lacking acetate are superior at opsonic and protective activity compared with antibodies directed to acetylated epitopes, but the molecular basis for this was unknown. Recently it was demonstrated for S. epidermidis that icaB encodes a de-acetylase. This chapter describes the similar role that IcaB plays in S. aureus, and the results revealed that an icaB mutant of S. aureus expressed significantly less surface-associated PNAG, did not produce a biofilm, was highly susceptible to Ab-independent opsonic killing and had reduced virulence in a murine model of bacteremia. Furthermore, the highly-acetylated secreted PNAG acted as a decoy, effectively at blocking opsonic killing mediated by a human Mab against PNAG. These findings provide a molecular mechanism explaining the superior opsonic and protective activity of Ab to cell surface partially deacetylated PNAG.

10.1. Experimental procedure

10.1.1. Strains and media

S. aureus strain MN8 was originally isolated by P. Schlievert, (Minneapolis, MN) from a patient with toxic shock syndrome. Strain MN8m is a spontaneous mutant isolated from a chemostat culture of strain MN8 [151]. Strain *S. aureus* NCTC 10833 (ATCC 25904) is a clumping factor positive variant of a throat swab isolate. Partial deletion of the *ica* locus to produce *S. aureus* strain 10833ica::tet was performed as described by Cramton *et al.* [51]. The strains were grown at 37ºC on TSA containing the appropriate antibiotic. Liquid cultures were either in TSB lacking glucose (17 g/l peptone from casein, 3 g/l peptone from soymeal, 5 g/l NaCl, 2.5 g/l K_2HPO_4) or in TSBG.

10.1.2. Plasmids, primers, and cloning and expression of genes in the *ica* locus

All plasmid purifications were performed with the QIAprep spin miniprep kit. All primers were custom synthesized by Qiagen Operon. Restriction enzymes and DNA modifying enzymes were purchased from Invitrogen. The pMUC plasmid was derived using a previously described vector [102] by ligating the constitutively transcribed *ica* locus from strain MN8m to the shuttle vector pRB473. To create plasmid pMUC∆icaB, a nonpolar, in-frame deletion which removed more than 80% of the *icaB* gene was generated by amplifying the plasmid by PCR with the following primer pair (icaBdelFWD; 5'-CCATCCAGTGTGCTTACAGGC-3' and icaBdelREV; 5'-TCCATTAAGAG ATGGGACGG ATTCC-3'). The ends of the PCR product were phosphorylated using T4 kinase, and the linear DNA was circularized using Ready-2-go T4 ligase. The plasmid was sequenced at the Harvard Medical School Microbiology Core Facility to confirm that the *icaB* deletion did not cause a frameshift mutation and that the rest of the *ica* locus was free from any other mutations. The plasmid was transduced to *S. aureus* 10833ica::tet to trans-complement the chromosomally-deleted *ica* locus and produce *S. aureus* strain 10833ica::tet+pMUC∆icaB.

In order to construct a vector for constitutive transcription of inserted DNA, the *ica* promoter was amplified from genomic DNA in the ica-constitutive strain MN8m by PCR using the following primer pair (icaprovectorFWD; 5'-GGGGGATCCCCCTACTGAAAATTAATCACA CTATG-3' and icaprovectorREV; 5'-CCCCCCGGGCAATTTCTTTACCTACCTTTCGTTAG-3') and cloned into the *SmaI* and *BamHI* sites of pRB473 to produce plasmid pKJ3. The *icaB* gene was amplified from MN8 genomic DNA using the primers (icaBFWD; 5'-GTGAAGTATAGAAAATTTATAATTTTAGTGTTGAG-3' icaBREV; 5'-GGGGAGCTCCTAATCT TTTTCATGGAATCCGTCC-3'), digested with *SstI* and cloned into pKJ3 to derive picaB. All plasmid constructs were initially transformed into the restriction-deficient *S. aureus* strain

RN4220 according to the method described by Lee [127]. Constructs were transferred to other strains of *S. aureus* by transduction using phage 80 [113].

10.1.3. RT-PCR

S. aureus cultures were grown in TSB at 37ºC overnight. The following day 1:10 dilutions of the cultures were made in TSBG and incubated at 37ºC for 4 H with shaking. RNA was extracted from 1×10^9 cells using the RNeasy Protect miniprep kit as described in the manufacturer's instructions except that cells were lysed by vortexing in the presence of 4 mm glass beads for 10 min. Turbo DNase was added to digest contaminating DNA that was then inactivated by heating according to manufacturer's instructions. RNA concentrations were determined OD_{260nm} and 1 mg of each sample was analyzed using the Superscript II One-Step RT-PCR kit and primers specific for either *icaA* (5'-GTCTATTTACTGGATTGTCGGTC-3' and 5'-GTCTGACTTCGCTTAATACAGCC-3'), *icaC* (5'-CCTTAGTGTTACAATTTTACATTCG and 5'-CGTTCGTAGTTATAACCCATATATGC-3'), or for *gyraseB*, as a positive control (5'-TTA TGGTGCTGGGCAAATACAAG-3' and 5'-CACCATGTAAACCACCAGATAC-3'). Agarose gels were stained with ethidium bromide and photographed. Each experiment was performed at least 3 times.

10.1.4. Biofilm assay

Microtiter plate assays for biofilm production were performed essentially as described in chapter 6.

10.1.5. Human monoclonal antibodies

The human monoclonal antibodies used in the study described in this chapter were produced by Kelly-Quintos *et al.* as described previously [115]. Briefly, B cells from a patient recovering from *S. aureus* infection were transformed with Epstein-Barr virus and screened for their ability to bind either acetylated PNAG or dPNAG. The F598 hybridoma (high binding to deacetylated PNAG) and the F628 hybridoma (high binding to acetylated PNAG) were chosen for further study. Variable regions were cloned into TCAE6 vector and transfected into CHO cells for IgG1 production.

10.1.6. Immunological detection of PNAG on the cell surface and in culture supernatants

PNAG blots were performed essentially as described in chapter 6, using cell surface extracts and culture supernatants.

10.1.7. Immunofluorescence microscopy

Glass bottom microwell plates were coated with 4% Celltak solution for 30 min, and then washed twice with sterile dH2O. Freshly harvested bacterial suspensions were added to the plates, allowed to sit 20 min at room temperature, and then washed twice with PBS. *S. aureus* 10833ica::tet+pMUC and *S. aureus* 10833ica::tet+pMUC∆icaB were fixed in 4% (wt/vol) formaldehyde in PBS, for 30 min at 4ºC, and then washed twice with PBS. Blocking solution containing 1% bovine serum albumin (BSA) and 2% normal rabbit serum (NRS) (to block non-specific binding to protein A) in PBS was added and incubated for 1 H at room temperature with rocking. After this time, the plates were washed, incubated with primary Ab solution (human Mab F598) diluted 1:100 in blocking buffer, and left for 2 H at room temperature with rocking. After being washed 4 times with PBS for 5 min each (with rocking), a secondary anti human IgG-Alexa 488, diluted 1:5,000 in blocking buffer was added. The plate was left rocking at room temperature for 1 H, then washed again 4 times with PBS for 5 min each with rocking at room temperature. The plates were examined by phase-contrast and fluorescence microscopy. Images of the same field viewed by the 2 different microscopic methods were acquired by a camera and images processed by computer using the LSM 5 image analysis system.

10.1.8. Opsonophagocytic assays

Opsonophagocytic assays were performed as described in chapter 9, using F598 and F628 monoclonal antibodies.

10.1.9. Inhibition of phagocytosis by competitive assay

PNAG was purified from a culture of *S. aureus* MN8m, as previously described [141]. A stock solution was made in PBS at 1,000 μg/ml. Since Mabs F598 and F628 mediate different levels of opsonic killing per μg of protein, the assay was standardized by using concentrations of the antibodies that would result in equivalent levels of opsonic killing. PNAG diluted in RPMI/FBS was used in the opsonophagocytic reactions described in chapter 9, at 2 different concentrations, based on the ratio of IgG used in each assay. Due to the low solubility of PNAG at neutral pH, a maximum concentration of 200 μg/ml of PNAG could be used on these assays. Control samples consisted of bacteria, leukocytes, complement, MAb and PBS without PNAG. The percentage of inhibition of killing was calculated by determining the ratio of the cfu surviving in the tubes with PNAG to the cfu surviving in the tubes without PNAG. The assay was done with triplicate samples and repeated 2 to 3 times.

10.1.10. Murine bacteremia model

The animal model used was previously described [143]. Briefly, groups of 6 mice (FVB-NJ; female, 5-7 weeks of age) were challenged intra-venous with a dose of $1.0X10^7$ cfu of *S. aureus* strains in 0.2 ml of PBS. Mice were sacrificed 90 min after bacterial challenge, blood samples withdrawn and number surviving of bacteria determined by serial diluting and plating of blood samples and the results expressed as cfu/ml of blood.

10.2. Results

10.2.1. Role of *icaB* in biofilm formation

The biofilm-forming capacity of *icaB* over-expressing and deletion mutant strains of *S. aureus* was first analyzed. *S. aureus* strain 10833 produced a moderate biofilm when grown in TSBG and the *ica* deletion mutant, which is unable to produce any PNAG, did not form a biofilm (figure 10.1). When the *icaB* gene was over-expressed in strain 10833, however, biofilm formation increased approximately 4-fold ($p<0.05$, unpaired t-test). When 10833ica::tet was complemented with pMUC, which contains the *ica* locus from the PNAG over-producing strain MN8m, it produced a heavy biofilm. In-frame deletion of the *icaB* gene from pMUC to produce pMUCΔicaB resulted in a strain was phenotypically similar to *S. aureus* 10833ica::tet lacking the *ica* genetic locus in that it could not produce a biofilm ($p<0.05$, unpaired t-test between strains carrying pMUC and pMUCΔicaB).

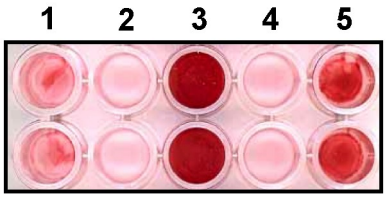

Figure 10.1. Safranin-stained biofilms of bacteria grown overnight in TSBG in microtiter wells; strains *S. aureus*: 1)10833, 2)10833ica::tet, 3) 10833ica::tet+pMUC, 4) 10833ica::tet+pMUCΔicaB and 5) 10833+pIcaB

Deletion of *icaB* in pMUC did not induce a frameshift mutation in the *ica* locus, nonetheless, it is possible that the mutation might affect transcription of the downstream gene, *icaC*. To assess transcription of the *ica* locus in the absence of *icaB*, a RT-PCR was performed to measure levels of *icaA* and *icaC* transcripts (*gyrB* transcript levels were measured as a control). As expected from previous findings that *ica* is constitutively transcribed in pMUC [102,104], *icaA* and *icaC* transcript levels in *S. aureus* 10833ica::tet+pMUC were much greater than in *S. aureus* 10833 and the levels of *icaA* and *icaC* RNA in *S. aureus* 10833ica::tet+pMUCΔicaB were comparable to those obtained from strain *S. aureus* 10833ica::tet+pMUC, indicating that the *icaB* deletion mutation does not

affect transcription of the *icaADC* genes in pMUCΔicaB (figure 10.2). Figure 10.2 also demonstrates, as expected, that over-expression of *icaB* in *S. aureus* strain 10833 does not affect transcription of the *icaA* and *icaC* genes.

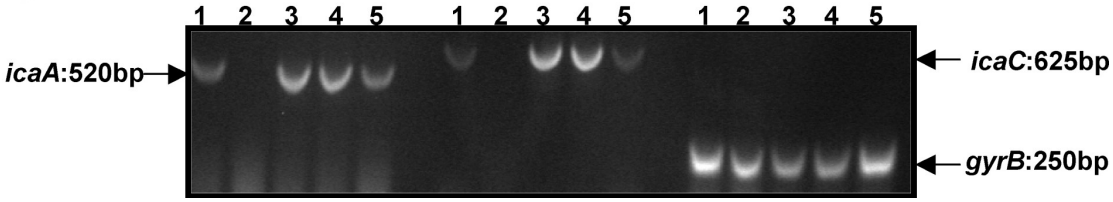

Figure 10.2. RT-PCR using RNA from (1) 10833, (2) 10833ica::tet, (3) 10833ica::tet +pMUC, (4) 10833ica::tet+ pMUCΔicaB, (5) 10833 + picaB.

10.2.2. Role of *icaB* in mediating association of PNAG to the bacterial cell surface

Immunoblots were used to characterize the levels of PNAG in bacterial cell surface extracts and culture supernatants from the different *S. aureus* 10833 strains. As expected, strain 10833ica::tet did not produce any detectable PNAG (figure 10.3).

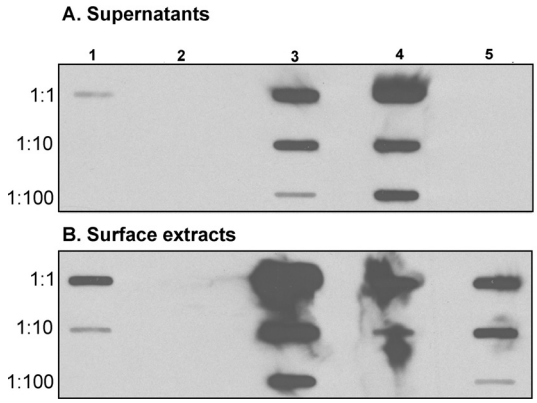

Figure 10.3. Immunoblots representing the levels of PNAG in culture supernatants (A) and bacterial cell surface extracts (B) from the different *S. aureus* strains: (1) 10833, (2) 10833ica::tet, (3) 10833ica::tet +pMUC, (4) 10833ica::tet+ pMUCΔicaB, (5) 10833 + picaB

Some of the PNAG produced by wild-type *S. aureus* strain 10833 was found in the supernatant whereas the majority of the polysaccharide was surface-associated. As expected, the pMUC plasmid, which leads to high levels of *ica* transcripts, increased PNAG production. Again, in *S. aureus* strain 10833ica::tet+pMUC, the majority of the PNAG was surface-associated. In *S. aureus* strain 10833ica::tet+pMUCΔicaB however, a minority of the PNAG was on the surface and most of it was secreted. In addition, the *icaB* over-expressing strain had more PNAG on the surface compared with the wild-type parental strain, and none was detected in the supernatant.

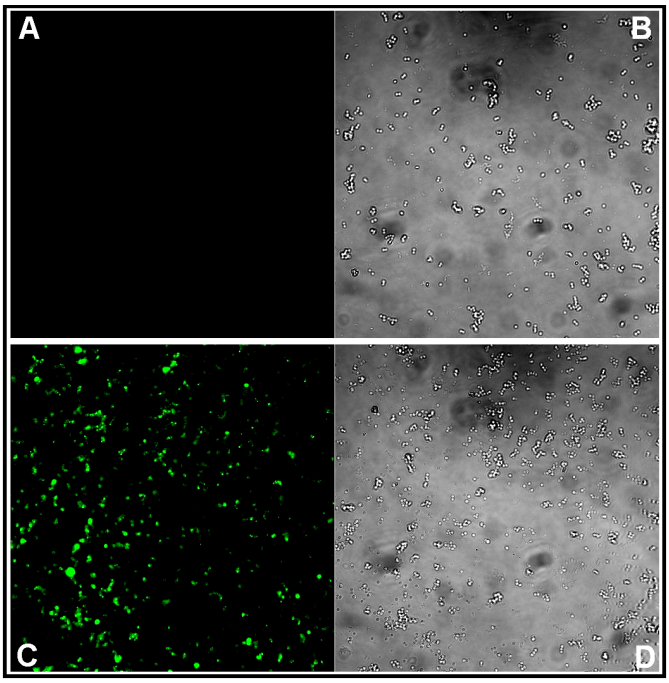

Figure 10.4: Evaluation of surface-associated PNAG by *S. aureus* strains by immunofluorescence. (A) Fluorescence and (B) phase contrast microscopy of immunostained *S. aureus* strain 10833ica::tet+pMUCΔicaB. (C) Fluorescence and (D) phase contrast microscopy of immunostained *S. aureus* 10833ica::tet+pMUC.

In this work it was also evaluated the surface-association of PNAG by immunofluorescent microscopic analyses. *S. aureus* strains 10833ica::tet+pMUC and 10833ica::tet+pMUCΔicaB were stained with dPNAG-specific Mab F598 and immunofluorescence analysis indicated that the Mab bound well to the surface of *S. aureus* 10833ica::tet+pMUC, but staining of *S. aureus* 10833ica::tet+pMUCΔicaB was very low (figure 10.4). Together these results indicate that, similar to *S. epidermidis*, *icaB* is required for optimal association of PNAG with the bacterial cell surface in *S. aureus* and formation of a strong biofilm in tissue-culture wells.

10.2.3. Opsonophagocytic assays

Phagocyte-dependent killing by human MAbs F598, which reacts as well to the dPNAG and it does to native PNAG, was compared with that by Mab F628, which reacts optimally with the highly acetylated residues on native PNAG and has decreased antigen binding when acetates are removed.

Killing of *S. aureus* 10883 and *S. aureus* 10833+picaB by Mabs F598 and F628 showed that the dPNAG-specific Mab F598 had higher killing activity compared with Mab F628 for both strains ($p<0.05$, unpaired t-test) (figure 10.5A). Over-expression of *icaB* in *S. aureus*

10833+picaB enhanced the killing by dPNAG-specific Mab F598 compared to the opsonic killing of wild-type *S. aureus* 10833 ($p<0.05$, unpaired t-test) (figure 10.5A).

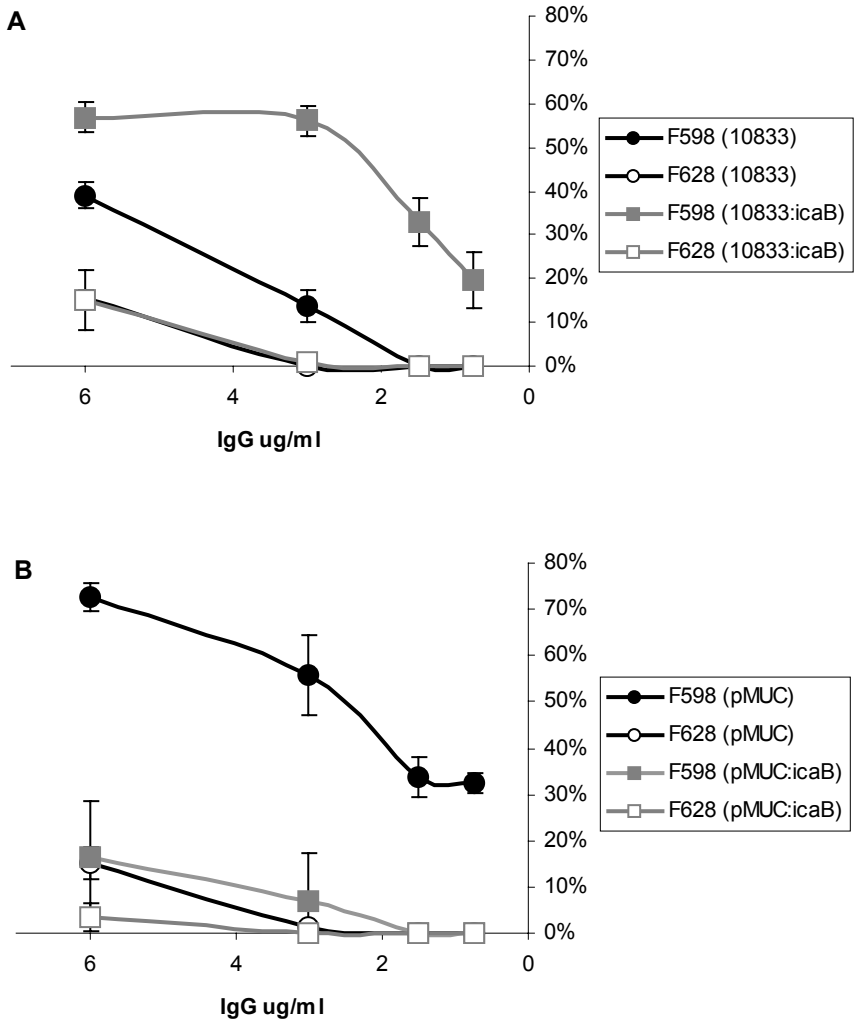

Figure 10.5: Opsonophagocytic activity of human IgG1 Mabs F598 (dPNAG-binding) and F628 (native PNAG-binding) at different concentrations against *S. aureus* strains. Error bars represent SD.

Figure 10.5B presents the results of the opsonic killing assays using *S. aureus* strains 10833ica::tet+pMUC and 10833ica::tet+pMUCΔicaB. The PNAG over-producing *S. aureus* strain, 10833ica::tet+pMUC, was effectively killed by Mab F598 but relatively resistant to the opsonic-killing effect of Mab F628. ($p<0.05$, unpaired t-test). Of note, in the absence of Ab, ~60% of *S. aureus* strain 10833ica::tet and 50% of *S. aureus* strain 10833ica::tet+pMUCΔicaB were killed, indicating loss of the cell surface PNAG resulted in marked sensitivity to Ab independent killing when compared to killing in the absence of either phagocytes or complement (figure 10.6). When Mabs F598 and F628 were tested for opsonic killing of *S. aureus* strain 10833ica::tet+pMUCΔicaB (figure 10.5B) there was no enhancement of killing

over that achieved in the presence of only bacteria, phagocytes and complement ($p>0.05$, unpaired t-test), consistent with the low level of PNAG on the surface of this strain.

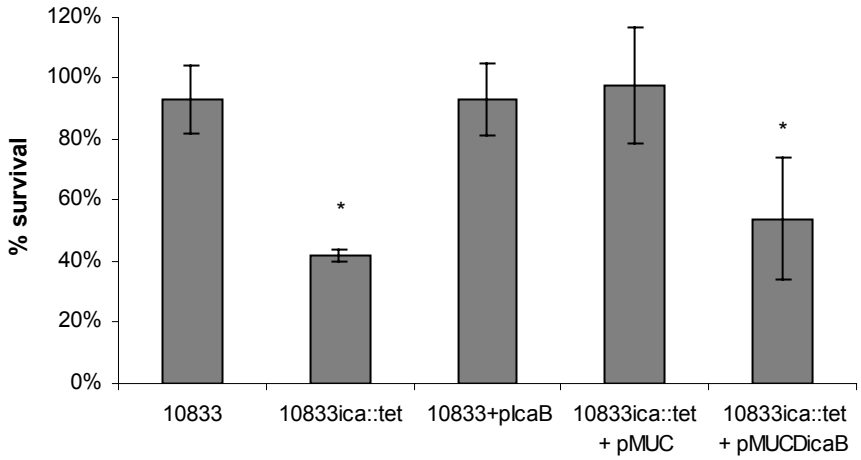

Figure 10.6. Ab-independent phagocytosis of *S. aureus* strains. Error bars represent SD. * represent a statistical difference (ANOVA, $p<0.05$).

10.2.4. Inhibition of phagocytosis by competitive assay

To test the hypothesis that non-cell-associated PNAG can act as a decoy to the PNAG-specific opsonic Ab, purified PNAG was added to opsonophagocytic reactions mediated either by Mab F598 or Mab F628 against *S. aureus* strain 10833. Table 10.1 presents the percentage inhibition of killing, compared to control reactions without added PNAG. When a 1 to 1 ratio of PNAG antigen to Ab was used, phagocytosis mediated by dPNAG-specific Mab F598 was inhibited only 6%. When native-PNAG-specific Mab F628 under the same conditions was used, the inhibition level, 36%, was significantly higher ($p<0.05$, unpaired t test). The greater ability of free PNAG to inhibit killing mediated by the Mab to native PNAG compared to the Mab to dPNAG was also verified with the other PNAG:IgG ratios (table 10.1). It was not possible to test inhibition by higher ratios of PNAG to Mab F628 due to the poor solubility of the antigen at neutral pH at higher concentrations.

Table 10.1: Inhibition of opsonophagocytic activity of human IgG1 Mabs F598 and F628 against *S. aureus* wild type strain 10833 by highly-acetylated PNAG.

Antibody used	Concentration	PNAG : IgG	% Inhibition
F598	6 μg/ml	1:1	6 ± 7
		4:1	25 ± 12
		10:1	36 ± 5
F628	50 μg/ml	1:1	32 ± 12
		4:1	57 ± 13

10.2.5. Virulence in murine bacteremia model

The role of *icaB* in *S. aureus* virulence was evaluated by comparing the *icaB* over-expressing strain with the wild-type parental strain and by comparing the *ica* deletion strain carrying pMUC with the same strain carrying pMUC∆icaB. When *icaB* was over-expressed in *S. aureus* 10833, significantly more bacteria survived in the blood after 90 min ($p<0.05$, unpaired t-test) compared with the wild-type parental strain (figure 10.7). On the other hand, when the *icaB* gene was deleted from the pMUC locus (figure 10.7) a significantly lower number of bacteria survived ($p<0.05$ unpaired t-test). Thus, over-expression of *icaB* enhanced surface retention of PNAG and enhanced resistance to mouse mediators of immunity to bloodstream infection, whereas deletion of *icaB* increased the clearance of this strain from the mouse blood.

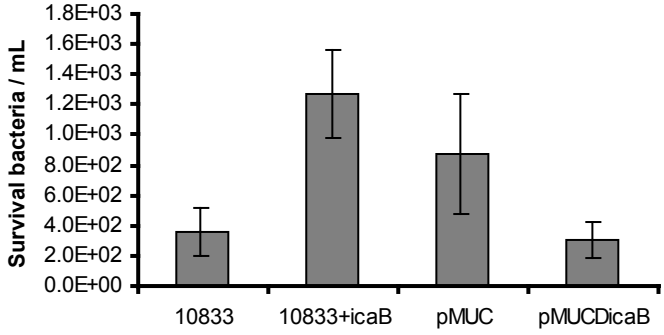

Figure 10.7. Murine bacteremia model demonstrates the role for *icaB* in enhanced survival of *S. aureus in vivo*. The bars represent the mean number of bacteria that were recovered from blood 90 min after IV infection and the error bars the SD.

10.3. Discussion

One known strategy that pathogens use to avoid host immune defenses it to elicit high levels of poorly protective antibodies. The protective efficacy of antibodies may be poor due to low Ab affinity, production of an inappropriate Ab isotype, or have specificity for non-protective epitopes [160,194,220]. This latter strategy appears applicable to the immune response to staphylococcal PNAG, wherein antibodies that bind best to the immunodominant, highly acetylated antigen, function poorly in opsonic killing and protection assays [143]. Overcoming this evasive strategy by immunizing animals with a conjugate vaccine containing poorly-acetylated PNAG (dPNAG), elicited antibodies that were superior to those to native PNAG in opsonic killing and protection against systemic *S. aureus* infection [143]. However, the molecular basis for the superior efficacy of the dPNAG-specific antibodies was not apparent.

The results from this work indicate that in the absence of the *icaB* protein, less PNAG is preferentially retained on the *S. aureus* cell surface, as it is for *S. epidermidis* [238],

presumably due to a lack of N-deacetylase activity in the absence of *icaB*. In the presence of *icaB* the PNAG retained on the *S. aureus* cell surface is less able to react with Ab to native PNAG and better able to bind Ab to dPNAG, improving opsonic killing and protection. Increasing the N-deacetylase activity by over-expression of *icaB* increased *S. aureus* susceptibility to killing by a human IgG1 Mab to dPNAG, but had no effect on killing by a human IgG1 Mab to native PNAG. Also, increased expression of *icaB* leads to greater survival of this strain in mouse blood, indicating a crucial role for surface associated PNAG in bacterial resistance to Ab-independent opsonic killing. In contrast, loss of *icaB* resulted in a strain with decreased surface retention of PNAG, increased susceptibility of the strain to Ab-independent killing and reduced survival in the blood of infected mice. These findings point to a key role for the *icaB* protein in pathogenesis due to its ability to influence the amount of PNAG on the *S. aureus* cell surface.

Vuong *et al.* initially determined that the *icaB* gene is responsible for the de-acetylation of PNAG (referred to as PIA) in *S. epidermidis*, and that the de-acetylation is necessary for the surface retention of PNAG [238]. The results from the present study confirmed that *icaB* is needed for surface retention of PNAG in *S. aureus* strains. Given the high homology of the *icaB* genes in *S. epidermidis* and *S. aureus* and the identical effects they mediate in regard to PNAG surface retention in both organisms, it is almost certain that *icaB* in *S. aureus* also functions as an N-deacetylase. Surface retention of PNAG promotes adherence between staphylococci and is necessary for biofilm formation. Therefore, without *icaB*, PNAG can no longer function in the role of a polysaccharide adhesin and biofilms cannot form in the absence of surface-retained PNAG. As it is well-established that biofilm formation renders bacterial cells more resistant to the immune system [128] and to antibiotic therapy [103] (as discussed on sections II and III) and biofilm formation is an important virulence factor in device-related infections, the *icaB* protein of staphylococci clearly plays a key role in the pathogenesis of biofilm infections by modulating attachment of PNAG to the staphylococcal cells surface.

The results presented in this chapter along with those of Vuong *et al.* [238] indicate that the PNAG polymer must be anchored to the bacterial cell to form biofilms; PNAG cannot merely function as a sort of intercellular glue binding cells together.

The findings of the present study also suggest that the secreted form of PNAG may act as a decoy by binding potentially opsonic antibodies away from the cell surface, preventing them from mediating killing. When the findings reported here are integrated with other studies that indicate that highly acetylated PNAG may also play a role in virulence by eliciting a less protective Ab response [143], it appears there are multiple properties of this molecule that contribute to the pathogenesis of staphylococcal infections.

The results from this work showing the effects of loss of expression of *icaB* and over-expression of *icaB* on *S. aureus* ability to form biofilms, resist Ab-independent opsonic killing and survive in mouse blood not only explain, in part, the role of PNAG in these varied aspects of *S. aureus* virulence, but also point to a reason why Ab to dPNAG has superior opsonic and protective efficacy. With preferential retention of the deacetylated form of the antigen on the cell surface, there is now a molecular basis for understanding why the antibodies to dPNAG function in a superior fashion compared to those that bind less well to the antigen when acetate groups are reduced. This insight should help guide further vaccine development based on the PNAG molecule, supporting the pursuit of the dPNAG form of the antigen as a superior vaccine candidate compared to the native, acetylated form of PNAG.

Chapter 11

Bacterial-bacterial cell interactions in biofilms: detection of PNAG by blotting and confocal microscopy

Summary

Standard methods to detect PNAG in Staphylococci are either based on dot- or slot-blots using specific, non-commercially available antibodies, or by confocal microscopy using commercially available lectins. In this chapter, a new method to detect PNAG, based on using a slot-blot technique, is presented. The innovation of this method lies on the fact that a commercially available lectin, instead of an antibody, is used. The specificity of the lectin for PNAG was verified by confocal laser microscopy using a PNAG-positive, biofilm-positive strain and a PNAG-negative strain.

Part of the work described in this chapter was published in 2006, in Methods of Molecular Biology, 341:119-126.

11.1. Experimental procedures

11.1.1 Strains

In the study described in this chapter 2 *S. aureus* and 2 CoNS strains were used: *S. aureus* MN8m and MN8mΔica [103], and also *S. epidermidis* M187 and *S. haemolyticus* M176. Detailed information about CoNS strains is present in the supplements section, page 179.

11.1.2. Biofilm assays and PNAG detection by Confocal Laser Scanning Microscopy

Biofilms were grown and prepared for CLSM analysis as described in chapter 6.

11.1.3. PNAG extraction and detection by immunoblotting

PNAG extraction and immunoblotting was performed as described in chapter 6.

11.1.4. PNAG extraction and detection by molecular-blotting

PNAG extraction was performed as described in chapter 6. The detection of PNAG by blotting was performed in a similar way as the immunoblot, but using a specific lectin that binds to N-acetyl-glucosamine: WGA. 100 µl of each PNAG extract were immobilized on a nitrocellulose filter that was then blocked with 1% BSA, and incubated for 30 min with 50 ng/ml of WGA conjugated with horseradish peroxidase. The membrane was washed 3 times, for 5 min, with TBST, and then PNAG was detected with the Amersham ECL (enhanced chemiluminescence) Western blotting system.

11.2. Results and Discussion

Interactions between bacterial cells, and adherence to a solid surface, are normally mediated in large part by exopolysaccharide intercellular adhesins, resulting in cohesive, structured communities known as biofilms [10,48,83]. Elaboration of adhesins is therefore a key factor in the switch from planktonic to biofilm growth [101]. Antibodies that react specifically to the adhesins of certain bacterial species have been produced and used to monitor, by immunoblotting, the effect of different mutations or environmental conditions on adhesin production [39,50,102,104]. However, adhesin-specific antibodies are not always readily available [111]. An alternative to antibodies is the use of lectins that bind to a specific carbohydrate moiety. Lectins have been widely used to detect adhesins in biofilms, using CSLM [125,163,164,193]. Regarding staphylococcal PNAG, the sugar residue N-acetyl-glucosamine is a ligand for the lectin WGA. Horseradish peroxidase- and fluorescently-labeled

WGA are commercially available, and can be used to detect adhesins semi-quantitatively [130].

Besides detecting the production of adhesins, CSLM analysis has other advantages: CSLM has been successfully used as a tool to determine the composition and structure of biofilms [106,130]. However, CSLM requires expensive equipment, which may be restrictive for many laboratories. Based of the specificity of WGA and previous CLSM studies, this work aimed to develop an easy and non-expensive technique that can be used to detect adhesin production by a number of bacterial species for which a specific anti-polysaccharide antibody is not readily available. Accordingly, a procedure in which PNAG was extracted from the cell surface and detected by a slot-blot system, using a WGA-peroxidase conjugate was developed.

To confirm the specificity of WGA, 2 strains of *S. aureus* were analyzed by CLSM. Since PNAG synthesis in *S. aureus* (and also *S. epidermidis*) is dependent on the proteins encoded by the intercellular adhesin (ica) locus, ica-positive and ica-negative mutants were used as controls. Strains were allowed to grow attached to a surface, and then were stained with fluorescently conjugated WGA and analyzed by CLSM, as represented in figure 11.1. WGA-binding was only detected in the PNAG producing strain, confirming the specificity of the commercially available WGA.

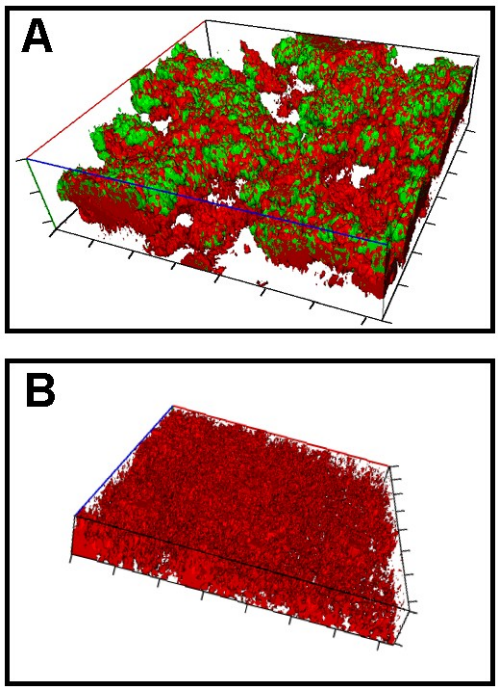

Figure 11.1. Detection of PNAG by confocal microscopy. A) the strong PNAG-producing *S. aureus* strain MN8m and B) the PNAG-negative *S. aureus* strain MN8Δica. Bacteria are presented in red and PNAG in green. Each bar segment represents 20 μm.

The PNAG from the cell surface of several additional staphylococcal strains, including *S. aureus*, *S. epidermidis* and *S. haemolyticus* that had been previously characterized regarding the production of PNAG were extracted. PNAG was then immobilized on a nitrocellulose membrane. The developed method to detect PNAG by WGA was based on the immunoblot procedure previously described by Cramton *et al.* [50], but with some changes. Blocking of the membrane was initially performed either with skim milk or BSA, but skim milk, which contains a variety of carbohydrates, was associated with some non-specific lectin binding. All subsequent assays were performed using 1% BSA as a blocking agent. After the blocking step, a WGA-horseradish peroxidase conjugate was added and the incubation time necessary to detect PNAG was optimized. While shorter incubation times yielded a low intensity signal, longer exposure times reduce the level of fluorescence. The incubation time was set to 30 min, which was sufficient to obtain a strong and clear signal. An advantage of this method is the reduced time consumption, compared with standard immunoblotting procedures, since with WGA is directly conjugated to HRP, eliminating the need for a secondary antibody. The full procedure, from PNAG extraction to detection, could be performed in less than 5 H, whereas the standard immunoblotting procedure took more than 8 H.

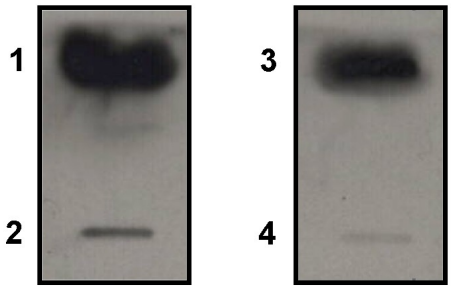

Figure 11.2. Analysis of PNAG production by blotting. (1) PNAG-hyper-producing *S. aureus* strain MN8m, (2) the PNAG-negative *S. aureus* strain MN8Δica::tet, (3) PNAG-producing *S. epidermidis* strain M187, (4) PNAG-negative staphylococcal species *S. haemolyticus* strain M176.

Figure 11.2 presents the detection of PNAG by WGA-blot: ica-positive strains yielded a strong signal whereas ica-negative strains yielded a very low or no signal. The presence of a very low signal likely results from a cross-reaction between WGA and the N-acetyl-glucosamine within the cell wall. It could also result from low level PNAG production by certain strains or from over-exposing the film. To differentiate between these possibilities, a known ica-negative strain should always be included when performing a blot, in order to provide a threshold negative value from the signal obtained with an ica-negative strain.

Section V

PNAG in other microorganisms

Section V cover image represents PNAG expression by several gram-negative bacteria, determined by dot-blot (at top) and biofilm formation of PNAG positive and PNAG negative Escherichia coli strains (at bottom). BWH, Harvard Medical School, Boston, USA.

Introduction

Although PNAG was first found in staphylococcal strains, and has been associated with intercellular adhesion and the production of biofilms, recently Romeo *et al.* [242] found that *Escherichia coli* has an *ica*-homologous genetic locus, termed *pga*, that encodes proteins able to synthesize an exo-polysaccharide that they designated PGA, which is biochemically equivalent to PNAG (see figure V). They also reported that *pga* locus homologues occur in a number of other important Gram-negative pathogens, like *Yersinia pestis*, *Yersinia pseudotuberculosis*, *Yersinia enterocolitica*, *Bordetella pertusis* and *Bordetella parapertussis* [111,242]. However, they did not demonstrate pga/PNAG production by these species so the full extent of the expression of PNAG among pathogens is not known.

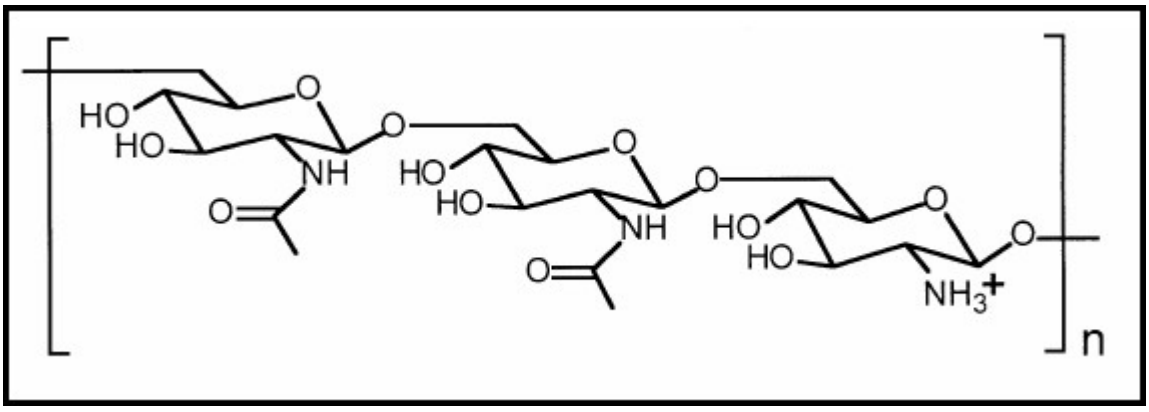

Figure V. Structure of PNAG. The polysaccharide is a linear homoglycan composed of β -1,6-linked N-acetylglucosamine residues; 20% of the residues are deacetylated and are thus positively charged. Adapted from J Infect Dis (1996), 174:881-884.

Since PNAG plays an important role in *S. epidermidis* pathogenesis (and also *S. aureus*), as described throughout this thesis, it was important to determine if the bacterial species identified by Romeo *et al.* as having *ica*-homologous genetic loci indeed produce a similar molecule to staphylococcal PNAG. As PNAG is a promising target for vaccine development [108,141,142,143,152,153], determining if the PNAG- homologous on the gram-negative pathogens was immunological similar to staphylococcal PNAG seemed of great importance, since it could mean that a vaccine against PNAG could potentially protect against several major human pathogens.

After the discovery of *E. coli* PGA, several studies focused on the role of PNAG/PGA in biofilm formation by a variety of bacterial species including *E. coli*, *Y. pestis*, *Y. enterocolitica*, *Y. pseudotuberculosis*, and *Actinobacillus pleuropneumoniae* among others [51,90,111,242].

In this last section, the investigation of the transcriptional activity of the *pga* promoter at different stages of growth, and in response to a variety of chemical stimuli using *E. coli* as a model is described. Furthermore, the presence of PNAG was also probed on the cell surface

on *E. coli*, *Yersinia spp*, and *Bordetella spp*, establishing that these organisms express a polysaccharide that is antigenically indistinguishable from staphylococcal PNAG. It was also verified that the antibodies elicited by an anti-staphylococcal vaccine was effective in killing *E. coli* clinical isolates from urinary tract infections and neonatal bacteremia *in vitro* and in protecting mice against lethal doses of bacteria.

Chapter 12

Molecular and immunological similarities between PNAG from Staphylococcus spp. and gram-negative bacteria

Summary

While PNAG was first detected in staphylococcal strains, the recent discovery that some gram-negative bacteria have genetic loci homologous to the staphylococcal ica locus (called the pga locus in E. coli), drove several research groups to focus their attentions on PNAG expression in gram-negative bacteria. In this last chapter, the ubiquitous presence of PNAG in gram-positive and gram-negative strains is described. The regulation of the E. coli pga promoter by environmental factors was studied. Furthermore, PNAG was immunologically detected on the cell surface of E. coli, Yersinia spp. and Bordetella spp. strains. The opsonic and protective effects of a staphylococcal PNAG-specific antiserum was evaluated using an E. coli pga mutant, as well as 30 E. coli clinical isolates from urinary tract and neonatal infections. Most of the E. coli pga positive strains were killed in an in vitro opsophagocitic assay. A representative set of E. coli strains was used in an in vivo murine intraperitoneal lethality model where the lethality of PGA/PNAG-positive strains was reduced by anti-PNAG antibody.

12.1. Experimental procedure

12.1.1 Strains and media

To evaluate the transcriptional activity of the *pga* promoter, the sequenced *E. coli* CFT073 strain was used to clone the *pga* locus and *E. coli* TOP10 was used as the host strain.

To evaluate the expression of PNAG by a broad range of bacteria, several strains were used: *S. aureus* MN8 [152] and *S. aureus* MN8Δica [50], *S. epidermidis* M187 [159], *E. coli* CFT073 [244] and *E. coli* UTI-J, *E. coli* UTI-JΔpga, UTI-JΔpga+pBAD (this study), *Y.pestis* KIM6+ and *Y. pestis* KIM6 [205], *Y.pestis* KIM6(pHMS1.2) [183], *Y. pseudotuberculosis* B46 and *Y. pseudotuberculosis* B46R, *B. pertussis* and *B. bronchoseptica*.

To further evaluate PNAG expression and the opsonic and protective activity of this antibody [143], 30 clinical isolates of *E. coli* from urinary tract infections (UTI) and from blood isolates from neonatal intensive care unit (NICU) were used.

S. epidermidis, *S. aureus* and *E. coli* strains were grown for 16 H at 37ºC in TSBG. *Y. pestis*, *Y. psedotuberculosis* and *Y. enterocolitica* were grown at 26 ºC for 48 H in brain hearth infusion (BHI). *B. pertussis* and *B. parapertussis* were grown for 72 H at 37ºC in blood agar plates.

12.1.2. Transcriptional activity of the *pga* promoter

To investigate the transcriptional activity of the *pga* promoter, the entire non-coding region between the *pga* locus and the *ycdT* gene was amplified from total DNA isolated from *E. coli* CFT073 by PCR and cloned into the pBLUE-TOPO vector to yield the construct pPGA. Empty pBLUE vector (pCTR) was used as a negative control. Both constructs were sequenced at the Microbiology Core Facility (Harvard Medical School, Boston, MA, USA) to confirm the absence of mutations. *E. coli* TOP10 cells served as the host strain. The strains were grown in a TSB modified medium lacking glucose. Growth curves were performed at 37ºC and both strains had similar growth kinetics (data not shown). The *pga* promoter activity under the influence of several environmental conditions was analyzed: growth at 21ºC and 37ºC, *pga* expression at different growth stages and also *pga* expression in the presence of glucose, ethanol, NaCl, MnCl2 and FBS. For that, approximately 1×10^9 bacteria growing at the different conditions were collected by centrifugation, lysed by bead-beating, and the supernatant was cleared by centrifugation. Total protein concentrations in the supernatants were analyzed by the Bradford assay, and β-galactosidase was quantified by standard ONPG assay. To calculate relative β-gal activity under different conditions, the basal activity per mg of extracted protein of strain pCTR was subtracted from the activity per mg protein of strain pBLUE.

12.1.3 Construction of *E. coli pga* mutant and complemented strains

The *pga* locus was replaced with a chloramphenicol acetyltransferase (CAT) cassette by the PCR-mediated one-step method of gene inactivation described by Datsenko and Wanner [55]. *E. coli* strains BW25311 and UTI-J containing the Red recombinase expression plasmid pKD46 were grown overnight at 25ºC in SOC medium containing 100 μg/ml of ampicillin and 10 mM L-arabinose. The following day the cells were collected, washed 3 times with de-ionized H2O containing 10% glycerol and concentrated 50-fold. A PCR product was generated using the following primer pair: pgadeleteFWD 5'- ccggactagcgctttttctgaaac caccatttttatttgcccctggctgggtgtagctggagctgcttc -3', and pgadeleteREV 5'- aagtagcagaaaaaggt gcccgaaaaccaaatgggctttgaaacttcttacatatgaatatcctccttag -3' with plasmid pKD3 as a template. The PCR product, which contained a CAT cassette with 5' and 3' ends homologous to the 5' and 3' ends of the *pga* locus, was gel purified using the QIAquick Gel Extraction kit. The electrocompetent bacteria were transformed with the purified PCR product by electroporation, and transformants were selected for on LB agar containing 30 μg/ml of chloramphenicol. Choramphenicol-resistant bacteria were analyzed by PCR for successful deletion of the *pga* locus and were cured of the pKD46 plasmid by 2 rounds of growth at 42ºC in the absence of ampicillin. To trans-complement the pga-deletion mutants, the entire *pga* locus was amplified by PCR using pgaexpressFWD (5'- ATGTATTCAAGTAGCAGAAAAAGGTGC -3') and pgaexpressREV (5'- GTGTTTACGCCCGGACTAGC -3') and cloned into the arabinose-inducible pBAD-TOPO vector. The resulting construct, pPGA, was sequenced and used to transform the *pga*-deletion mutant strains by electroporation. Transformants were selected for on LB agar containing 100 μg/ml of ampicillin. Addition of arabinose to the growth medium was not necessary for sufficient expression levels in pPGA-complemented strains.

12.1.4. PNAG production by bacteria and immunological detection

PNAG blots were performed as described in chapter 6.

12.1.5. Detection of the pga locus in *E. coli* clinical isolates by PCR

Genomic DNA from *E. coli* strains was extracted using a DNeasy Tissue kit. For the detection of *pgaC* gene the following primers were used: 5'-ATGATTAATCG CATCGTATCG-3' and 5'-CATCGGTTCCACAATATATGC-3'. For the detection of *pgaA* gene, the following primers were used: 5'-GGCTTTGAAACTTCTTACTGC-3' and 5'-CCTGTTTATCTTGC CCGGCC-3'. All primers were custom synthesized by Qiagen Operon. For the PCR reaction 25 μl of PCR supermix high fidelity was added, 0.5 μl of each primer and 2 μl of DNA. PCR conditions comprise an initial 5 min denaturation step at 94ºC, followed by 32 cycles of 30 s at 94ºC, 30 s at 50ºC and 45 s at 72ºC, and a final extension step of 5 min at 72ºC.

12.1.6. Opsonophagocytic assays with *E. coli* clinical isolates

White blood cells were prepared as described previously [154]. The complement source (1 ml of baby rabbit serum diluted 1:10 in RPMI/FBS) was adsorbed twice at 4ºC for 45 min with continual mixing using bacteria resuspended from a pellet containing ~10^9 cfu of *E. coli* BW25113. The goat antibody [143] used was diluted 1:10 in RPMI/FBS and adsorbed twice at 4ºC for 45 min with continual mixing using bacteria resuspended from a pellet containing ~10^9 cfu of *E. coli* BW25113Δpga. After adsorption the complement solution and the antibody were centrifuged and filter sterilized. The bacterial strains to be evaluated for phagocyte-dependent killing activities of antibody were grown overnight in TSBG and then adjusted to an OD_{640nm} of 0.4. Then, a 1:100 dilution was then made in RPMI/FBS for using in the killing assay.

The opsonophagocytic assay was performed as described in chapter 9. Several controls were used: each individual component was used in all possible combinations. To evaluate antibody-mediated killing the antibody was replaced with RPMI/FBS. The percentage of killing was calculated by determining the ratio of the cfu surviving in the tubes with bacteria, leukocytes, complement and antibody, to the cfu surviving in the tubes with bacteria, complement, leukocytes and RPMI/FBS. The assay was done with triplicates and repeated 2 to 3 times.

12.1.7. Murine lethality model

To evaluate the *in vivo* protection ability of anti-PNAG antibody, an intra-peritoneal murine model was used, as previously described [143]. Briefly, groups of 8 mice (FVB, female, 6-8 weeks of age) were immunized IP 24 H before and 4 H after infection with 0.3 ml of NGS or immune goat sera raised against staphylococcal PNAG. Bacteria were grown overnight in TSBG, and then resuspended in sterile PBS to approximately 5×10^8 cfu/ml to 5×10^9 cfu/ml, depending on the strain. For each strain, a minimal dose that would kill at least 75% of the mice was selected. Mice were challenged IP with a dose of 1.25×10^8 cfu to 1×10^9 cfu in 0.2 ml of PBS and monitored at least twice daily.

12.2. Results

12.2.1. Effect of growth conditions on *E. coli* pga promoter activity

To determine *pga* promoter activity during different growth phases, and in response to chemical stimuli, the predicted promoter of the locus *pgaABCD* was cloned into the a β-galactosidase (β-gal) reporter plasmid, and the plasmid transformed into a competent *E. coli* strain. The β-gal expression per mg total protein was compared at 21ºC and 37ºC (figure 12.1A) and the results showed that the activity was significantly higher at 37ºC ($p<0.05$, paired

samples t-test). Expression of the *pga* promoter was also significantly greater ($p<0.05$, paired samples t-test) during stationary phase (figure 12.1B).

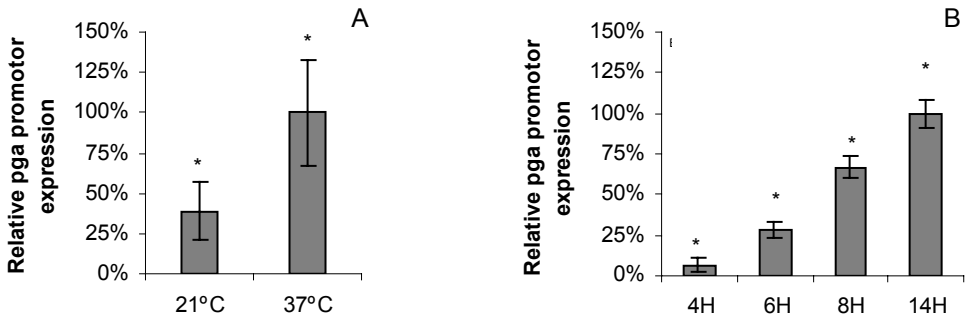

Figure 12.1. Expression of the *E. coli pga* promoter in modified TSB medium without glucose; A) growth at 21 or 37ºC, at the beginning of the stationary phase; B) growth at 37ºC, at different points of the growth phase: early log phase (4 H), mid log phase (6H), late log phase (8 H) and late stationary phase (14 H). Maximum activity was defined as 100% activity. Error bars represent the SD. * represent a statistical difference ($p<0.05$, paired samples t-test).

All cultures were subsequently grown to stationary phase at 37ºC. Addition of the stress-inducing factors like 1% ethanol and 1% NaCl in the growth medium resulted in a significant increase ($p<0.05$, paired samples t-test) in β-gal activity, whereas 1mM MnCl2 and 5% FBS had little effect (figure 12.2). Addition of 1% glucose was the only factor that had a strong inhibitory effect on expression (figure 12.2). The inhibitory effect of glucose was concentration dependent, and as little as 0.5% of glucose inhibited ~50% of the promoter activity (data not shown).

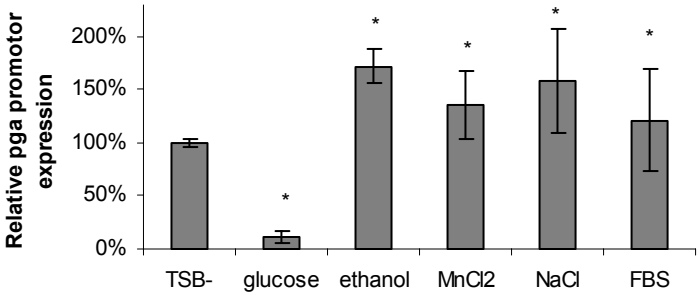

Figure 12.2. Expression of the *E. coli pga* promoter at 37ºC and stationary phase, due to the effect of 1% glucose, 1% ethanol, 1% NaCl 1mM MnCl2 and 5% FBS. The activity obtained with the modified TSB medium (TSB-) without added factors was defined as 100% activity. Error bar represent the SD. * represent a statistical difference to the control ($p<0.05$, paired samples t-test).

Although glucose repressed *pga* promoter activity, biofilm formation was enhanced (data not shown). This phenomena was also described in *S. epidermidis* strains [59], suggesting that glucose is required for biofilm formation but that there must be an yet unidentified factor regulating glucose repression of the *ica* and *pga* locus and biofilm formation.

12.2.2. Presence of PNAG in several gram-negative bacteria

Figure 12.3 presents PNAG expression in a broad range of gram-positive and gram-negative bacteria. *S. aureus* MN8 and *S. aureus* MN8Δica were used as positive and negative controls.

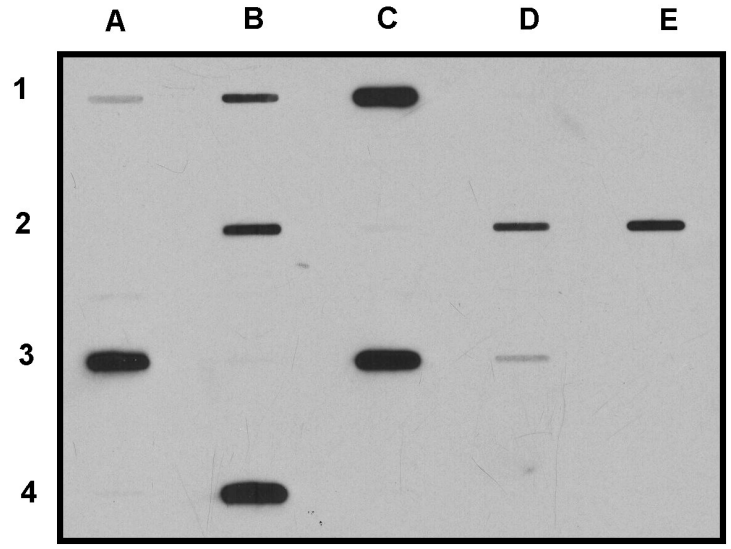

Figure 12.3. PNAG expression in gram-positive and gram-negative bacteria. Cell surface extracts with EDTA 0.5M of *S. aureus* MN8 (A1), *S. aureus* MN8Δica (A2), *S. epidermidis* M187 diluted 1,000× (A3), *E. coli* CTF073 (B1), *E. coli* UTI-J (B2), *E. coli* UTI-JΔpga (B3), *E. coli* UTI-JΔpga+pPGA (B4), *Y. pestis* Kim6+ (C1), *Y. pestis* Kim6 (C2), *Y. pestis* Kim6(pHMS1.2) (C3), *Y. pseudotuberculosis* B46 (D1), *Y. pseudotuberculosis* B46red (D2), *Y. enterocolitica* (D3), *B. pertussis* (E1) and *B. bronchoseptica* (E2).

S. epidermidis M187 was also used, however the cell surface extract was diluted 1,000 fold since the amount of PNAG produced by *S. epidermidis* M187 was a lot more than the rest of the bacteria used. The fact that *S. epidermidis* produced a lot more PNAG than *S. aureus* is not surprising, since PNAG *S. epidermidis* strains normally form thicker biofilms than *S. aureus* [39,103], and PNAG is the major component of *S. epidermidis* biofilm matrix. However, this presented a technical problem in the development of the immunoblot film, since the signal of a non diluted *S. epidermidis* M187 cell surface extract was too intense, even after only 20 s film exposure, and after 2 min of exposure, the film was over exposed due to this strong signal. After 1,000 fold dilution of the sample, a clean blot was obtained, being able to detect PNAG in the remaining strains.

Lanes B to E present the gram-negative bacteria tested. PNAG was detected in *E. coli Yersinia* and *Bordetella* strains. *E. coli* CFT073 (sequenced strain) and *E. coli* UTI-J (clinical isolate) produced PNAG. An *E. coli pga* mutant (UTI-JΔpga) lost the ability to produce PNAG, and this ability was restored when complemented with a plasmid with the *pga* locus (pPGA). The same observation was made for *Y. pestis*: while *Y. pestis* Kim6+ produce PNAG, a *hms* mutant strain did not produce PNAG, but when the mutant strain was complemented with a plasmid with the *hms* locus (pHMS1.2), PNAG production was restored. It was also demonstrated that there are *Y. pseudotuberculosis* and *Y. enterocolitica* strains that produce PNAG. *Y. pseudotuberculosis* B46red is a clinical isolate that has been found to agglutinates when grown on blood agar plates [183].

PNAG production was also determined in *B. pertussis* and *B. bronchiseptica*, and a strong signal in *B. bronchiseptica* was found, providing the first evidence that *Bordetella spp.* also produce a polysaccharide immunologically similar to staphylococcal PNAG.

12.2.3. Molecular and immunological characterization of the *E. coli* isolates

Table 12.1 summarizes the characterization of the 30 *E. coli* clinical isolates, and also control strains *E. coli* BW25133, BW25133Δpga, UTI-J, UTI-JΔpga.

Table 12.1. Molecular and Immunological characterization of *E. coli* clinical isolate strains

Group	Number of strains	DNA [1]		PNAG Blot [2]			Opsonophagocytic killing		
		-	+	-	+	++	<10%	11-30%	>31%
Control	4	2	2	2	1	1	2	0	2
UTI	18	2	16	4	9	5	4	5	9
NICU	12	2	10	3	5	4	5	0	7

1) Number of strains with (+) or without (-) pga locus, determined by PCR amplification of *pgaA* and *pgaC* gene; 2) number of strains producing PNAG detected by immunoblot: (-) no signal detected, (+) week signal detected, (++) strong signal detected.

In most of the *E. coli* strains (87%) the *pga* locus was detected, as determined by PCR probing of the *pgaA* and *pgaC* genes. While the *pga* negative strains did not produced PNAG (as expected) as detectable by immunoblot, some of the pga positive strains also did not produced detectable levels of PNAG. This can be due to low levels of PNAG expression, or even some mutation in the pga ORF.

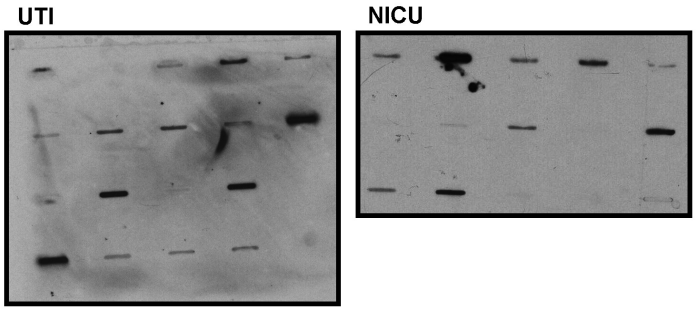

Figure 12.4. PNAG blot of *E. coli* urinary tract infections (UTI) and neonate intensive care unit bacteremia (NICU) isolates.

However, most of these strains (73%) produced detectable levels of PNAG (figure 12.4). When the opsonic killing of *E. coli* by a rabbit polyclonal antibody raised to deacetylated staphylococcal PNAG was evaluated (figure 12.5), pga-negative strains were resistant to killing, and approximately 81% of pga-positive strains were partially killed *in vitro*, with 62% demonstrated high levels of killing.

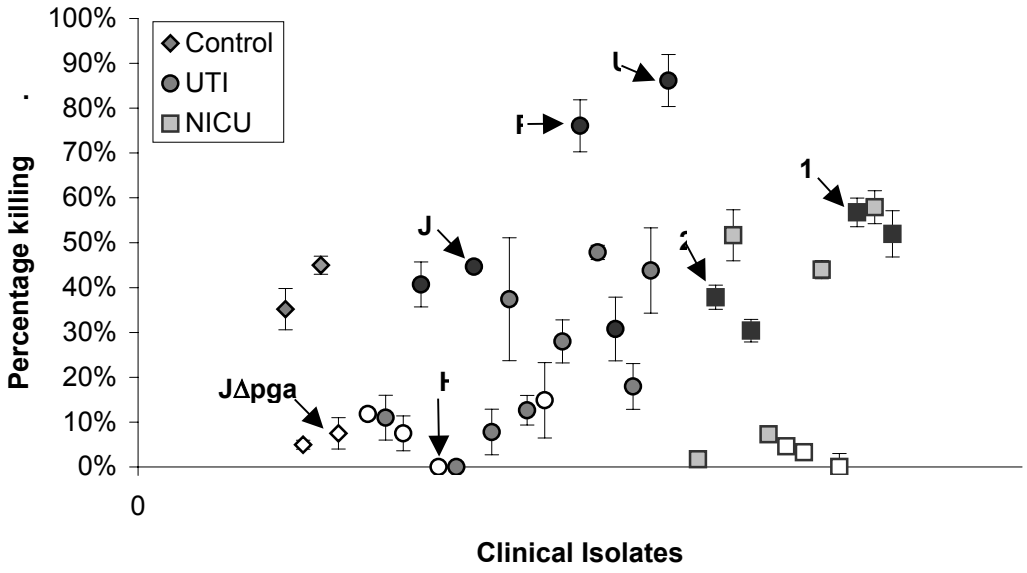

Figure 12.5. Opsonophagocytosis of the *E. coli* clinical isolates. Control strains are represented in diamonds. UTI isolates are in circles. NICU are in squares. Dark colors represent strong PNAG producers; light colors represent weak PNAG producers; white represent no PNAG detectable. *E. coli* UTI-J, UTI-JΔpga, UTI-H, UTI-P, UTI-U, NICU-2 and NICU-10 were selected for further studies.

12.2.4. dPNAG and PNAG opsonic activity

Figure 12.6 presents the differential opsonic activity of several dilutions of a rabbit polyclonal antibody raised to deacetylated staphylococcal PNAG (dPNAG) or to highly acetelytated staphylococcal PNAG (PNAG) against some *E. coli* clinical isolates. Both dPNAG and PNAG polyclonal sera were previously characterized, both having similar titers [143].

For *E. coli* UTI-J and NICU10 (killed well in the initial opsonic assay) and also *E. coli* UTI-P and UTI-U (highly killed in the initial opsonic assay) were selected for further studies. For all strains at any sera dilution, dPNAG antibody was superior compared to PNAG antibody. Furthermore, PNAG polyclonal antibody looses its ability to kill at a higher titer than dPNAG. For instance, with *E. coli* UTI-U, PNAG antibody stop killing bacteria at titers lower than 1:320 while dPNAG antibody could kill approximately 50% of the bacteria at a titer of 1:640.

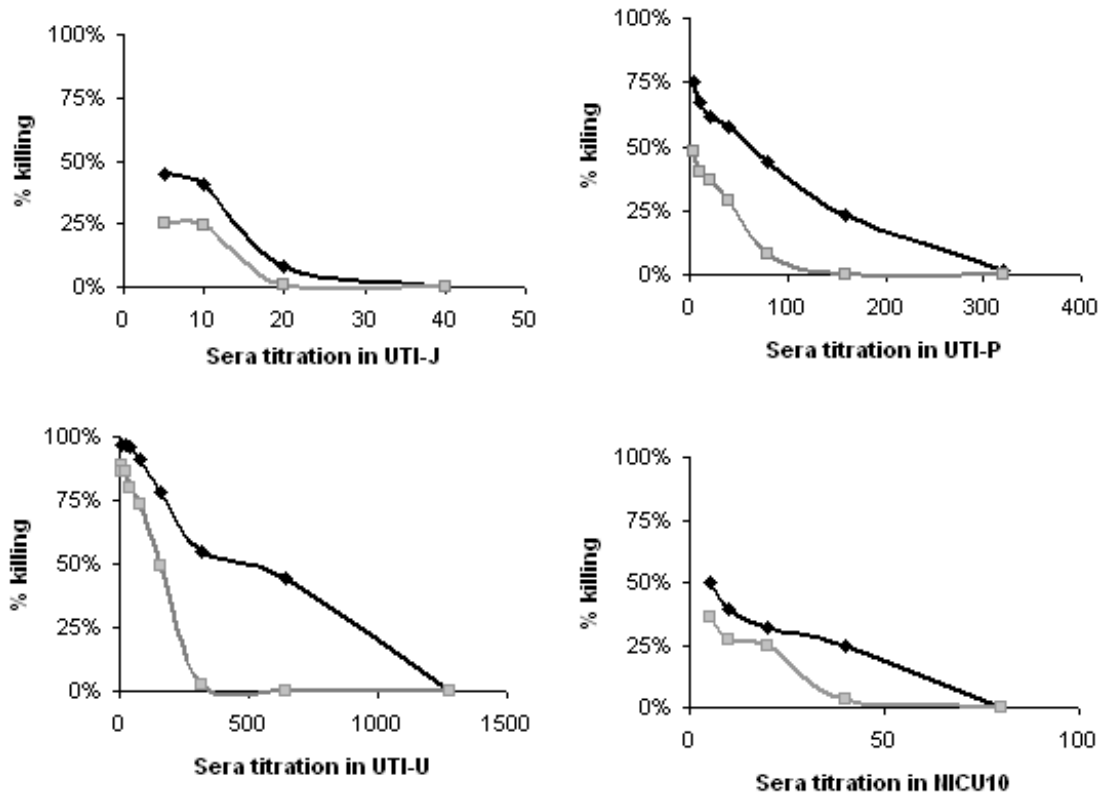

Figure 12.6. Opsonophagocytosis with dPNAG and PNAG sera titration, against *E. coli* UTI-J, UTI-P, UTI-U and NICU10 clinical isolates.

12.2.5. Protection studies

Table 12.2 summarizes the protective activity of the rabbit dPNAG polyclonal antibody against a selection of *E. coli* strains, in a murine intraperitonial infection model. *E. coli* UTI-J was used as a positive control and *E. coli* UTI-JΔpga as a negative control. *E. coli* UTI-H (pga-negative) was also included as a second negative control. *E. coli* NICU2 and NICU10 were modestly killed in the *in vitro* opsonic assays, while *E. coli* UTI-P and UTI-U were highly killed in the *in vitro* opsonic assay. The minimum bacterial concentration necessary to kill at least 75% of the mice was first determined, and then this concentration was used on the protection assays.

Table 12.2. Protection studies in an intraperitoneal murine model

Strain	Dose per mice	Normal Goat Sera	Immune Goat Sera
UTI-J	$2.5x10^8$ cfu	0/8 (0%)	5/8 (63%)
UTI-JΔpga	$1.0x10^9$ cfu	2/8 (25%)	2/8 (25%)
UTI-H	$5x10^8$ cfu	0/8 (0%)	0/8 (0%)
UTI-P	$2.5x10^8$ cfu	0/8 (0%)	7/8 (88%)
UTI-U	$5x10^8$ cfu	1/8 (13%)	7/8 (88%)
NICU-2	$1.25x10^8$ cfu	0/8 (0%)	7/8 (88%)
NICU-10	$1.25x10^8$ cfu	0/8 (0%)	4/8 (50%)

Data is presented as number of surviving mice over the total mice used, with the percentage survival between brackets.

Interestingly, while it was only necessary to use 2.5×10^8 cfu per mouse of *E. coli* UTI-J to kill all the mice, it was necessary to increase the concentration of *E. coli* UTI-JΔpga 4 fold (1×10^9 cfu per mice) to have a lethal dose to most of the mice. This provides evidence that PNAG is a virulence factor in *E. coli*, as it is in *S. aureus* [121]. As expected, it was possible to protect mice from UTI-J but not from UTI-JΔpga. Infection with UTI-H also resulted in the death of the mice, since this strain does not have the *pga* locus and does not produce PNAG. For most strains a high percentage of protection was achieved, having an average of ~75% of survival for all the strains used (excluding the negative controls).

12.3. Discussion

Recently, it was been described that in *E. coli* there is a homologous locus to the Staphylococcal *icaABCD*, called *pgaABCD*, which is required for the production of a polymer of β-1,6-N-acetyl-D-glucosamine, called PGA in *E. coli* [242]. *E. coli* is an important cause of gastrointestinal diseases [200,201], urinary tract infections [6,114,218,248] and neonatal meningitis and sepsis [107,251]. PGA promotes biofilm formation, is cell surface associated, and has a virtually identical structure to the staphylococcal PNAG [242]. PNAG was previously unknown from gram-negative bacteria [242] but had been previously found in *S. aureus* [51,152] and *S. epidermidis* [42,90,151]. Furthermore, it has been recently found that a glycosyl hydrolase from *Actinobacillus actinomycetemcomitans*, dispersin B, uses PNAG as a substrate [111]. The role of PNAG in biofilm formation in *S. epidermidis* and *E. coli*, was further elucidated, when dispersin B was used to effectively disrupt biofilm formed by these bacteria [99]. In the study described in this chapter it was shown that transcriptional activity of *pga* promoter has similarities with *ica* promoter in *S. epidermidis*. It was also demonstrated that *E. coli* PNAG is immunological similar to *S. aureus* PNAG, using a sequenced strain (*E. coli* CFT073) and also a clinical isolate (*E. coli* UTI-J). A *pga* mutant of *E. coli* UTI-J does not produce PNAG and a complemented strain with the *pga* locus inserted on a plasmid (pPGA) restores PNAG production (figure 12.3).

Although PNAG was not identified in *Yersinia* and *Bordetella spp* (until the present study), recent evidence shown that these organisms have a *pga*/*ica* homologous locus [111,242].

In the present study, PNAG was also found to be immunologically similar to the polysaccharide produced by *hmsHFRS* locus, as *hms*+ *Y. pestis* produces a signal detectable by immunoblot whereas a strain deleted for *hms* does not. Furthermore, a complemented strain with the *hms* locus restores the production of *Yersinia* PNAG (figure 12.3). The *hmsHFRS* locus in *Y. pestis* (homologous to *pgaABCD*) is required for biofilm formation *in vitro* [117] and hms HFRS-mediated biofilm formation is thought to play a role in transfer of

plague from fleas to mammals by causing blockage of the flea proventriculus and subsequent regurgitation of the organism into the bite wound [92]. It has been found that the *hms* proteins are temperature sensitive and can be degraded at 37ºC, with higher levels of expression found at 26ºC [182]. *Yersinia* strains were grown at 26ºC and 37ºC and the PNAG levels detected by immunoblot blot were higher at 26ºC, but still detectable at 37ºC (data not shown). This suggests that PNAG is likely synthesized in mammals and may be a vaccine candidate for plague. Strains of *Y. pseudotuberculosis* and *Y. enterocolitica* were also found to make PNAG.

B. pertussis and *B. bronchiseptica* cause whooping cough in humans, which is a highly contagious acute respiratory illness. *B. bronchiseptica* can also cause infection in other mammals, while *B. pertussis* is a strict human pathogen [150]. While no known role for PNAG in *Bordetella spp* has been described, it was interesting to determine if PNAG is present in these bacteria due to the possibility of cross-reaction with the *S. aureus* PNAG. Indeed, a strong signal was detected in an immunoblot, demonstrating that at least *B. bronchiseptica* produces PNAG. No signal was detected for *B. pertussis*, meaning that *B. pertussis* is not a strong PNAG producing strain.

In order to prove that PNAG production is a characteristic of the *E. coli* species, 30 *E. coli* clinical isolates were used for further studies. The strains were screened for the presence of the *pga* locus, by PCR, and PNAG production was detected by immunoblot. The opsonic-killing assay revealed a modestly good correlation of killing level with antigen expression level, although there were some exceptions. Nevertheless, it was already demonstrated that *S. aureus* MN8 (figure 12.3) is a low PNAG producer, but *in vivo* protection against this strain can be achieved [143].

The work described in chapter 10 provided evidence that an antibody raised against a partially de-acetylated form of PNAG is more effective than an antibody raised against highly acetylated PNAG, in the opsonic killing against *S. aureus* [143]. To verify if the same occurs in *E. coli*, 4 clinical isolates were selected and the killing effect of both antibodies compared. The same phenomenon was verified in the *E. coli* strains.

The protective efficacy of the antibody raised to the partially de-acetylated form of PNAG [143] was then analyzed in an *in vivo* murine model, against several *E. coli* strains expressing high or moderate levels of PNAG by immunoblot along with some negative controls (*E. coli* strains without the *pga* locus). In comparison to NGS, the anti-PNAG goat serum effectively protected against lethal sepsis following intraperitoneal infection, except in the negative controls, as expected.

The vaccine potential of PNAG as a target to Ab was previously demonstrated for *S. aureus* [143] and *S. epidermidis* [153] and the present results provide evidence that this vaccine may also give protection against *E. coli*.

The protective efficacy of antibody to PNAG against neonatal isolates of *E. coli* opens the possibility of a single passive therapeutic reagent for evaluation of prevention of serious infection by the 3 most consequential pathogens in neonatal intensive care units (*E. coli*, *S. aureus* and *S. epidermidis*) [251]. Furthermore, the immunological similarities between *Yersinia spp* and *Bordetella spp* PNAG with *S. aureus* PNAG open the possibility of a broad vaccine against some of the major human pathogens. Further studies most evaluate the vaccine potential of PNAG against these major human pathogens.

Concluding Remarks

Concluding remarks cover image is a SEM observation with 5000x magnification of a S. epidermidis 9142 biofilm in acrylic. Centre of Materials, University of Minho, Braga, Portugal.

Concluding remarks

Throughout this thesis, several aspects of coagulase negative staphylococci (especially *S. epidermidis*) virulence were addressed, namely: (a) the ability to adhere to different inert surfaces following by the (b) ability to form a biofilm on those same surfaces. It was also tested the (c) resistance of biofilms to several antibiotics, highlighting the differences between planktonic and biofilm cultures. Some strategies to overcome biofilm antibiotic resistance were tested, including (d) the use of sub-inhibitory concentrations of antibiotics to inhibit adhesion and biofilm formation and (e) the use of bacteriophage to eradicate biofilms. Furthermore, aspects involved in the immune evasion of *S. epidermidis* biofilms were tested using (f) *in vitro* phagocytic assays and (g) *in vivo* murine challenge models. Also, (h) molecular mechanisms of the production and chemical modification of PNAG were studied, revealing a key role in the immune evasion of Staphylococcal strains. Adding to this, the ubiquous presence of PNAG in other major human pathogens was briefly probed, indicating a major role for PNAG in the pathogenesis of other organisms beside *Staphylococcus spp*.

Adhesion and biofilm formation methods strongly influence the outcome of the experimental results

While one may think that biofilm formation depends only on the strain used, this is far from reality: initial adhesion and biofilm formation are strongly influenced by the growth medium and by the hydrodynamic conditions. These conditions must be optimized for accurate comparisons between strain's ability to adhere and to form biofilms.

Clinical isolates of *S. epidermidis* present different surface characteristics, resulting in different adhesion and biofilm formation abilities

Different strains of the same species can be phenotypically and genetically different. Strain variability within the same bacterial species is sufficient enough to yield a range of phenotypes. When testing different species for biofilm formation, a sufficient number of strains of each species should be used. Conclusions regarding any bacterial species ability to adhere to any surface or to form a biofilm based on just 1 strain can lead to a wrong conclusion. For instance, just by looking to *S. epidermidis* IE75 or even M129, one could come to the conclusion that *S. epidermidis* can adhere to several surfaces but is a week biofilm producer, and this is far for being true, since *S. epidermidis*, as a species, is a major biofilm producer.

Initial adhesion and subsequent biofilm formation are 2 distinct phenomena among clinical isolates of *S. epidermidis*

While it was been previously demonstrated that a *S. epidermidis* mutant strain impaired in the ability to produce PNAG would adhere extensively to glass but nevertheless could not form a biofilm, it was not known if clinical isolates of *S. epidermidis* would behave the same way. Since the factors involved in both processes are different (hydrophobic interactions play a major role in initial adhesion while specific biochemical factors play a major role in biofilm maturation), it is not surprising that some clinical isolates of *S. epidermidis* adhering to high extents could not form a biofilm, confirming that adhesion and biofilm formation are 2 distinct phenomena.

Biofilms are more resistant to antibiotics than planktonic cultures

While it has been widely accepted that biofilms are more resistant to antibiotics than planktonic cells, appropriate methods to quantify this resistance are scarce. The use of MIC values or even the more recent MBEC is really not appropriate to compare resistance between biofilm and planktonic populations, since MIC is used to measure susceptibility of low concentration planktonic cultures while MBEC uses high-density biofilm cultures. The work described in this thesis provided a direct comparison of equivalent bacterial populations and quantified the resistance of biofilms to antibiotics. The results revealed that while biofilms were more resistant than planktonic cells, as suggested by the literature, this resistance was found to be only 2 to 7 fold higher than planktonic cultures. Although this is still clinically significant, these values are much lower than the reported 1,000-fold increase resistance found in biofilms.

The use of sub-inhibitory concentrations of antibiotics partially reduces biofilm formation but can induce changes in biofilm phenotype

A suggested strategy to reduce biofilm formation was the prophylactic use of low concentrations of antibiotics. The work described in this thesis showed that, under the experimental conditions used, both adhesion and biofilm formation were significantly reduced. Nevertheless *S. epidermidis* strains were able to form a biofilm in the presence of antibiotics. Moreover, changes in the bacterial phenotype and on the biofilm structure, like an increase in antibiotic resistance and biofilm matrix constitution, present as serious obstacle to the implementation of prophylactic therapy using low concentrations of antibiotics.

Staphylococcal phages may present an alternative to antibiotics against biofilm infections

The high resistance of Staphylococcal biofilms to antibiotics is the driving force for the development of alternatives to resolve biofilm infections. The work described in the thesis proved that *S. epidermidis* biofilms do not pose a physical barrier to phage penetration, and the biofilm mass is effectively reduced by anti-staphylococcal phage K. Interestingly biofilm cells are lysed at slower rates than exponentially growing planktonic cells but at similar rates to stationary phase planktonic cells. This is not entirely surprising since phage activity depends on the metabolism of the host, and biofilms or stationary growth cells have lower growth rates, and therefore result in intrinsically lower phage-mediated lytic rates.

Biofilm cells are sufficiently phenotypically different, compared to planktonic cells, in order to induce a distinct immune response

While it has been demonstrated that bacteria encased in a biofilm structure are protected from the immune system, nothing was known regarding the contribution of biofilm-grown bacteria individually phenotype to this resistance. The work described within this thesis demonstrated that *S. epidermidis* cells resuspended from a biofilm are more resistant to killing in an *in vitro* opsonic-phagocytosis assay than their planktonic counterparts. Moreover, the induced immune response in a murine model was distinct, with planktonic bacteria recruiting more innate and adaptive immune response effectors than biofilm-grown cells.

Besides the intercellular adhesion function, chemically modified PNAG can act as a decoy against the host immune response

PNAG was first identified in *S. epidermidis* and was called PIA, due to its described function as a polysaccharide intercellular adhesin. In the last few years, PNAG was also detected in *S. aureus*, and a new function was described: PNAG enhanced the resistance of bacteria to antibody-independent phagocytosis. The studies described in the thesis demonstrated a third role for PNAG, which is based on the acetylation of PNAG by *icaB* gene, where partial de-acetylation of PNAG results in its retention on the bacterial cell surface whereas highly-acetylated PNAG can be secreted, acting as a decoy to the adaptive response of the immune system.

PNAG is present in several major human pathogens and is immunologically similar to staphylococcal PNAG

Besides all the described biological functions of PNAG, this molecule has been used as a target for vaccine development by the group of Gerald Pier, in Harvard Medical School, Boston, USA. The discovery of an immunologically similar molecule to staphylococcal PNAG in several major human pathogens indicates that this anti-staphylococcal vaccine might be used against other infectious diseases agents. The results demonstrated the protective efficacy of antibody to dPNAG against neonatal isolates of *E. coli*, which opens the possibility of a single passive therapeutic reagent for evaluation of prevention of serious infection by the 3 most consequential pathogens in neonatal intensive care units (*E. coli*, *S. aureus* and *S. epidermidis*).

Future perspectives

The findings derived from the work described in this thesis enlight some aspects of *S. epidermidis* virulence, but also opened more questions that need to be answered. Some of the work that should be explored includes:

1- Testing the hypothesis of PNAG as a decoy in a murine *in vivo* model.

2- Expanding the knowledge provided by the *in vivo* immune system assays (chapter 9) by performing more immunological *in vivo* experiments using the same animal model and also trying to implement a new animal model based on an urinary tract infection associated with catheter use.

3- Testing phage therapy in a murine *in vivo* model, by isolating new anti-staphylococcal phages and analyzing not only the phage efficacy but also the phage half-life once injected in the mouse.

4- Further characterizing the set of clinical isolates used for other virulence factors, like the *AtlE* gene, *sarA* family and the *agr* quorum sensing system, and to verify the global effect on clinical isolates ability to form a biofilm.

Supplements

S.1. Origin of the CoNS strains

CoNS strain	Origin of strains
9142	Biofilm positive control strain [135]
9142-M10	Biofilm negative control strain [135]
IE75 IE186 IE214 IE246	Strains isolated from infective endocarditis patients, at Brigham and Women's Hospital, Boston MA, USA
M129 M176 M187	Strains isolated from dialysis-associated peritonitis patients, at Brigham and Women's Hospital, Boston MA, USA
FJ6 JI6 LE7 PE9	Strains isolated from the skin, at Brigham and Women's Hospital, Boston MA, USA

S.2. Identification of the species using API STAPH kit

CoNS strain	Primary identification	Secondary identification
9142	96.1% *S. epidermidis*	-
9142-M10	98.2% *S. epidermidis*	-
IE75	93.2% *S. epidermidis*	-
IE186	95.3% *S. epidermidis*	4.3% *S. hominis*
IE214	95.3% *S. epidermidis*	4.3% *S. hominis*
IE246	90.2% *S. haemolyticus*	-
M129	85.2% *S. epidermidis*	12.8% *S. capitis*
M176	90.2% *S. haemolyticus*	-
M187	93.2% *S. epidermidis*	-
FJ6	93.2% *S. epidermidis*	-
JI6	95.3% *S. epidermidis*	4.3% *S. hominis*
LE7	95.3% *S. epidermidis*	4.3% *S. hominis*
PE9	96.1% *S. epidermidis*	-

S.3. Metabolic diversity by API STAPH kit

Test	CoNS strain												
	9142	M10	IE75	IE186	IE214	IE246	M129	M176	M187	FJ6	JI6	LE7	PE9
GLU	+	+	+	+	+	+	+	+	+	+	+	+	+
FRU	+	+	+	+	+	-	+	-	+	+	+	+	+
MNE	+	-	+	-	-	-	+	-	+	+	-	-	+
MAL	+	+	+	+	+	+	+	+	+	+	+	+	+
LAC	+	+	+	+	+	+	-	+	+	+	+	+	+
TRE	-	-	-	-	-	+	-	+	-	-	-	-	-
MAN	-	-	-	-	-	+	-	+	-	-	-	-	-
XLT	-	-	-	-	-	-	-	-	-	-	-	-	-
MEL	-	-	-	-	-	-	-	-	-	-	-	-	-
NIT	+	+	+	+	+	+	+	+	+	+	+	+	+
PAL	+	+	+	+	+	+	+	+	+	+	+	+	+
VP	-	-	-	-	-	-	+	-	-	-	-	-	-
RAF	-	-	-	-	-	-	-	-	-	-	-	-	-
XYL	-	-	-	-	-	-	-	-	-	-	-	-	-
SAC	+	+	+	+	+	+	+	+	+	+	+	+	+
MDG	-	-	-	-	-	-	-	-	-	-	-	-	-
NAG	-	-	-	-	-	+	-	+	-	-	-	-	-
ADH	-	+	+	-	-	+	+	+	+	+	-	-	-
URE	+	+	+	+	+	-	+	-	+	+	+	+	+

S.4. Physiological diversity

	9142	M10	M187	IE75	IE186	IE214	IE246	M129	M176	FJ6	LE7	JI6	PE9
Duplication time (a)	38	43	32	36	34	54	33	40	26	30	39	46	41
Coaggregation (b)	+	-	+	-	+	++	+	+	+	+	-	-	+
Growth temperature (c)	45-49	45-49	40-44	40-44	45-49	40-44	45-49	40-44	40-44	45-49	40-44	40-44	45-49

(a) minimum duplication time in the log phase at 37ºC and 130rpm, in TSB medium; (b) coaggreagation detected after overnight growth, at 37ºC and 130rpm, in TSB medium; (c) maximum growth temperature range (in 5ºC intervals).

S.5. Biofilm Image Gallery

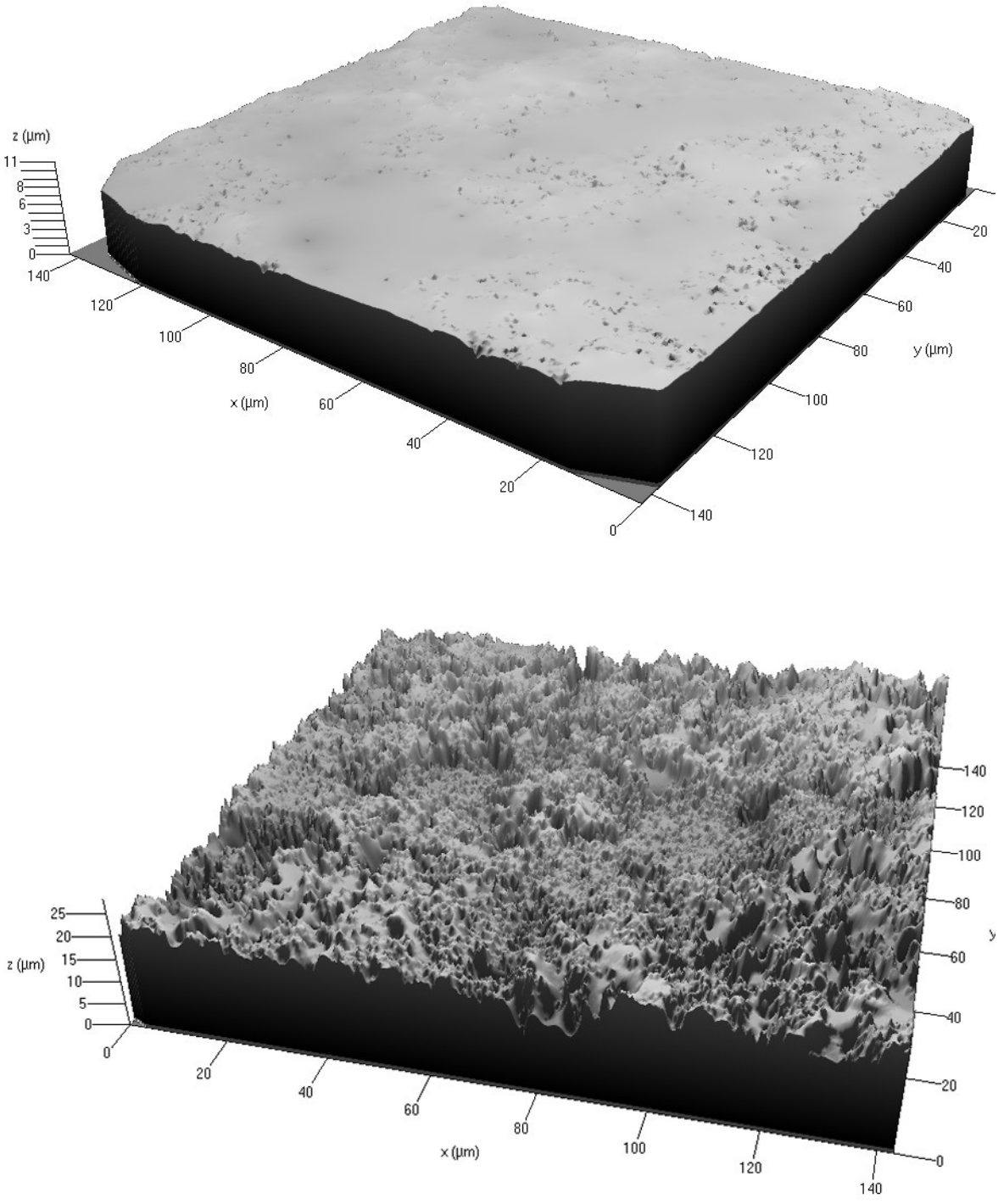

Figure S.5.A. Difference between a 24 H (top) and 48 H (bottom) biofilm of *S. epidermidis* 9142 on a glass surface (CLSM representation).

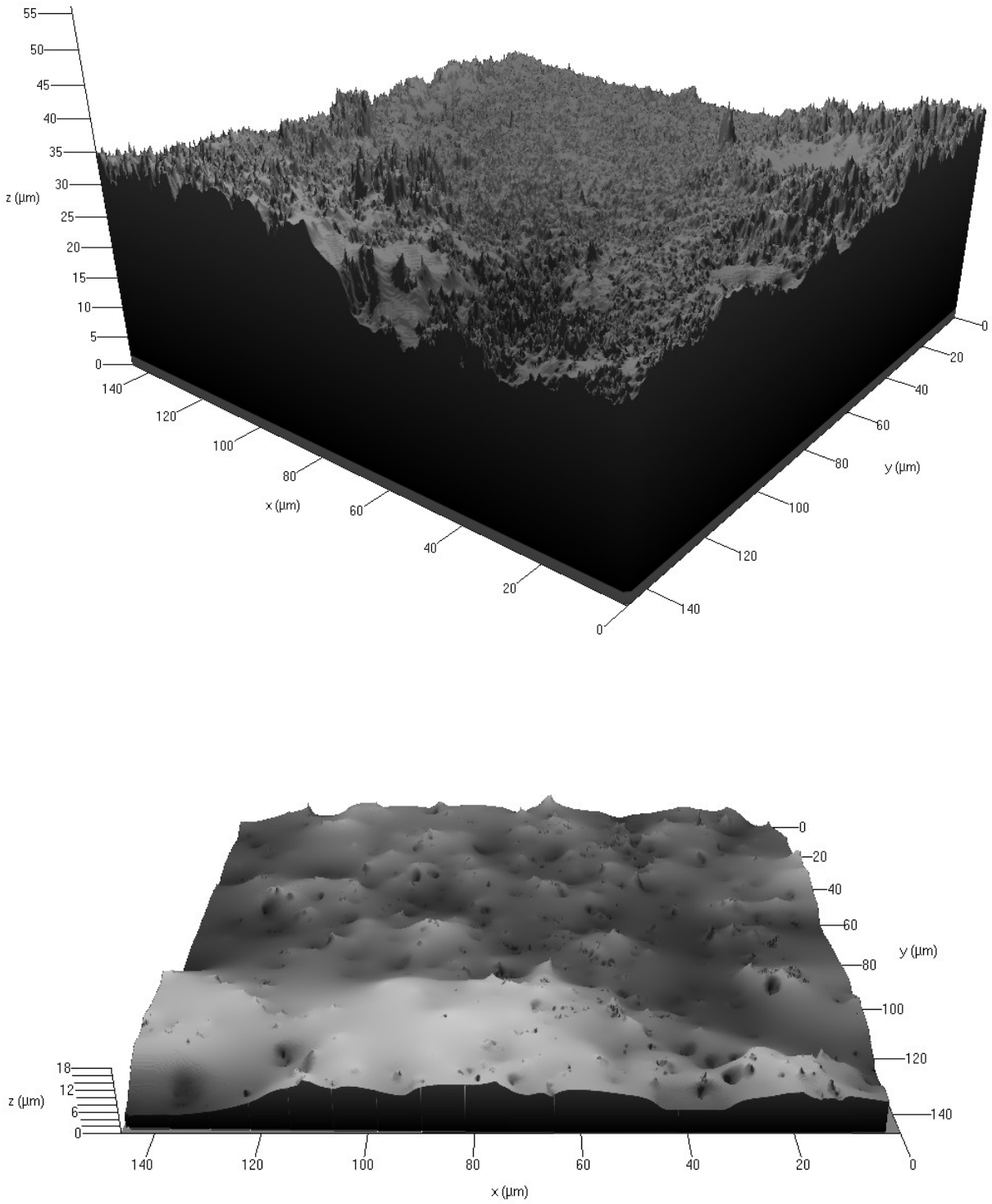

Figure S.5.B. Difference between of *S. epidermidis* (top) and *S. haemolyticus* (bottom) 48 H biofilm on a glass surface (CLSM representation).

Equipment List

2 ml centrifuge. Silent spin, Continental Lab Products, USA

25 gauss syringe. Artsana, Italy

Video camera. Sony CCD, Japan (for inverted microscope) and Axiocam Hrc, Germany (for contrast-phase).

40× ultra-long working distance objective. ELWD, 40x/0.50, Nikon, Netherlands

40× water immersion objective. Phaco2 40x/0.65W, Leitz, Germany

50 ml centrifuge. Sigma 4K10, B. Braun, Germany

63× water immersion objective. Achroplan 63x/0.95W, Zeiss, Germany

96 well ELISA plate reader. Spectra Rainbow, Tecan, Austria

Automated contact angle device. OCA20, Dataphysics, Germany

Blot developing cassette. ECL Direct nucleic acid labeling and detection system, Amersham Biosciences, UK

CellQuest software. Becton Dickinson, USA

CSLM device. LSM 510 Meta attached to an Axioplan II microscope, Zeiss, Germany

Cytospins slide. Cytospin2, Shandon, USA

Digital scale. Sartorius BL120S. Germany

FACScan device. Becton Dickinson, USA

LSM 510 software. Zeiss, Germany

Lyophilizator. Christ Alpha2-4, B.Braun, Germany

Contrast-phase Microscope. Leitz Labourluz S, Germany

Neubauer chamber. Marienfeld, Germany

Orbital shaker. SI50, Stuart Scientific, UK (sections I – III) and Rollerdrum, New Brunswick Scientific Co, USA (sections IV and V)

PCR thermocycler. TC312, Techne, UK

Peristaltic roller pump. Reglo, Lsmatec, Switzerland

Phase-contrast inverted microscope. Nikon Diaphot 300, Netherlands

Photographic developer. Kodak M35A X-OMAT, USA

Sigma Scan Pro software. Aspire Software International, USA

Slot-blot apparatus. The convertible, Gibco BRL, USA

Sonicator. VC600, Sonics, USA

Spectrophtometer. Spectonic 20 Genesys, Spectronic Instruments, USA

Vortex. Vortex-genie 2, Scientific Industries, USA

Western blotting system. Amersham Sciences, USA

XPS device. ESCALAB 200A, Thermo Electron Corporation, USA

Reagents and Materials List

ρ-nitrophenyl phosphate. Sigma, USA

0.2 μm nitrocellulose filter. Amersham Sciences, USA

0.45 μm cellulose filter. Whatman, UK

6 well polystyrene tissue-culture plates. Startedt, USA

96 well polystyrene microtiter plates. Orange Scientific, Belgium (sections I and II) or Corning Incorporated, USA (sections III, IV and V) or Nunc, Denmark (chapter 9)

Acrylic. Repsol, Denmark

Agarose. American Bioanalytical, USA

Anti human IgG-Alexa 488. Molecular Probes, USA

Antibiotics. Sigma, USA

Antibodies for ELISA assay. Southern Biotechnology Associates, USA

Antibodies for flow citometry. PharMingen, USA (all except goat anti-mouse IgM FITC conjugate, from Southern Biotechnology Associates, USA)

Anti-rabbit IgG-Alexa green. Molecular Probes, USA

Baby bunny complement. Cedarlane, Canada.

BHI. Bacto, USA

BSA. American Bioanalytical, USA

BSS. Sigma, USA

Celltak solution. BD Biosciences, USA

Commercial detergent. Sonazol Pril, Portugal

Contact angles references liquids. Merck, Germany

DNeasy Tissue kit. Qiagen, USA

Dubois Reagents. Sigma, USA

EDTA. Sigma, Germany

Eppendorf tubes. Brinkmann Instruments Inc, USA

Ethidium bromide. Sigma, USA

FBS. Hyclone, USA

General chemicals. Merck, Germany

Glass. Industrial Quality, Germany

Glass bottom microwell plates. Mattek, USA

Glucose. Merck, Germany

Hemacolour stain. Sigma, USA

Horse erythrocyte solution. Biomerieux, France

Horseradish peroxidase-conjugated anti-rabbit IgG antibody. SouthernBiotech, USA

LB. Bacto, USA

Liquid Nitrogen. Praxair, Portugal

Lowry Reagents. Sigma, USA

ONPG assay. Invitrogen, USA

pBAD-TOPO vector. Invitrogen, USA

pBLUE-TOPO vector. Invitrogen, USA

PCR primers. Qiagen Operon, USA

PCR supermix high fidelity, Invitrogen, USA

PMS. Sigma, USA

Proteinase K. Qiagen, Germany

QIAprep spin miniprep kit. Qiagen, USA

QIAquick Gel Extraction kit. Qiagen, USA

Ready-2-go T4 ligase. Amersham Sciences, USA

Restriction and DNA modifying enzymes. Invitrogen, USA

RPMI. Sigma, USA

RNeasy Protect miniprep kit. Qiagen, USA

Safranin solution. Merck, Germany

Saline Solution (NaCl). Pronalab, Portugal

SOC. Sigma, USA

Skin milk. Difco Laboratories, USA

Superscript II One-Step RT-PCR. Invitrogen, USA

TBS. American Bioanalytical, USA

TSA. Merck, Germany (sections I, II and III) and Bacto, USA (sections IV and V)

TSB. Merck, Germany (sections I, II and III) and Bacto, USA (sections IV and V)

Turbo Dnase. Ambion, USA

Tween. American Bioanalytical, USA

Ultra-pure water. From Seralpur Pro 90CN, Spain

WGA. Molecular Probes, USA

XTT. Sigma, USA

Reference List

1. Ackermann HW, Krisch HM, (1997) A catalogue of T4-type bacteriophages. Arch Virol, 142: 2329-2345.

2. Akiyama H, Yamasaki O, Kanzaki H, Tada J, Arata J, (1998) Adherence characteristics of *Staphylococcus aureus* and coagulase-negative staphylococci isolated from various skin lesions. J Dermatol Sci, 18: 132-136.

3. Amorena B, Gracia E, Monzón M, Leiva J, Oteiza C, Perez M, Alabart J, Hernandez-Yajo J, (1999) Antibiotic susceptibility assay for *Staphylococcus aureus* in biofilms developed *in vitro*. J Antimicrob Chemother, 44: 43-55.

4. An Y, Friedman R, (1997) Laboratory methods for studies of bacterial adhesion. J Microb Meth, 30: 141-152.

5. Anderl J, Franklin M, Stewart P, (2000) Role of antibiotic penetration limitation in *Klebsiella pmeumoniae* biofilm resistance to ampicillin and ciprofloxacin. Antimicrob Agents Chemother, 44: 1818-1824.

6. Andreu A, Alos JI, Gobernado M, Marco F, de La RM, Garcia-Rodriguez JA, (2005) Etiology and antimicrobial susceptibility among uropathogens causing community-acquired lower urinary tract infections: a nationwide surveillance study. Enferm Infecc Microbiol Clin, 23: 4-9.

7. Arciola C, Campoccia D, Montanaro L, (2002) Effects on antibiotic resistance of *Staphylococcus epidermidis* following adhesion to polymethylmethacrylate and to silicone surfaces. Biomaterials, 23: 1495-1502.

8. Arciola C, Montanaro L, Caramazza R, Sassoli V, Cavedagna D, (1998) Inhibition of bacterial adherence to a high-water-content polymer by a water.solube nonsteroidal, anti-inflammatory drug. J Biomed Mater Res, 42: 1-5.

9. Azeredo J, Henriques M, Sillankorva S, Oliveira R, (2003) Extraction of exopolymers from biofilms: the protective effect of glutaraldehyde. Water Sci Technol, 47: 175-179.

10. Azeredo J, Oliveira R, (2000) The role of expolymers produced by *Sphingomonas paucimobilis* in biofilm formation and composition. Biofouling, 16: 17-27.

11. Azeredo J, Oliveira R, (2003), The role of hydrophobicity and exopolymers in initial adhesion and biofilm formation ***in*** Biofilms in Medicine, Industry and Environmental Biotechnology - Characteristics, Analysis and Control, 16-31. IWA Publishing, London

12. Babalova EG, Katsitadze KT, Sakvarelidze LA, Imnaishvili NS, Sharashidze TG, Badashvili VA, Kiknadze GP, Meipariani AN, Gendzekhadze ND, Machavariani EV, Gogoberidze KL, Gozalov EI, Dekanosidze NG, (1968) [Preventive value of dried dysentery bacteriophage]. Zh Mikrobiol Epidemiol Immunobiol, 45: 143-145.

13. Bakker D, Busscher H, van der Mei H, (2002) Bacterial deposition in a parallel plate and a stagnation point flow chamber: microbial adhesion mechanisms depend on the mass transport conditions. Microbiology, 148: 597-603.

14. Baldassarri L, Doneelli G, Gelosia A, Voglino M, Simpson WA, Christensen GD, (1996) Purification and characterization of the staphylococcal slime-associated antigen and its occurence among *Staphylococcus epidermidis* clinical isolates. Infect Immun, 64: 3410-3415.

15. Baveja J, Wilcox M, Hume E, Kumar N, Odell R, Poole-Warren L, (2004) Furanones as potential anti-bacterial coating on biomaterials. Biomaterials, 25: 5003-5012.

16. Berkowitz FE, (1995) Antibiotic resistance in bacteria. South Med J, 88: 797-804.

17. Beveridge T, Makin S, Kadurugamuwa J, Li Z, (1997) Interactions between biofilms and the environment. FEMS Microbiol Rev, 20: 291-303.

18. Bos R, van der Mei H, Busscher H, (1999) Physico-chemistry of initial microbial adhesive interactions: its mechanisms and methods for study. FEMS Microbiol Rev, 23: 179-230.

19. Bosch J, van der Mei H, Busscher H, (1991) Statistical analisis of bacterial species based on a physico-chemical surface proteins. Biofouling, 4: 141-150.

20. Briandet R, Herry J, Bellon-Fontaine N, (2001) Determination of the van der Waals, electron donor and electron acceptor surface tension components of static gram-positive microbial biofilms. Colloids Surf B Biointerfaces, 21: 299-310.

21. Brown MR, Barker J, (1999) Unexplored reservoirs of pathogenic bacteria: protozoa and biofilms. Trends Microbiol, 7: 46-50.

22. Bruinsma G, van der Mei H, Busscher H, (2001) Bacterial adhesion to surface hydrophilic and hydrophobic contact lenses. Biomaterials, 22: 3217-3224.

23. Brussow H, (2005) Phage therapy: the *Escherichia coli* experience. Microbiology, 151: 2133-2140.

24. Brussow H, Canchaya C, Hardt WD, (2004) Phages and the evolution of bacterial pathogens: from genomic rearrangements to lysogenic conversion. Microbiol Mol Biol Rev, 68: 560-602, table.
25. Bruttin A, Brussow H, (2005) Human volunteers receiving *Escherichia coli* phage T4 orally: a safety test of phage therapy. Antimicrob Agents Chemother, 49: 2874-2878.
26. Bryant MP, Wolin EA, Wolin MJ, Wolfe RS, (1967) *Methanobacillus omelianskii*, a symbiotic association of 2 species of bacteria. Arch Mikrobiol, 59: 20-31.
27. Buckling A, Rainey PB, (2002) Antagonistic coevolution between a bacterium and a bacteriophage. Proc Biol Sci, 269: 931-936.
28. Bull JJ, Levin BR, DeRouin T, Walker N, Bloch CA, (2002) Dynamics of success and failure in phage and antibiotic therapy in experimental infections. BMC Microbiol, 2: 35-
29. Busscher H, Bos R, van der Mei H, (1995) Initial microbial adhesion is a determinant for the strenght of biofilm adhesion. FEMS Microbiol Lett, 128: 229-234.
30. Busscher H, Geertsema-Doornbusch G, van der Mei H, (1997) Adhesion to silicone rubber of yeasts and bacterial isolated from voice prostheses: influence of salivary conditioning films. J Biomed Mater Res, 34: 201-210.
31. Busscher H, van Hoogmoed C, Geertsema-Doornbusch G, van der Kuijl-Booij M, van der Mei H, (1997) *Streptococcus thermophilus* and its biosurfactants ihnibit adhesion by *Candida spp*. on silicone rubber. Appl Environ Microbiol, 63: 3810-3817.
32. Busscher H, Weerkamp A, (1987) Specific and non-specific interactions in bacterial adhesion to solid substrata. FEMS Microbiol Rev, 46: 165-173.
33. Busscher H, Weerkamp A, van der Mei H, van Pelt A, De Jong H, Arends J, (1984) Measurement of the surface free-energy of bacterial-cell surfaces and its relevance for adhesion. Appl Environ Microbiol, 48: 980-983.
34. Busscher H, Bruinsma G, van Weissenbruch R, Leunisse,C, van der Mei H, Dijk F, Albers FW, (1998) The effect of buttermilk consumption on biofilm formation on silicone rubber voice prostheses in an artificial throat. Eur Arch Otorhinolaryngol, 255: 410-413.
35. Canchaya C, Proux C, Fournous G, Bruttin A, Brussow H, (2003) Prophage genomics. Microbiol Mol Biol Rev, 67: 238-76.
36. Carsenti-Etesse,H, Durant,J, Bernard,E, Mondain,V, Entenza,J, Dellamonica,P (1992) Effect of subinhibitory concentrations of cefamandole and cefuroxime on adherence of *Staphylococcus aureus* and *Staphylococcus epidermidis* to polystyrene culture plates. Eur J Clin Microbiol Infect Dis, 11: 732-737.
37. Cerca N, Martins S, Cerca F, Jefferson K, Pier G, Oliveira R, Azeredo J, (2005) Comparative assessment of the susceptibility of coagulase-negative Staphylococcal cells in biofilm versus planktonic culture to antibiotic killing as assedded by bacterial enumeration or rapid XTT colorimetry. J Antimicrob Chemother, 56: 331-336.
38. Cerca N, Martins S, Pier G, Oliveira R, Azeredo J, (2005) The relationship between inhibition of bacterial adhesion to a solid surface by sub-mic concentrations of antibiotics and the subsequent development of a biofilm. Res Microbiol, 156: 650-655.
39. Cerca N, Martins S, Sillankorva S, Jefferson K, Pier G, Oliveira R, Azeredo J, (2005) Effects of growth in the presence of subinhibitory concentrations of dicloxacillin on *Staphylococcus epidermidis* and *Staphylococcus haemolyticus* Biofilms. Appl Environ Microbiol, 71: 8677-8682.
40. Cerca N, Pier G, Oliveira R, Azeredo J, (2004) Comparative evaluation of coagulase-negative staphylococci (CoNS) adherence to acrylic by a static method and a parallel-plate flow dynamic method. Res Microbiol, 155: 755-760.
41. Cerca N, Pier G, Vilanova M, Oliveira R, Azeredo J, (2004) Influence of batch or fed-batch growth on *Staphylococcus epidermidis* biofilm formation. Lett Appl Microbiol, 39: 420-424.
42. Cerca N, Pier GB, Vilanova M, Oliveira R, Azeredo J, (2005) Quantitative analysis of adhesion and biofilm formation on hydrophilic and hydrophobic surfaces of clinical isolates of *Staphylococcus epidermidis*. Res Microbiol, 156: 506-514.
43. Ceri H, Olson M, Stremick C, Read R, Morck D, Buret A, (1999) The calgary biofilm device: new technology for rapid determination of antibiotic susceptibilities of bacterial biofilms. J Clin Microbiol, 37: 1771-1776.
44. Chapman R, Ostuni E, Liang M, Meluleni G, Kim E, Yan L, Pier G, Warren S, Whitesides G, (2001) Polymeric thin films that resist the adsoption of proteins and the ahdesion of bacteria. Langmuir, 17: 1225-1233.
45. Chibani-Chennoufi S, Dillmann ML, Marvin-Guy L, Rami-Shojaei S, Brussow H, (2004) *Lactobacillus plantarum* bacteriophage LP65: a new member of the SPO1-like genus of the family Myoviridae. J Bacteriol, 186: 7069-7083.

46. Christensen GD, Barker L, Mawhinney T, Baddour L, Simpson WA, (1990) Identification of an antigen marker of slime production for *Staphylococcus epidermidis*. Infect Immun, 58: 2906-2911.
47. Collins FS, (1992) Cystic fibrosis: molecular biology and therapeutic implications. Science, 256: 774-779.
48. Costerton JW, (1995) Overview of microbial biofilms. J Ind Microbiol, 15: 137-140.
49. Costerton JW, Stewart PS, Greenberg EP, (1999) Bacterial biofilms: a common cause of persistent infections. Science, 284: 1318-1322.
50. Cramton S, Ulrich M, Gotz F, Doring G, (2001) Anerobic conditions induce expression of polysaccharide intercellular adhesin in *Staphylococcus aureus* and *Staphylococcus epidermidis*. Infect Immun, 69: 4079-4085.
51. Cramton S, Gerke C, Schnell NF, Nichols WW, Gotz F, (1999) The intercellular adhesion (*ica*) locus is present in *Staphylococcus aureus* and is required for biofilm formation. Infect Immun, 67: 5427-5433.
52. Cunliffe D, Smart C, Alexander C, Vulfson E, (1999) Bacterial adhesion at synthetic surfaces. Appl Environ Microbiol, 65: 4995-5002.
53. Dankert J, Hogt A, Feijen J, (1986) Biomedical polymers: bacterial adhesion, colonization and infection. CRC Critic Rev Biocomp, 2: 219-301.
54. Dart J, (1996), Contact lens and prosthesis infections ***in*** Duane's foundations of clinical ophthalmology, 1-30. Lippincott-Raven, Philadelphia, USA
55. Datsenko KA, Wanner BL, (2000) One-step inactivation of chromosomal genes in *Escherichia coli* K-12 using PCR products. Proc Natl Acad Sci U S A, 97: 6640-6645.
56. Davey M, O'Toole G, (2000) Microbial biofilms: from ecology to molecular genetics. Microbiol Mol Biol Rev, 64: 847-867.
57. De Beer D, Srinivasan R, Stewart PS, (1994) Direct measurement of chlorine penetration into biofilms during disinfection. Appl Environ Microbiol, 60: 4339-4344.
58. de Silva G, Kantzanou M, Justice A, Massey R, Wilkinson A, Day N, Peacock S, (2002) The *ica* operon and biofilm production in coagulase-negative staphylococci associated with carriage and disease in a neonatal intensive care unit. J Clin Microbiol, 40: 382-388.
59. Dobinsky S, Kiel K, Rohde H, Bartscht K, Knobloch JK, Horstkotte MA, Mack D, (2003) Glucose-related dissociation between *icaADBC* transcription and biofilm expression by *Staphylococcus epidermidis*: evidence for an additional factor required for polysaccharide intercellular adhesin synthesis. J Bacteriol, 185: 2879-2886.
60. Donland R, Costerton J, (2002) Biofilms: survival mechanisms of clinical relevant microorganisms. Clin Microbiol Rev, 15: 167-193.
61. Doyle R, (2000) Contribution of the hydrophobic effect to microbial infection. Microbes Infect, 2: 391-400.
62. Dubois M, Gilles K, Hamilton J, Rebers P, Smith F, (1956) Colorimetric method for determination of sugars and related substances. Anal Chem, 28: 350-356.
63. Dunne W, (2002) Bacterial adhesion: seen any good biofilms lately? Clin Microbiol Rev, 15: 155-166.
64. Dunne W, Mason EO, Kaplan SL, (1993) Diffusion of rifampin and vancomycin through a *Staphylococcus epidermidis* biofilm. Antimicrob Agents Chemother, 37: 2522-2526.
65. Elliott TS, Moss HA, Tebbs SE, Wilson IC, Bonser RS, Graham TR, Burke LP, Faroqui MH, (1997) Novel approach to investigate a source of microbial contamination of central venous catheters. Eur J Clin Microbiol Infect Dis, 16: 210-213.
66. Evans DJ, Allison DG, Brown MR, Gilbert P, (1991) Susceptibility of *Pseudomonas aeruginosa* and *Escherichia coli* biofilms towards ciprofloxacin: effect of specific growth rate. J Antimicrob Chemother, 27: 177-184.
67. Everaert E, Mahieu H, Chung R, Verkerke G, van der Mei H, Busscher H, (1997) A new method for *in vivo* evaluation of biofilms on surface-modified silicone rubber in a parallel plate flow chamber in the absence and presence of nutrient broth. Microbiology, 143: 1569-1574.
68. Fang H, Chan K, Xu L, (2000) Quantification of bacterial adhesion forces using atomic force microscopy. J Microb Meth, 40: 89-97.
69. Finkelstein R, Rabino G, Mashiah T, Bar-El Y, Adler Z, Kertzman V, Cohen O, Milo S, (2002) Vancomycin versus cefazolin prophylaxis for cardiac surgery in the setting of a hight prevalence of methicillin-resistant staphylococcal infections. Surg acq cardiov dis, 123: 326-332.
70. Fluit A, Schmitz F, Verhoef J, (2001) Multi-resistance to antimicrobial agenst for the ten most frequently isolated bacterial pathogens. Int J Antimicrob Agents, 18: 147-160.
71. Fonseca P, Granja P, Nogueira J, Oliveira R, Barbosa M, (2001) *Staphylococcus epidermidis* RP62A ahdesion to chemically modified cellulose derivatives. J Mat Science: Mat Med, 12: 543-548.

72. Friberg O, Jones I, Sjoberg L, Soderquist B, Vikerfors T, Kallman J, (2004) Antibiotic concentrations in serum and wound fluid after local gentamicin or intravenous dicloxacillin prophylaxis in cardiac surgery. Scand J Infect Dis, 35: 251-254.
73. Fung-Tome J, Clark J, Minassiam B, Pucci M, Tsai Y, Gradelski E, Lamb L, Medina I, Huczko E, Kolek B, Chaniewski S, Ferraro C, Washo T, Bonner D, (2002) *in vitro* and *in vivo* activities of a novel cephalosporin, BMS-247243, against methicillin-resistant and susceptible Staphylococci. Antimicrob Agents Chemother, 46: 971-976.
74. Furneri P, Garozzo A, Musumarra M, Scuderi A, Russo A, Bonfiglio G, (2003) Effects on adhesiveness and hydrophopbicity of sub-inhibitory concentrations of netilmicin. Int J Antimicrob Agents, 22: 164-167.
75. Galbart J, Allignet J, Tung H, Ryden C, Solh N, (2000) Screening for *Staphylococcus epidermidis* markers discriminating between skin-flora strains and those responsible for infections of joint prostheses. J Infect Dis, 182: 351-355.
76. Ganderton L, Chawla J, Winters C, Wimpenny J, Stickler D, (1992) Scanning electron microscopy of bacterial biofilms on indwelling bladder catheters. Eur J Clin Microbiol Infect Dis, 11: 789-796.
77. Gerke C, Kraft A, Sussmuth R, Schweitzer O, Gotz F, (1998) Characterization of the N-acetylglucosaminyl-transferase activity involved in the biosynthesis of the *Staphylococcus epidermidis* polysaccharide intercellular adhesin. J Biol Chem, 273: 18586-18593.
78. Gilbert P, Das J, Foley I, (1997) Biofilm susceptibility to antimicrobials. Adv Dent Res, 11: 160-167.
79. Gillis R, Iglewski B, (2004) Azithromycin retards Pseudomonas aeruginosa biofilm formation. J Clin Microbiol, 42: 5842-5845.
80. Giridhar G, Kreger A, Myrvik Q, Gristina A, (1994) Inhibition of staphylococcus adherence to biomaterials by extracellular slime of *S. epidermidis* RP12. J Biomed Mater Res, 28: 1289-1294.
81. Gómez-Suárez C, Busscher H, van der Mei H, (2001) Analysis of bacterial detachment from substratum surfaces by the passage of air-liquid interfaces. Appl Environ Microbiol, 67: 2531-2537.
82. Gómez-Suárez C, Noordmans J, van der Mei H, Busscher H, (1999) Detachment of colloidal particles from collector surfaces with different electrostatic charge and hydrophobicity by attachment to air bubbles in a parallel plate flow chamber. Phys Chem, 1: 4423-4427.
83. Gotz F, (2002) Staphylococcus and biofilms. Mol Microbiol, 43: 1367-1378.
84. Gristina AG, Dobbins JJ, Giammara B, Lewis JC, DeVries WC, (1988) Biomaterial-centered sepsis and the total artificial heart. Microbial adhesion vs tissue integration. JAMA, 259: 870-874.
85. Gross M, Cramton S, Gotz F, Peschell A, (2001) Key role of teichoic acid net charge in *Staphylococcus aureus* colonization of artificial surfaces. Infect Immun, 69: 3423-3426.
86. Haessler D, Reverdy M, Neidecker J, Brule P, Ninet J, Lehot J, (2003) Antibiotic prophylaxis with cefazolin and gentamicin in cardiac surgery for children less than ten kilograms. J Cardiothorac Vasc Anesth, 17: 221-225.
87. Hawser S, Norris H, Jessup C, Ghannoum M, (1998) Comparison of a 2,3-bis(2-methoxy-4-nitro-5-sulfophenyl)-5[(phenyl-amino)carbonyl]-2H-tetrazolium hydroxide (XTT) colorimetric method with the standardized national committee for clinical laboratory standards method of testing clinical yeast isolates for susceptibility to antifungal agents. J Clin Microbiol, 36: 1450-1452.
88. Heilmann C, Gerke C, Perdreau-Remington F, Gotz F, (1996) Characterization of Tn917 insertion mutants of *Staphylococcus epidermidis* affected in biofilm formation. Infect Immun, 64: 277-282.
89. Heilmann C, Hussain M, Peters G, Gotz F, (1997) Evidence for autolysin-mediated primary attachment of *Staphylococcus epidermidis* to a polystyrene surface. Mol Microbiol, 5: 1013-1024.
90. Heilmann C, Schweitzer O, Gerke C, Vanittanakom N, Mack D, Gotz F, (1996) Molecular basis of intercellular adhesion in the biofilm-forming *Staphylococcus epidermidis*. Mol Microbiol, 20: 1083-1091.
91. Hermsen E, Hovde L, Hotchkiss K, Rotschafer J, (2003) Increased killing of staphylococci and streptococci by daptomycin compared with cefazolin and vancomycin in an *in vitro* peritoneal dialysate model. Antimicrob Agents Chemother, 47: 3764-3767.
92. Hinnebusch BJ, Fischer ER, Schwan TG, (1998) Evaluation of the role of the *Yersinia pestis* plasminogen activator and other plasmid-encoded factors in temperature-dependent blockage of the flea. J Infect Dis, 178: 1406-1415.
93. Hoban D, Bouchillon S, Johnson J, Zhanel G, Butler D, Saunders K, Miller L, Poupard J, (2001) Comparative *in vitro* potency of amoxycillin-clavulanic acid and four oral agents against recent North American clinical isolates from a global surveillance study. Int J Antimicrob Agents, 21: 425-453.
94. Hoellman D, Lin G, Ednie L, Ashok R, Jacobs M, Appelbaum P, (2003) Antipneumococcal and antistaphylococcal activities of ranbezolid (RBX 7644), a new oxazolidinone, compara to those of other agents. Antimicrob Agents Chemother, 47: 1148-1150.

95. Hoyle BD, Alcantara J, Costerton JW, (1992) *Pseudomonas aeruginosa* biofilm as a diffusion barrier to piperacillin. Antimicrob Agents Chemother, 36: 2054-2056.
96. Hoyle BD, Costerton J, (1991) Bacterial resistance to antibiotics: the role of biofilms. Prog Drug Res, 37: 91-105.
97. Huff WE, Huff GR, Rath NC, Balog JM, Donoghue AM, (2002) Prevention of *Escherichia coli* infection in broiler chickens with a bacteriophage aerosol spray. Poult Sci, 81: 1486-1491.
98. Hume E, Baveja J, Muirf B, Schubert T, Kumar N, Kjelleberg S, Griesser H, Thissen H, Read R, Poole-Warren L, Schindhelm K, Wilcox M, (2004) The control of *Staphylococcus epidermidis* biofilm formation and *in vivo* infection rates by covalent bound furanones. Biomaterials, 25: 5023-5030.
99. Itoh Y, Wang X, Hinnebusch BJ, Preston JF III, Romeo T, (2005) Depolymerization of beta-1,6-N-acetyl-D-glucosamine disrupts the integrity of diverse bacterial biofilms. J Bacteriol, 187: 382-387.
100. Jansen B, Kristinsson K, Jansen S, Peters G, Pulverer G, (1992) In-vitro efficacy of a central venous catheter complexed with iodine to prevent bacterial colonization. J Antimicrob Chemother, 30: 135-139.
101. Jefferson K, (2004) What drives bacteria to produce a biofilm? FEMS Microbiol Lett, 236: 163-173.
102. Jefferson K, Cramton S, Gotz F, Pier G, (2003) Identification of a 5-nucleotide sequence that controls expression of the ica locus in *Staphylococcus aureus* and characterization of the DNA-binding properties of IcaR. Mol Microbiol, 889-899.
103. Jefferson K, Goldmann D, Pier G, (2005) Use of confocal microscopy to analyze the rate of vancomycin penetration throught *Staphylococcus aureus* biofilms. Antimicrob Agents Chemother, 49: 2467-2473.
104. Jefferson K, Pier D, Goldmann D, Pier G, (2004) The teicoplanin-associated locus regulator (TcaR) and the intercellular adhesin locus regulator (icaR) are transcriptional inhibitors of the ica locus in *Staphylococcus aureus*. J Bacteriol, 186: 2449-2456.
105. Jesaitis AJ, Franklin MJ, Berglund D, Sasaki M, Lord CI, Bleazard JB, Duffy JE, Beyenal H, Lewandowski Z, (2003) Compromised host defense on *Pseudomonas aeruginosa* biofilms: characterization of neutrophil and biofilm interactions. J Immunol, 171: 4329-4339.
106. Johnsen AR, Hausner M, Schnell A, Wuertz S, (2000) Evaluation of fluorescently labeled lectins for noninvasive localization of extracellular polymeric substances in *Sphingomonas* biofilms. Appl Environ Microbiol, 66: 3487-3491.
107. Jones B, Peake K, Morris AJ, McCowan LM, Battin MR, (2004) *Escherichia coli*: a growing problem in early onset neonatal sepsis. Aust N Z J Obstet Gynaecol, 44: 558-561.
108. Joyce J, Abeygunawardana C, Xu Q, Cook J, Hepler R, Przysiecki C, Grimm K, Roper K, Yu C, Cope L, Montgomery D, Chang M, Campie S, Brown M, McNeely T, Zorman J, Maira-Litrán T, Pier G, Keller,´P, Jansen K, Mark G, (2003) Isolation, structure characterization, and immunological evaluation of a high-molecuar-weight exopolysaccharide from *Staphylococcus aureus*. Carbohydr Res, 338: 903-922.
109. Jucker B, Harms H, Zehnder A, (1996) Adhesion of the positively charged bacterium *Stenotrophomonas (Xanthomonas) maltophilia* 70401 to glass and teflon. J Bacteriol, 178: 5472-5479.
110. Kadry A, Tawfik A, El-Asrar A, Shibi A, (1999) Reductiong of mucoid *Staphylococcus epidermidis* adherence to intraocular lenses by selected antimicrobial agents. Chemotherapy, 45: 56-60.
111. Kaplan JB, Velliyagounder K, Ragunath C, Rohde H, Mack D, Knobloch JK, Ramasubbu N, (2004) Genes involved in the synthesis and degradation of matrix polysaccharide in *Actinobacillus actinomycetemcomitans* and *Actinobacillus pleuropneumoniae* biofilms. J Bacteriol, 186: 8213-8220.
112. Karchmer A, Gibbons G, (1994), Infections of prosthetic hearth valves and vascular grafts ***in*** Infections associated with indewelling medical devices , 213-249. ASM, Washington DC, USA
113. KasatiyaSS, Baldwin JN, (1967) Nature of the determinant of tetracycline resistance in *Staphylococcus aureus*. Can J Microbiol, 13: 1079-1086.
114. Katouli M, Brauner A, Haghighi LK, Kaijser B, Muratov V, Mollby R, (2005) Virulence characteristics of *Escherichia coli* strains causing acute cystitis in young adults in Iran. J Infect, 50: 312-321.
115. Kelly-Quintos C, Kropec A, Briggs S, Ordonez C, Goldmann D, Pier G, (2005) The role of epitope specificity in the human opsonic antibody response to Staphylococcal surface polysaccharide PNAG. J Infect Dis, 11:2012-2019
116. Keren I, Kaldalu N, Al S, Wang Y, Key L, (2004) Persister cells and tolerence to antimicrobials. FEMS Microbiol Lett, 230: 13-18.

117. Kirillina O, Fetherston J, Bobrov A, Abney J, Perry R, (2004) *HmsP*, a putative phosphodiesterase, and *HmsT*, a putative diguanylate cyclase, control Hms-dependent biofilm formation in *Yersinia pestis*. Mol Microbiol, 54: 75-88.
118. Klingenberg C, Aarag E, Ronnestad A, Sollid JE, Abrahamsen TG, Kjeldsen G, Flaegstad T, (2005) Coagulase-Negative Staphylococcal Sepsis in Neonates: Association Between Antibiotic Resistance, Biofilm Formation and the Host Inflammatory Response. Pediatr Infect Dis J, 24: 817-822.
119. Knobloch J, von Osten H, Horstkotte M, Rohde H, Mack D, (2002) Minimal attachment killin (MAK): a versatile method for susceptibility testing of attached biofilm-positive and -negative *Staphylococcus epidermidis*. Med Microbiol Immunol, 191: 107-114.
120. Koerner R, Butterworth L, Mayer I, Dasbach R, Busscher H, (2002) Bacterial adhesion to titanium-oxy-nitride (TiNOX) coatings with different resistivities: a novel approach for the development of biomaterials. Biomaterials, 23: 2835-2840.
121. Kropec A, Maira-Litrán T, Jefferson K, Grout M, Cramton S, Gotz F, Goldmann D, Pier G, (2005) Poly-N-acetyl glucosamine production in *Staphylococcus aureus* is essential for virulence in murine models of systemic infection. Infect Immun, 73: 6868-6876.
122. Kuhn DM, Balkis M, Chandra J, Mukherjee PK, Ghannoum MA, (2003) Uses and limitations of the XTT assay in studies of *Candida* growth and metabolism. J Clin Microbiol, 41: 506-508.
123. Lacy M, Tessier P, Nicolau D, Nightingale C, Quintiliani R, (2000) Comparison of vancomycin pharma-codynamics (1 g every 12 or 24 h) against methicillin-resistant staphylococci. Int J Antimicrob Agents, 15: 25-30.
124. Lalla F, (1999) Antimicrobial chemotheraphy in the control of surgical infectious complications. J Chemoth, 11: 440-445.
125. Lawrence JR, Swerhone GD, Leppard GG, Araki T, Zhang X, West MM, Hitchcock AP, (2003) Scanning transmission X-ray, laser scanning, and transmission electron microscopy mapping of the exopolymeric matrix of microbial biofilms. Appl Environ Microbiol, 69: 5543-5554.
126. Lebaron P, Bauda P, Lett MC, Duval-Iflah Y, Simonet P, Jacq E, Frank N, Roux B, Baleux B, Faurie G, Hubert JC, Normand P, Prieur D, Schmitt S, Block JC, (1997) Recombinant plasmid mobilization between *E. coli* strains in seven sterile microcosms. Can J Microbiol, 43: 534-540.
127. Lee JC, (1993) Electrotransformation of Staphylococci.
128. Leid JG, Shirtliff ME, Costerton JW, Stoodley AP, (2002) Human leukocytes adhere to, penetrate, and respond to *Staphylococcus aureus* biofilms. Infect Immun, 70: 6339-6345.
129. Leid JG, Willson CJ, Shirtliff ME, Hassett DJ, Parsek MR, Jeffers AK, (2005) The exopolysaccharide alginate protects *Pseudomonas aeruginosa* biofilm bacteria from IFN-{gamma}-mediated macrophage killing. J Immunol, 175: 7512-7518.
130. Leriche V, Sibille P, Carpentier B, (2000) Use of an enzyme-linked lectinsorbent assay to monitor the shift in polysaccharide composition in bacterial biofilms. Appl Environ Microbiol, 66: 1851-1856.
131. Logu A, Pellerano M, Sanna A, Pusceddu M, Uda P, Saddi B, (2003) Comparison of the susceptibility testing of clinical isolates of *Mycobacterium tuberculosis* by the XTT colorimetric method and the NCCLS standards method. Int J Antimicrob Agents, 21: 244-250.
132. Lowry O, Rosebrough N, Farr A, Randall R, (1951) Protein measurement with the Folin phenol reagent. J Biol Chem, 193: 265-275.
133. Lydyard P, Grossi C, (1998), Cells involved in the immune response ***in*** Immunology, 14-30. Mosby, London, UK
134. Mack D, Fischer W, Krokotshc A, Leopold K, Hartmann R, Egge H, Laufs R, (1996) The intercellular adhesin involved in biofilm accumulation of *Staphylococcus epidermidis* is a liner beta-1.6-linked glucosaminoglycan: purification and structural analysis. J Bacteriol, 178: 175-183.
135. Mack D, Nedelmann M, Krokotshc A, Schwarzkopf A, Heesemann J, Laufs R, (1994) Characterization of transposon mutants of biofilm-producing *Staphylococcus epidermidis* Impaired in the accumulative Phase of biofilm production: genetic identification of a hexosamine-containing polysaccharide intercellular adhesin. Infect Immun, 62: 3244-3253.
136. Mack D, Riedewald J, Rohde H, Magnus T, Feucht H, Elsner H, Laufs R, Rupp M, (1999) Essential functional role of the polysaccharide intercellular adhesin of *Staphylococcus epidermidis* in hemagglutination. Infect Immun, 67: 1004-1008.
137. Mack D, Rohde H, Dobinsky S, Riedewald J, Nedelmann M, Knobloch J, Elsner H, Feucht H, (2000) Identification of 3 essential regulatory gene loci governing expression of *Staphylococcus epidermidis* polysaccharide intercellular adhesin and biofilm formation. Infect Immun, 68: 3799-3807.
138. Madigan M, Martinko J, Parker J, (1997), Concepts of Immunology ***in*** Brock, Biology of Microorganisms, 813-862. Prentice Hall, London, UK

139. Madigan M, Martinko J, Parker J, (1997), Host-parasite relationships ***in*** Brock, Biology of Microorganisms, 785-812. Prentice Hall, London, UK
140. Mah T, O'Toole G, (2001) Mechanisms of biofilm resistance to antimicrobial agents. Trends Microbiol, 9: 34-39.
141. Maira-Litrán T, Kropec A, Abeygunawardana C, Joyce J, Mark G, Goldmann D, Pier G, (2002) Immunochemical properties of the staphylococcal poly-N-acetylglucosamine surface polysaccharide. Infect Immun, 70: 4433-4440.
142. Maira-Litrán T, Kropec A, Goldmann D, Pier G, (2004) Biologic properties and vaccine potential of the staphylococcal poly-N-acetyl glucosamin surface polysaccharide. Vaccine, 22: 872-879.
143. Maira-Litran T, Kropec A, Goldmann D, Pier G, (2005) Comparative opsonic and protective activities of *Staphylococcus aureus* conjugate vaccines containing native or deacetylated Staphylococcal Poly-N-acetyl-beta-(1-6)-glucosamine. Infect Immun, 73: 6752-6762.
144. Maki DG, Stolz SM, Wheeler S, Mermel LA, (1997) Prevention of central venous catheter-related bloodstream infection by use of an antiseptic-impregnated catheter. A randomized, controlled trial. Ann Intern Med, 127: 257-266.
145. Male D, (1998), Cell migration and inflammation ***in*** Immunology, 62-70. Mosby, London, UK
146. Male D, Roitt I, (1998), Introduction to the Immune System ***in*** Immunology, 1-13. Mosby, London, UK
147. Marrie TJ, Costerton JW, (1983) A scanning and transmission electron microscopic study of the surfaces of intrauterine contraceptive devices. Am J Obstet Gynecol, 146: 384-394.
148. Mathee K, Ciofu O, Sternberg C, Lindum PW, Campbell JI, Jensen P, Johnsen AH, Givskov M, Ohman DE, Molin S, Hoiby N, Kharazmi A, (1999) Mucoid conversion of *Pseudomonas aeruginosa* by hydrogen peroxide: a mechanism for virulence activation in the cystic fibrosis lung. Microbiology, 145 (Pt 6): 1349-1357.
149. Matsuzaki S, Yasuda M, Nishikawa H, Kuroda M, Ujihara T, Shuin T, Shen Y, Jin Z, Fujimoto S, Nasimuzzaman MD, Wakiguchi H, Sugihara S, Sugiura T, Koda S, Muraoka A, Imai S, (2003) Experimental protection of mice against lethal *Staphylococcus aureus* infection by novel bacteriophage phi MR11. J Infect Dis, 187: 613-624.
150. Mattoo S,Cherry JD, (2005) Molecular pathogenesis, epidemiology, and clinical manifestations of respiratory infections due to *Bordetella pertussis* and other *Bordetella* subspecies. Clin Microbiol Rev, 18: 326-382.
151. McKenney D, Hubner J, Muller E, Wang Y, Goldmann D, Pier G, (1998) The *ica* locus of *Staphylococcus epidermidis* encodes productiong of the capsular polysaccharide/adhesin. Infect Immun, 66: 4711-4720.
152. McKenney D, Pouliot K, Wang Y, Murthy V, Ulrich M, Doring G, Lee J, Goldmann D, Pier G, (1999) Broadly protective vaccine for *Staphylococcus aureus* based on an *in vivo*-expressed antigen. Science, 284: 1523-1527.
153. McKenney D, Pouliot K, Wang Y, Murthy V, Ulrich M, Doring G, Lee J, Goldmann D, Pier G, (2000) Vaccine potential of poly-1-6-B-D-N-succinylglucosamine, and immunoprotective surface polysaccharide of *Staphylococcus aureus* and *Staphylococcus epidermidis*. J Biotech, 83: 37-44.
154. Meluleni GJ, Grout M, Evans DJ, Pier G, (1995) Mucoid *Pseudomonas aeruginosa* growing in a biofilm *in vitro* are killed by opsonic antibodies to the mucoid exopolysaccharide capsule but not by antibodies produced during chronic lung infection in cystic fibrosis patients. J Immunol, 155: 2029-2038.
155. Millsap K, Reid G, van der Mei H, Busscher H, (1996) Adhesion of *Lactobacillus* species in urine and phophate buffer to silicone rubber and glass under flow. Biomaterials, 18: 87-91.
156. Mohamed N, Teeters M, Patti J, Hook M, Ross J, (1999) Inhibition of *Staphylococcus aureus* adherence to collagen under dynamic conditions. Infect Immun, 67: 589-594.
157. Monzón M, Oteiza C, Leiva J, Lamata M, Amorena B, (2002) Biofilm testing of *Staphylococcus epidermidis* clinical isolates: low performance of vancomycin in relation to other antibiotics. Diagn Microbiol Infect Dis, 44: 319-324.
158. Moran FJ, Garcia C, Perez-Giraldo C, Hurtado C, Blanco MT, Gomez-Garcia AC, (1998) Phagocytosis and killing of slime-producing *Staphylococcus epidermidis* bypolymorphonuclear leukocytes. Effects of sparfloxacin. Rev Esp Quimioter, 11: 52-57.
159. Muller E, Hubner J, Gutierrez N, Takeda S, Goldmann D, Pier G, (1993) Isolation and characterization of transposon mutants of *Staphylococcus epidermidis* deficient in capsular polysaccharide/adhesin and slime. Infect Immun, 61: 551-558.
160. Naess LM, Aarvak T, Aase A, Oftung F, Hoiby EA, Sandin R, Michaelsen TE, (1999) Human IgG subclass responses in relation to serum bactericidal and opsonic activities after immunization with 3 doses of the Norwegian serogroup B meningococcal outer membrane vesicle vaccine. Vaccine, 17: 754-764.

161. NCCLS, (1997) National Committee for Clinical Laboratory Standards. Methods for dilution antimicrobial susceptibility test for bacteria that grow aerobically. 5th Edition. Approved standard M7-A5. Volume 20. National Committee for Clinical Laboratory Standards, Wayne, PA:
162. Neu T, de Boer C, Ververke G, Schutte H, Rakhorst G, van der Mei H, Busscher H, (1994) Film development in time on a silicone rubber voice prosthesis - a case study. Microb Eco Health dis, 7: 27-33.
163. Neu T, Swerhone GD, Lawrence JR, (2001) Assessment of lectin-binding analysis for *in situ* detection of glycoconjugates in biofilm systems. Microbiology, 147: 299-313.
164. Neu TR, Lawrence JR, (1999) Lectin-binding analysis in biofilm systems. Methods Enzymol, 310: 145-152.
165. Nichols WW, Dorrington SM, Slack MP, Walmsley HL, (1988) Inhibition of tobramycin diffusion by binding to alginate. Antimicrob Agents Chemother, 32: 518-523.
166. Nichols WW, Evans MJ, Slack MP, Walmsley HL, (1989) The penetration of antibiotics into aggregates of mucoid and non-mucoid *Pseudomonas aeruginosa*. J Gen Microbiol, 135: 1291-1303.
167. Nickel JC, Costerton JW, (1993) Bacterial localization in antibiotic-refractory chronic bacterial prostatitis. Prostate, 23: 107-114.
168. Nickel JC, Ruseska I, Wright JB, Costerton JW, (1985) Tobramycin resistance of *Pseudomonas aeruginosa* cells growing as a biofilm on urinary catheter material. Antimicrob Agents Chemother, 27: 619-624.
169. Nyvad B, Kilian M, (1990) Comparison of the initial streptococcal microflora on dental enamel in caries-active and in caries-inactive individuals. Caries Res, 24: 267-272.
170. O'Flaherty S, Coffey A, Meaney WJ, Fitzgerald GF, Ross RP, (2005) Inhibition of bacteriophage K proliferation on *Staphylococcus aureus* in raw bovine milk. Lett Appl Microbiol, 41: 274-279.
171. O'Flaherty S, Ross RP, Meaney W, Fitzgerald GF, Elbreki MF, Coffey A, (2005) Potential of the polyvalent anti-Staphylococcus bacteriophage K for control of antibiotic-resistant staphylococci from hospitals. Appl Environ Microbiol, 71: 1836-1842.
172. O'Gara J, Humphreys H, (2001) *Staphylococcus epidermidis* biofilms: importance and implications. J Med Microbiol, 50: 582-587.
173. O'Toole GA, Gibbs KA, Hager PW, Phibbs PV Jr, Kolter R, (2000) The global carbon metabolism regulator Crc is a component of a signal transduction pathway required for biofilm development by *Pseudomonas aeruginosa*. J Bacteriol, 182: 425-431.
174. O'Toole GA, Kolter R, (1998) Initiation of biofilm formation in *Pseudomonas fluorescens* WCS365 proceeds via multiple, convergent signalling pathways: a genetic analysis. Mol Microbiol, 28: 449-461.
175. Oga M, Arizono T, Sugioka Y, Naylor P, Myrvik O, Gristina A, (1992) The inhibition of bacterial adhesion to a tobramycin-impragnated apolymethylmethacryllate substractum. J Long Term Eff Med Implants, 1: 321-328.
176. Ostuni E, Chapman R, Liang M, Meluleni G, Pier G, Ingber D, Whitesides G, (2001) Self-assembled monolayers that resist the adsorption of proteins and the adhesion of bacterial and mammalian cells. Langmuir, 17: 6336-6343.
177. Otto M, (2001) *Staphylococcus aureus* and *Staphylococcus epidermidis* peptide pheromones produces by the accesory gene regulator agr system. Peptides, 22: 1603-1608.
178. Otto M, (2004) Quorum-sensing control in Staphylococci - a target for antimicrobial drug theraphy? FEMS Microbiol Lett, 241: 135-141.
179. Pagano P, Buchanan L, Dailey C, Haas J, Enk R, Gibson J, (2004) Effects of linezolid on staphylococcal adherence versus time of treatment. Int J Antimicrob Agents, 23: 226-234.
180. Palacios G, Gonzalez S, Perez F, Cuevas S, Solorzano S (2001) Cefuroxime vs dicloxacillin/chloram-phenicol combination for the treatment of parapneumonic pleural effusion and empynema in children. Pulm Pharmacol Ther, 15: 17-23.
181. Perez-Giraldo C, Cruz-Villalon G, Sanchez-Silos R, Martinez-Rubio R, Blanco M, Gomez-Garcia A, (2003) *in vitro* activity of allicin against *Staphylococcus epidermidis* and influence of subinhibitory concentrations on biofilm formation. J Appl Microbiol, 95: 709-711.
182. Perry RD, Bobrov AG, Kirillina O, Jones HA, Pedersen L, Abney J, Fetherston JD, (2004) Temperature regulation of the hemin storage (Hms+) phenotype of *Yersinia pestis* is posttranscriptional. J Bacteriol, 186: 1638-1647.
183. Perry RD, Pendrak ML, Schuetze P, (1990) Identification and cloning of a hemin storage locus involved in the pigmentation phenotype of *Yersinia pestis*. J Bacteriol, 172: 5929-5937.
184. Pier G, (1998) *Pseudomonas aeroginosa*: a key problem in cystic fibrosis. ASM News, 64: 339-347.
185. Pitts B, Hamilton M, Zelver N, Stewart P, (2003) A microtiter-plate screening method ofr biofilm disinfection and removal. J Microb Meth, 54: 269-276.

186. Poulsen LK, Ballard G, Stahl DA, (1993) Use of rRNA fluorescence *in situ* hybridization for measuring the activity of single cells in young and established biofilms. Appl Environ Microbiol, 59: 1354-1360.
187. Pringle JH, Fletcher M, (1986) Influence of substratum hydration and adsorbed macromolecules on bacterial attachment to surfaces. Appl Environ Microbiol, 51: 1321-1325.
188. Quirynen M, Bollen CM, Vandekerckhove BN, Dekeyser C, Papaioannou W, Eyssen H, (1995) Full- vs. partial-mouth disinfection in the treatment of periodontal infections: short-term clinical and microbiological observations. J Dent Res, 74: 1459-1467.
189. Rachid S, Ohlsen K, Witte W, Hacker J, Zieburh W, (2000) Effect of subinhibitory antibiotic concentrations on polysaccharide intercellular adhesin expression in biofilm-forming *Staphylococcus epidermidis*. Antimicrob Agents Chemother, 40: 3357-3363.
190. Resch A, Rosenstein R, Nerz C, Gotz F, (2005) Differential gene expression profiling of *Staphylococcus aureus* cultivated under biofilm and planktonic conditions. Appl Environ Microbiol, 71: 2663-2676.
191. Rijnaarts H, Norde W, Bouwer E, Lyklema J, Zehnder A, (1993) Bacterial adhesion under static and dynamic conditions. Appl Environ Microbiol, 59: 3255-3265.
192. Roberts AP, Pratten J, Wilson M, Mullany P, (1999) Transfer of a conjugative transposon, Tn5397 in a model oral biofilm. FEMS Microbiol Lett, 177: 63-66.
193. Roldan M, Thomas F, Castel S, Quesada A, Hernandez-Marine M, (2004) Noninvasive pigment identification in single cells from living phototrophic biofilms by confocal imaging spectrofluorometry. Appl Environ Microbiol, 70: 3745-3750.
194. Romero-Steiner S, Musher DM, Cetron MS, Pais LB, Groover JE, Fiore AE, Plikatys BD, Carlone GM (1999) Reduction in functional antibody activity against *Streptococcus pneumoniae* in vaccinated eldery individuals highly correlates with decreased IgG antibody avidity. Clin Infec Dis, 29: 281-288.
195. Rupp M, Archer G, (1992) Hemagglutination and adherence to plastics by *Staphylococcus epidermidis*. Infect Immun, 60: 4322-4327.
196. Rupp M, Hamer K, (1998) Effect of subinhibitory concentrations of vancomycin, cefazolin, ofloxacin, L-oflocaxin and D-ofloxacin on adherence to intravascular catheters and biofilms formation by *Staphylococcus epidermidis*. J Antimicrob Chemother, 41: 155-161.
197. Rupp M, Ulphani JS, Fey PD, Mack D, (1999) Characterization of *Staphylococcus epidermidis* polysaccharide intercellular adhesin/hemagglutinin in the pathogenesis of intravascular catheter-associated infection in a rat model. Infect Immun, 67: 2656-2659.
198. Sadavskaya I, Vinogradov E, Flahaut S, Kogan G, Jabbouri S, (2005) Extracellular carbohydrate-containing polymers of a model biofilm-producing strain, *Staphylococus epidermidis* RP62A. Infect Immun, 73: 3007-3017.
199. Schink B, (1997) Energetics of syntrophic cooperation in methanogenic degradation. Microbiol Mol Biol Rev, 61: 262-280.
200. Sherlock O, Schembri MA, Reisner A, Klemm P, (2004) Novel roles for the AIDA adhesin from diarrheagenic *Escherichia coli*: cell aggregation and biofilm formation. J Bacteriol, 186: 8058-8065.
201. Sherlock O, Vejborg RM, Klemm P, (2005) The TibA adhesin/invasin from enterotoxigenic *Escherichia coli* is self recognizing and induces bacterial aggregation and biofilm formation. Infect Immun, 73: 1954-1963.
202. Shi L, Ardehall R, Caldwell K, Valint P, (2000) Mucin coating on polymeric material surfaces to suppress bacterial adhesion. Colloids Surf B Biointerfaces, 17: 229-239.
203. Shiau AL, Wu CL, (1998) The inhibitory effect of *Staphylococcus epidermidis* slime on the phagocytosis of murine peritoneal macrophages is interferon-independent. Microbiol Immunol, 42: 33-40.
204. Shiro H, Muller E, Gutierrez N, Boisot S, Grout M, Tosteson T, Goldmann D, Pier G, (1994) Transposon mutants of *Staphylococcus epidermidis* deficient in elaboration of capsular polysaccharide/adhesin and slime are avirulent in a rabbit model of endocarditis. J Infect Dis, 169: 1042-1049.
205. Sikkema DJ, Brubaker RR, (1987) Resistance to pesticin, storage of iron, and invasion of HeLa cells by *Yersiniae*. Infect Immun, 55: 572-578.
206. Sillankorva S, Oliveira R, Vieira M, Suthereland IW, Azeredo J, (2004) Bacteriophage f-S1 infection of *Pseudomonas fluorescens* planktonic cells versus biofilms. Biofouling, 20: 133-138.
207. Smith HW, Huggins MB, (1982) Successful treatment of experimental *Escherichia coli* infections in mice using phage: its general superiority over antibiotics. J Gen Microbiol, 128: 307-318.
208. Spoering A, Lewis K, (2001) Biofilms and planktonic cells of *Pseudomonas aeruginosa* have similar resistance to killing by antimicrobials. J Bacteriol, 183: 6744-6751.

209. Stanley PM, (1983) Factors affecting the irreversible attachment of *Pseudomonas aeruginosa* to stainless steel. Can J Microbiol, 29: 1493-1499.
210. Stewart M, Male D, (1998), Immunological techiques ***in*** Immunology, 381-396. Mosby, London, UK
211. Stewart P, Costerton J, (2001) Antibiotic resistance of bacteria in biofilms. Lancet, 358: 135-138.
212. Stewart P, (1998) A review of experimental measurements of effective diffusive permeabilities and effective diffusion coefficients in biofilms. Biotechnol Bioeng, 59: 261-272.
213. Stoodley AP, Boyle D, Dodds I, Lappin-Scott H, (1997) Consensus model of biofilm structure ***in*** Biofilms: community interactions and controls, 1-9. BioLine, Cardiff, Uk
214. Stoodley AP, Boyle D, Dodds I, Lappin-Scott H, (1998) Influence of hydrodynamics and nutrients on biofilm structure. J Appl Microbiol, 85: 19S-28S.
215. Suci PA, Mittelman MW, Yu FP, Geesey GG, (1994) Investigation of ciprofloxacin penetration into *Pseudomonas aeruginosa* biofilms. Antimicrob Agents Chemother, 38: 2125-2133.
216. Suthereland IW, Hughes KA, Skillman LC, Tait K, (2004) The interaction of phage and biofilms. FEMS Microbiol Lett, 232: 1-6.
217. Szomolay B, Klapper I, Dockery J, Stewart PS, (2005) Adaptive responses to antimicrobial agents in biofilms. Environ Microbiol, 7: 1186-1191.
218. Tal S, Guller V, Levi S, Bardenstein R, Berger D, Gurevich I, Gurevich A, (2005) Profile and prognosis of febrile elderly patients with bacteremic urinary tract infection. J Infect, 50: 296-305.
219. Tambe S, Modak S, (2001) *in vitro* evaluation of the risk of developing bacterial resistante to antiseptics and antibiotics used in medical devices. J Antimicrob Chemother, 47: 589-595.
220. Tamura Y, Kijima M, Ohishi K, Takahashi T, Suzuki S, Nakamura M, (1992) Antigenic analysis of Clostridium chauvoei flagella with protective and non-protective monoclonal antibodies. J Gen Microb, 138: 537-542.
221. Teixeira P, Oliveira R, (1999) Influence of surface characterisitcs on the adhesion of *Alcaligenes denitrificans* to polymerics substrates. J Adhes Science Tech, 13: 1287-1294.
222. Tenover FC, Hughes JM, (1996) The challenges of emerging infectious diseases. Development and spread of multiply-resistant bacterial pathogens. JAMA, 275: 300-304.
223. Thiel K, (2004) Old dogma, new tricks--21st Century phage therapy. Nat Biotechnol, 22: 31-36.
224. Tojo M, Yamashita N, Goldmann D, Pier G, (1988) Isolation and characterization of a capsular polyssacharide adhesin from *Staphylococcus epidermidis*. J Infect Dis, 157: 713-722.
225. Tunkel A, Mandell G, (1992) Infecting microorganisms ***in*** Infective endocarditis, 85-97. Raven Press, New York, USA
226. Tunney M, Ramage G, Field T, Moriarty T, Storey D, (2004) Rapid colorimetric assay for antimicrobial susceptibility testing of *Pseudomonas aeruginosa*. Antimicrob Agents Chemother, 48: 1879-1881.
227. Tuomanen E, Cozens R, Tosch W, Zak O, Tomasz A, (1986) The rate of killing of *Escherichia coli* by beta-lactam antibiotics is strictly proportional to the rate of bacterial growth. J Gen Microbiol, 132 (Pt 5): 1297-1304.
228. van der Mei H, de Vries J, Busscher H, (2000) X-ray photoelectron spectroscopy for the study of microbial cell surfaces. Surf Science Rep, 39: 1-24.
229. van Oss C, (1995) Hydrophobicity of biosurfaces - origin, quantitative determination and interaction energies. Colloids Surf B Biointerfaces, 5: 91-110.
230. van Oss C, Giese R, (1995) The hydrophilicity and hydrophobocity of clay minerals. Clay Min, 43: 474-477.
231. Vermont C, Hartwig N, Fleer A, de Man P, Verbrugh H, van der Anker J, de Groot R, van Belkun A, (1998) Persistance of clones of coagulase-negative staphylococci among premature neonates in neonatal intensive care units: 2-center study of bacterial genotyping and patient risk factors. J Clin Microbiol, 36: 2485-2490.
232. Viedma D, Rabadán P, Díaz M, Cercenado E, Bouza E, (2000) Heterogeneous antimicrobial resistance patterns in polyclonal populations of coagulase-negative staphylococci isolated from catheters. J Clin Microbiol, 38: 1359-1363.
233. Vilanova M, Teixeira L, Caramalho I, Torrado E, Marques A, Madureira P, Ribeiro A, Ferreira P, Gama M, Demengeot J, (2004) Protection against systemic candidiasis in mice immunized with secreted aspartic proteinase 2. Immunology, 111: 1-9.
234. Vinh D, Embil J, (2005) Device-related infections: a review. J Long Term Eff Med Implants, 15: 467-488.
235. von Eiff C, Heilmann C, Peters G, (1999) New aspects in the molecular basis of polymer-associated infections due to staphylococci. Eur J Clin Microbiol Infect Dis, 18: 843-846.
236. Vuong C, Otto M, (2002) *Staphylococcus epidermidis* infections. Microbes Infect, 4: 481-489.

237. Vuong C, Voyich J, Fischer E, Braughton K, Whitney A, DeLeo F, Otto M, (2004) Polysaccharide intercellular adhesin (PIA) protects *Staphylococcus epidermidis* against major components of the human innate immune system. Cell Microb, 6: 269-275.
238. Vuong C, Kocianova S, Voyich JM, Yao Y, Fischer ER, DeLeo FR, Otto M, (2004) A crucial role for exopolysaccharide modification in bacterial biofilm formation, immune evasion, and virulence. J Biol Chem, 279: 54881-54886.
239. Vuong C, Otto M, (2002) *Staphylococcus epidermidis* infections. Microbes Infect, 4: 481-489.
240. Vuong C, Voyich JM, Fischer ER, Braughton KR, Whitney AR, DeLeo FR, Otto M, (2004) Polysaccharide intercellular adhesin (PIA) protects *Staphylococcus epidermidis* against major components of the human innate immune system. Cell Microbiol, 6: 269-275.
241. Wang J, Lory S, Ramphal R, Jin S, (1996) Isolation and characterization of *Pseudomonas aeruginosa* genes inducible by respiratory mucus derived from cystic fibrosis patients. Mol Microbiol, 22: 1005-1012.
242. Wang X, Preston Jr III, Romeo T, (2004) The *pgaABCD* locus of *Escherichia coli* promotes the synthesis of a polysaccharide adhesin required for biofilm formation. J Bacteriol, 186: 2724-2734.
243. Watnick P, Kolter R, (2000) Biofilm, city of microbes. J Bacteriol, 182: 2675-2679.
244. Welch RA, Burland V, Plunkett G III, Redford P, Roesch P, Rasko D, Buckles EL, Liou SR, Boutin A, Hackett J, Stroud D, Mayhew GF, Rose DJ, Zhou S, Schwartz DC, Perna NT, Mobley HL, Donnenberg MS, Blattner FR, (2002) Extensive mosaic structure revealed by the complete genome sequence of uropathogenic *Escherichia coli.* Proc Natl Acad Sci U S A, 99: 17020-17024.
245. Williams I, Venables W, Lloyd D, Paul F, Critchley I, (1997) The effects of adherence to silicone surfaces on antibiotic susceptibility in *Staphylococcus aureus*. Microbiology, 143: 2407-2413-
246. Wolf AS, Krieger D, (1986) Bacterial colonization of intrauterine devices (IUDs). Arch Gynecol, 239: 31-37.
247. Wozniak D, Keyser R, (2004) Effects of subinhibitory concentrations of macrolide antibiotics on Pseudomonas aeruginosa. Chest, 125: 62-69.
248. Wu CY, Chiu PC, Hsieh KS, Chiu CL, Shih CH, Chiou YH, (2004) Childhood urinary tract infection: a clinical analysis of 597 cases. Acta Paediatr Taiwan, 45: 328-333.
249. Yarwood J, Schievert P, (2003) Quorum sensing in staphylococcus infections. J Clin Invest, 112: 1620-1625.
250. Yasuda H, Ajiki Y, Aoyama J, Yokota T, (1994) Interaction between human polymorphonuclear leucocytes and bacteria released from in-vitro bacterial biofilm models. J Med Microbiol, 41: 359-367.
251. Zaidi AK, Huskins WC, Thaver D, Bhutta ZA, Abbas Z, Goldmann D, (2005) Hospital-acquired neonatal infections in developing countries. Lancet, 365: 1175-1188.

FUNDAÇÃO CALOUSTE GULBENKIAN